The characterization of ancestral lignin degrading enzyme

A Doctoral Thesis

Yasuyuki Semba

Tokyo University of Pharmacy and Life Sciences

The characterization of ancestral lignin degrading enzyme

極限環境生物学研究室
指導教授　山岸　明彦
学位申請者　仙波　康之

1. Background

Improving enzyme stability is one of the major subjects in protein engineering. In the early stage of the protein engineering, it was done by the method so called rational engineering: improving the packing of the hydrophobic core, introducing disulfide bond and extending ion pair network. Despite of many researches, it is still a challenging task to stabilize a particular enzyme of interest. The directed evolution is the alternative method. This method is based on the evolutionary process: mutation and selection. Later, the consensus approach was proposed, which is based on the dependence of the amino acid frequency in homologous amino acid sequences. These two methods do not need physical principle and tertiary structural information of the target enzyme. Our laboratory has developed ancestral mutation method, based on the phylogenetic analysis: (1) collecting amino acid sequences from database, (2) multiple sequence alignment, (3) phylogenetic tree construction, (4) estimation of ancestral sequence, (5) introduction of ancestral amino acid residue(s) into the target enzyme, (6) Enzyme expression and characterization. Some ancestral mutants have been created starting for isocitrate dehydrogenase (ICDH), 3-isopropylmalate dehydrogenase (IPMDH), glycyl-tRNA synthetase (GlyRS) and *β*-amylase. The dataset of ICDH, IPMDH and GlyRS contained archaea, bacteria and eukarya. That of *β*-amylase was constructed with bacteria and eukarya. The ancestral mutation method based on the dataset constituted only of eukarya hasn't been investigated.

The lignin is the polymer in the cell wall and protects plant bodies from biodegradation. In 1983, lignin degrading enzyme has been discovered from white rot fungi: lignin peroxidase (LiP), manganese peroxidase (MnP) and versatile peroxidase (VP). LiP oxidizes veratryl alcohol (VA) and the product $VA^{+\cdot}$ plays a role of mediator. MnP oxidizes manganese (II) to manganese (III) and manganese (III) forms complex with dicarboxylic acid. This complex attacks to lignin. VP has both activities. These enzymes have potential to be applied to the degradation of lignin. The application of these enzymes on degrading lignin is expected to contribute to lower the energy cost and by-products. However the low stability of these enzymes has been the obstacle to the industrial application.

The purpose of this study is to create stable lignin degrading enzyme by ancestral mutation method and resurrection of ancestral lignin degrading enzyme based on the dataset constituted only of eukaryal sequences.

2. Ancestral mutants of LiP

In chapter 2 we created stable LiP by ancestral mutation method.

2.1. Method

The amino acid sequences of lignin degrading enzymes were collected from NCBI database by Protein Blast search using wild-type lignin peroxidase from *Phanerochaete chrysosporium* strain UAMH3641 as a query sequence. The sequences were aligned by the program ClustalX with its default parameters and then manually adjusted. Well-conserved regions were collected by Gblocks 0.91. The maximum likelihood tree was constructed with Treefinder and PhyML 2.4.4. The WAG substitution model was used as the substitution matrix for amino acids. Ancestral sequence was estimated by CODEML in PAML 3.14. Comparing amino acid sequences of ancestral and wild-type, eleven mutation sites were selected. The point mutations were introduced by QuikChange Lightning Site-Directed Mutagenesis Kit. Enzymes were expressed in *Escherichia coli* BL21 (DE3) and were accumulated as inclusion body. After washing inclusion body, the enzyme was unfolded with urea and refolded. Crude sample was purified with DEAE-sepharose and HiTrapQ columns.

The enzyme activity was measured by monitoring the oxidation of veratryl alcohol to veratryl aldehyde (veratryl alcohol + H_2O_2 → veratryl aldehyde + H_2O). The thermal inactivation of LiP was done by incubating enzyme at 37 ^{o}C. The resistance for H_2O_2 was estimated by incubating enzyme with 0.1 mM H_2O_2 at 25 ^{o}C. The structural stability was estimated by measuring circular dichroism at 222 nm.

2.2. Result

The phylogenetic tree was constructed from 198 positions of the 49 fungal peroxidase sequences. LiP from Ascomycota was used as outgroup. The sequences at the branching point of Basidiomycota and Ascomycota, two ancestors of LiP and MnP were estimated. Eleven ancestral mutants were created.

The enzyme activity of six ancestral mutants was increased. Especially the activity of H239F/T240L/I241L was 2.3-fold higher than the wild-type. The optimum temperature of H239F/T240L/I241L was increased by 10 ^{o}C than the wild-type. Five ancestral mutants showed high remaining activity than wild-type after thermal inactivation. Furthermore five ancestral mutants showed high H_2O_2 resistance than the wild-type. The T_m values, half-denaturation temperature, of H239F/T240L/I241L and the wild-type were 51.9 ± 0.7 ^{o}C and 50.1 ± 0.2 ^{o}C, respectively.

2.3. Discussion

We have extended the method to select the ancestral mutation site relying on the primary amino acid sequence. We estimated the relationship between thermal stability and the conservation of the neighboring amino acids within seven residues in the primary sequence. If a wild-type residue and the ancestral residue were identical, the likelihood value was taken as the conservation value. However, if the wild-type and ancestral residue differed then the conservation value was defined as 0. Finally, an averaged conservation value for neighboring residues on the primary amino acid sequence was calculated. This value is referred to linear ACV. The linear ACV values were plotted against the remaining activity after incubation at 37 ^{o}C or in 0.2 mM H_2O_2. When the linear ACV value is greater than 0.9, mutants with improved thermal stability were obtained at high efficiency. Three of four mutants whose linear ACV was >0.9 showed improved thermal stability. A similar trend was observed when the window size was increased to eleven residues. A similar relationship between the linear ACV value and the effect of ancestral mutation was found for the ancestral mutants of *β*-amylase and IPMDH reported previously. These results suggest that the mutants with higher linear ACV tend to show increased thermal stability. Thus, the linear ACV value can be used to select residues for mutation that will improve the thermal stability of the protein.

3. Ancestral lignin degrading enzyme

In chapter 3, we resurrected the ancestral lignin degrading enzyme whose amino acid sequence was entirely made of ancestral amino acids.

3.1. Method

LiP homologous 83 sequences were collected and aligned with MAFFT. The multiple sequence alignment was adjusted manually and well-conserved region was selected by Gblocks. The WAG+G+F model was selected as the amino acid substitution model by Prottest. Phylogenetic tree was constructed with PhyML. The ancestral sequence was estimated with CODEML in PAML and the gap position was estimated with GASP. Obtained ancestral sequence was named ancestral ligninase. Ancestral ligninase was expressed in *E. coli* BL21 (DE3). Enzyme was purified and the enzyme activities measured.

3.2. Result

The ancestral ligninase has two activities, MnP and LiP activities, although the former activity was lower than the counterpart from *P. chrysosporium*. The remaining LiP and MnP activities of ancestral ligninase were higher than LiP and MnP from *P. chrysosporium* after the 15 min heat treatment. The T_m value was defined as the half denaturation temperature. The T_m values of MnP, LiP and ancestral ligninase were 50 ^{o}C, 58 ^{o}C and 66 ^{o}C, respectively. The

ancestral ligninase showed higher T_m value than LiP and MnP from *P. chrysosporium*.

3.3. Discussion

Most residues of ancestral ligninase at the glycosylation site were the same as those of extent glycosylated enzymes. Then ancestral ligninase probably must have been glycosylated in its nascent organism. Nie *et al*. reported that the glycosylation is contributing to enzyme stability (*Arch Biochem. Biophys*. 1999. **2**. 328). Because the stability of glycosylated LiP and MnP were higher than wild-type enzyme, glycosylated ancestral ligninase must also show higher stability than non-glycosylated ancestral ligninase.

In the previous studies of resurrecting ancestral enzymes, the high thermal stabilities were interpreted to represent the high environ temperature of the host organism. In the current study, the ancestral sequence represents the age around 270 million years ago (*Science* 2012. **336**. 1715), when the whole earth temperature is not very high. However, the stability of enzyme is often much higher than the growth temperature of the host organisms. For example, the T_m value of ribonuclease T1 from *Aspergillus oryzae* is 59.3 ^oC and the optimum growth temperature is 26 ^oC (*J. biol. Chem*. 1988. **24**. 11820). The ancestral ligninase was much more stable than the growth temperature of the host.

4. Conclusion

In the ancestral mutants of LiP, we introduced ancestral mutations into wild-type LiP from *P. chrysosporium* to improve its thermal stability. The recombinant ancestral mutant, m10 (H239F/T240L/I241L), showed improved thermal stability comparable to that of the glycosylated wild-type enzyme. Specific activity and k_{cat}/K_M of one of the ancestral mutants, m10, was improved by amino acid substitution. This is the first investigation to successfully improve enzyme stability by introducing ancestral residues inferred from the dataset constructed from eukaryotic sequences. The linear ACV value can be used to select ancestral residues to efficiently enhance the thermal stability of enzymes.

In the ancestral lignin degrading enzyme, we constructed dataset constructed with only Basidiomycota. By selecting position locating near peroxidases from *A. ramosus* and *C. cinerea* as ancestral node, our ancestral ligninase showed two activities. The ancestral ligninase showed high enzyme stability than modern enzymes. The resurrecting ancestral enzyme from limited dataset could be used to design thermally stable enzyme.

Abbreviations

Anc: ancestor
DTT: dithiothreitol
EDTA: ethylenediaminetetraacetic acid
IPTG: isopropyl-β-$_{D}$-thiogalactopyranoside
LiP: lignin peroxidase
ML: maximum likelihood
MnP: manganese peroxidase
PCR: polymerase chain reaction
PMSF: phenylmethylsulfonyl fluoride
PcLiP: lignin peroxidase from *Phanerochaete chrysosporium*
PcMnP: manganese peroxidase from *Phanerochaete chrysosporium*
TE: 10 mM Tris-HCl (pH8.0) and 1 mM EDTA solution
VA: veratryl alcohol
VP: versatile peroxidase

Chapter 1. General introduction

1. Stability of the enzyme

Enzyme is useful tool for civilization. For example, cellulase, lipase and protease were contained in detergent. These enzymes make detergent powerful and usage reduce. Glucose oxidase is used for glucose sensor. Enzyme has a possibility to contribute to not only industry but another field like medicine, agriculture and food. However, the designing and/or improving enzyme to be efficient for use is very difficult. In particular, the stability of the enzyme was big issue; increasing enzyme stability is the one of the great challenge of protein engineering.

1.1. The rational engineering method

Many researchers tried to improve enzyme stability.

Mathews *et al*. was successes in improving thermal stability of T4 lysozyme by replacing a residue by a proline (Pro, P), and replacing a glycine (Gly, G) by alanine (Ala, A)[1]. The half denaturation temperature of mutant, A82P, was increased by 0.8 ^{o}C (pH 2.0) and 2.1 ^{o}C (pH 6.5) than wild-type. These substitutions didn't effect on enzyme activity.

Hydrogen bonds contributes to the thermodynamic stability[2]. Alber *et al.* used phage T4 lysozyme. Thirteen substitutions were introduced in threonine (Thr, T) 157. This residue has two hydrogen bonds between neighboring residue T157 and aspartate (Asp, D) 159. When T157 was mutated into another thirteen amino acids, the thermal stability of these variants was decreased than wild-type enzyme.

According to Sandberg and Terwilliger, interior packing and hydrophobicity was effects on the stability of protein[3]. This is shown by using gene V protein from bacteriophage F1. They introduced mutations, valine (Val, V) 35 isoleucine (Ile, I), I47V. Two single mutants and one double mutants, V35I/I47V, were decreased its stability due to change packing and hydrophobicity in hydrophobic core.

Introducing disulfide bonds was also effective[4]–[7]. Peter *et al.* engineered disulfide bond in T4 lysozyme[4]. Isoleucine (Ile, I) 3 was mutated to cysteine (Cys, C) to create new disulfide bond between Cys3 and Cys97. And the variant was more stable than the wild type when enzyme was treated at 67 ^{o}C. Matsumura *et al.* also engineered another four disulfide bonds in phage T4 lysozyme by theoretical calculations and computer modeling[7]. The protein melting temperature of two mutants was increased by 6 ^{o}C and 11 ^{o}C than wild-type. Wells and Powers engineered disulfide bonds in subtilisin, a kind of protease, from *Bacillus amyloliquefaciens*[5]. Sauer *et al.* introduced disulfide bond at the dimer interface of the N-terminal domain of λ repressor and its stability against thermal denaturation and urea

denaturation was increased[6].

Metal ions were contributed to enzyme stability. Kuroki *et al*, designed and creation of a Ca^{2+} binding site, Gln86Asp and Ala92Asp, in human lysozyme to enhance structural stability[8]. The enzyme activity of mutant human lysozyme was 2-fold higher than that of the native lysozyme and the optimum temperature was also higher than that of wild-type. In addition, mutant human lysozyme was more stable against protease treatment. The authors conclude that the creation of the calcium binding site in human lysozyme enhances its structural stability.

Extending ion pair network is important factor for enzyme stabilities[9]–[11]. Sakuraba *et al*. determined the crystal structure of $_{L}$-aspartate oxidase from *Sulfolobus tokodaii* and compared the structure with $_{L}$-aspartate oxidase from *Escherichia coli*[9]. They discovered large ion-pair network between the FAD-binding and C-terminal domains of the enzyme from *S. tokodaii*, on the other hands, there are no large ion-pair network in the enzyme from *E. coli*. This ion-pair network contributes to be the main factors contributing to the high thermostability.

Despite the existence of many investigations, there are no critical methods to improve enzyme stability. This caused by that mutated amino acid residue itself have unpredictable influence to another amino acid. To adapt these rational engineering methods were required too many information about the target enzyme, which means insufficient.

1.2. Direct evolutionary engineering

The direct evolutionary engineering was developed as alternative method to increase enzyme stability. This method was based on the evolution process. In this method, evolutionary library was constructed and select ideal mutants by screening or selection.

Laccase from *Myceliophthora thermophila* was improved by directed evolution engineering[12]. Laccase has the possibility as application for pulp bleaching and delignification for the paper industry. This laccase was expressed in *Saccharomyces cerevisiae* and direct evolved. Enzyme activity was enhanced 170-fold and k_{cat} value increased 22-fold. Not only enzyme activity but expression level was also improved by 7.7-fold.

Sutilisin S41 from psychrophilic is a kind of protease and its stability was lower than mesophilic and thermophilic homologs. Miyazaki and Arnold was tried to increase thermal stability of sutilisin S41 by direct evolution and saturation mutagenesis[13]. By directed evolution, they found the position that the possibility to increase stability. Next they applied saturation mutagenesis. As a result, thermal stable mutants were created. The half life at 60 ^{o}C of mutants and wild-type was 84 min and 8 min, respectively.

Many enzymes were improved its stability and/or enhanced its enzyme activities[14], [15].The effort of this method is not necessary of much information. The disadvantage is the

low efficiency. In random mutation library, almost variants were neutral or deleterious. So the construction of the library was devised. For example, Alcolombri *et al.* constructed library with ancestral mutants[16]. Flores and Ellington combined modified consensus approach[17]. However, the directed evolution method is still laborious and costly.

1.3. Ancestral mutation method

We developed ancestral mutation method as alternative method to increase enzyme stability. This method was based on the hypothesis; the universal common ancestor of life, Commonote, was thermophile and its enzyme has high thermal stability. Recently, Akanuma *et al.*, showed experimental evidence by reconstruction of ancestral nucleoside diphosphate kinase (NDK) of bacteria and archaea[18]. The bacterial and archaeal NDK has high thermal stability.

The process is described below. (1) Collecting amino acid sequences of homologes from NCBI database. (2) Constructing multiple sequence alignment. (3) Phylogenetic analysis, construction of phylogenetic tree. (4) Estimating of ancestral sequence. (5) Comparing amino acid sequence between target enzyme and ancestral sequence. (6) Point or multi ancestral mutation in target enzyme (7) Expression, purification and characterization.

We succeed in increasing some enzyme stabilities by this method. Iwabata *et al.* used isocitrate dehydrogenase (ICDH) from *Caldococcus noboribetus*[19]. To estimate ancestral sequence, 18 sequences from archaea, bacteria and eukarya were used. Five ancestral mutants were created and four mutants of them were increased thermal stability than wild-type.

Watanabe *et al.* 3-isopropylmalate dehydrogenase (IPMDH) from *Thermus thermophilus*[20]. The dataset of this study was the same as Iwabata's dataset. 12 ancestral mutants were created and at least six of them were increased thermal stability than wild-type. In addition, the combination of improved mutants were tested and two mutants containing multiple mutants, showed high thermal stability[21]. The additivity was observed and the mutation points were well separated in primary sequence is the key.

ICDH is related to TCA cycle and IPMDH is related to leucine biosynthetic pathway. Another type of enzymes were tried to apply ancestral mutation method. Glycyl-tRNA synthetase is related to translation. Shimizu *et al.* used Glycyl-tRNA synthetase from *T. thermophilus*[22]. 28 sequences from archaea, bacteria and eukarya was collected and estimate ancestral sequence. 8 mutants were constructed and 6 mutants were improved its stability than wild-type and 7 mutants were increased enzyme activity. There was the tendency that the mutants where mutation points located on the loops and β-sheets were increased stability. But this tendency was conflict with the result of IPMDH.

β-amylase is attractive enzyme to commercial usage. Yamashiro *et al.* introduced ancestral mutation to *β*-amylase from *Bacillus circulans*[23]. There was no definitively

identifical archaeal β-amylase sequence, no archaeal sequence was in the dataset. They constructed 18 ancestral mutants and 7 mutants were increased its stability. They didn't estimate the commonote's sequence, however they succeed in increasing enzyme stability.

In these investigations, ancestral amino acids were introduced single and/or double. The full length of amino acid sequence was also constructed with ancestral amino acid were constructed. Akanuma *et al.* resurrected full length of ancestral DNA gyrase B subunit[24]. DNA gyrase is a type II DNA topoisomerase and related to replication. B subunit has ATPase domain. The thermal stability of ancestral DNA gyrase B subunit was more similar to that of the subunit from *Thermus thermophilus*.

2. Lignin degrading enzymes

Recently, biofuel production from cellulosic biomass was developing. Lignin is the heterogeneous polymer in the cell wall. Lignin makes plants rigid and protects plants from biodegradation. The only fungi can brake lignin down to CO_2 and H_2O with secreting high power lignin degrading enzymes[25].Lignin peroxidase, manganese peroxidase and versatile peroxidase were well known as lignin degrading enzyme. These enzymes contain heme in the center. The details of these enzymes are written in below.

2.1. Lignin peroxidase

In 1983, Tien *et al.*, discovered lignin peroxidase[26]. Lignin peroxidase (LiP, EC 1.11.1.14) is one kind of the lignin degrading enzymes. LiP catalyzes aromatic compounds, such as veratryl alcohol (3, 4-dimethoxybenzyl alcohol, VA), 1, 4-methoxybenzene[27], $_L$-Dopa[28], which indicate that the substrate specificity of LiP was low. $VA^{+\cdot}$ as mediator[29]. This mediator $VA^{+\cdot}$ attacks lignin, however there is a possibility that LiP attacks lignin directly[30], [31].

Researcher often used VA as a substrate. In this reaction, the optimum pH is <2.5. The heterologous expression techniques were developed. Doyle and Smith used *Escherichia coli* to express LiP from *Phanerochaete chrysosporium*[32]. Miki *et al.* also used *E. coli* for LiP from *Trametes cervina*[27]. Johnson and Li. used baculovirus and LiP from *P. chrysosporium* was expressed[33]. Especially, the expression system with *E. coli* was powerful tool, For example, for active site search. As a result, tryptophan (Trp, W) 170 was determined as active site[34]. The tertiary structure was determined[35] and shown in Figure 1-1.

2.2. Manganese peroxidase

Manganese peroxidase (MnP, EC 1.11.1.13) is one kind of the lignin degrading enzymes. This enzyme catalyzes oxidizing manganese (II) to manganese (III) with hydrogen peroxide.

$$Mn\ (II) + H_2O_2 \rightarrow Mn\ (III) + H_2O$$

Mn (III) form complex with dicarbonic acid like oxalic acid, malonic acid and succinic acid[36]. This complex attacks lignin. The degrading lignin occurs far from enzyme active site. Not only lignin, but also another polymer would have a possibility degraded by MnP.

In MnP, the expression system with using *E. coli* was constructed[37], [38]. The active site is constructed with glutamate (Glu, E) 36, glutamate (Glu, E) 40 and aspartate (Asp, D) 180[39], [40]. The tertiary structure was determined[41] and shown in Figure 1-2.

Native MnP, secreted in fungi, is also glycosylated enzyme. The glycosylated MnP is more stable than non-glycosylated MnP[42].

2.3. Versatile peroxidase

Versatile peroxidase (VP) is hybrid enzyme. This enzyme has two activity; LiP activity and MnP activity[43]. Tertiary structure was determined[44] and it was shown in Figure 1-3.

2.4. Protein engineering of lignin degrading enzymes

Researchers tried to improve MnP stability.

MnP has two or four calcium. There is a report that these calcium are very important for the enzyme stability[45]. And the peroxidase from peanut have a disulfide bond near the calcium binding site. Reading *et al,* focused on the region near the calcium binding site and they introduced disulfide bond to fix the structure[46]. The remaining enzyme activity of native MnP which is glycosylated MnP, recombinant MnP which expressed in E. coli and MnP which introduced disulfide bond was measured. As a result, MnP which has disulfide bond was the same remaining activity as native MnP.

Miyazaki *et al.*, improved H_2O_2 stability of MnP[47], they substituted methionine (Met, M) to leucine (Leu, L) because of methionine was sensitive for oxidizing stress. After 3 mM H_2O_2 treatment for 1 hour at 37 ^oC, the residual activity of variant and wild-type was about 30 % and 0 %, respectively.

Furthermore Miyazaki *et al.* used direct evolution method and select mutants improved H_2O_2 stability [48]. MnP was expressed in inclusion body with *E. coli* expression system. So they used cell-free expression system named SIMPLEX (Single-molecule-PCR-linked *in vitro* expression). They selected 4 mutants improved H_2O_2 stability from 10^4 samples.

Not only improving enzyme stability, but also engineering enzyme activity was investigated. The tertiary structure was very similar to MnP and LiP. The superposition model LiP and MnP was drawn by PyMol in Figure 1-4. The RMSD (Root Mean Square Deviation) value was 0.716 Å. Timofeevski *et al.* were introduced LiP active site into MnP from *Phanerochaete chrysosporium*[49]. This variant Ser168Trp retained Mn (II) oxidizing activity

and VA oxidizing activity.

Conversely, Tünde and Tien introduced MnP active site into LiP[50]. Three mutations, Asn182Asp, Asp183Lys and Ala36Glu, were introduced into LiP from *P. chrysosporium*. This mutant was able to oxidize Mn (II) and VA. In this mutant, the optimum pH of VA and Mn (II) oxidation were also altered. The optimum pH of oxidizing VA of wild-type and mutant were 2.5 and 3.5, respectively. The optimum pH of oxidizing Mn (II) of wild-type and mutant were 4 and 5.5, respectively.

Native LiP and MnP, expressed in fungi, was glycosylated. Recombinant LiP expressed in *Escherichia coli* wasn't glycosylated and its stability was lower than native LiP[42]. Then the expression system in Yeast *Pichia pastoris* was developed[51]. Although the MnP expressed in *P. pastoris* was slightly less thermo-stable than MnP from *P. chrysosporium*, it seems that the stability of MnP expressed in *P. pastoris* was higher than MnP expressed in *E coli*.

Direct evolution method was applied for VP[52]. In this paper, VP from *Pleurotus eryngii* was expressed in *Saccharomyces cerevisiae*. After 6 rounds of direct evolution, 4 mutants increased VP activity (129 fold). Additionally, temperature, peroxide and alkaline pH tolerant.

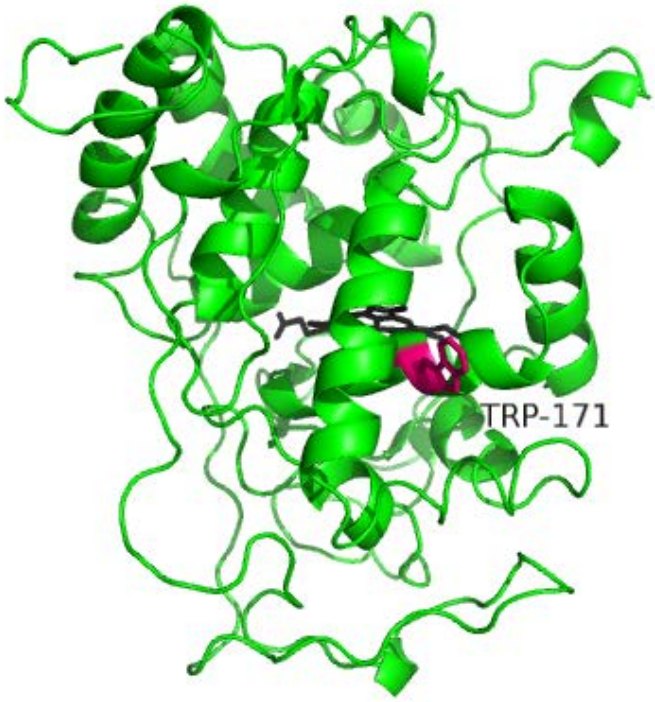

Figure 1-1. The tertiary structure of the LiP.

PDB file was 1LLP and described by PyMol. Trp171, active site, was colored magenta and black stick was heme. This figure was drown by using PyMol (http://www.pymol.org).

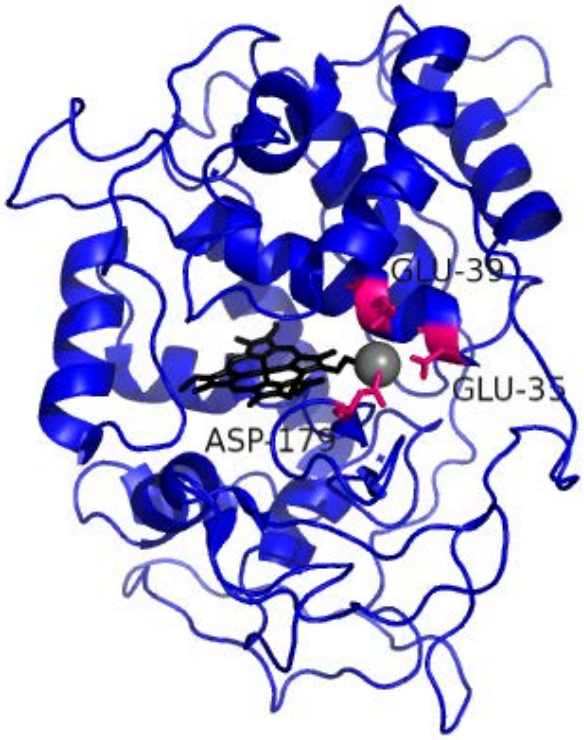

Figure 1-2. The tertiary structure of MnP.

PDB file was 1MNP and described by PyMol. The residues constructed with active site, were colored magenta. Gray sphere was manganese and black stick was heme.

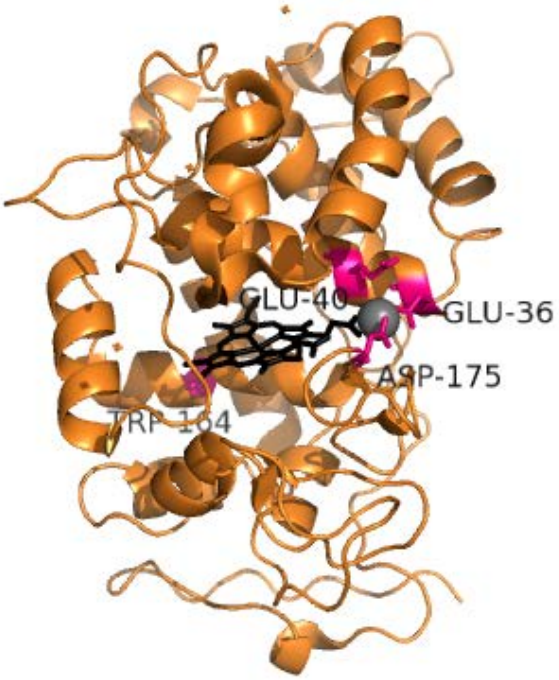

Figure 1-3. The tertiary structure of VP.

PDB file was 2BOQ and described by PyMol. The active site was colored magenta. TRP-164 was LiP active site. GLU-36, GLU-40 and ASP-175 construct MnP active site. Gray sphere was manganese and black stick was heme.

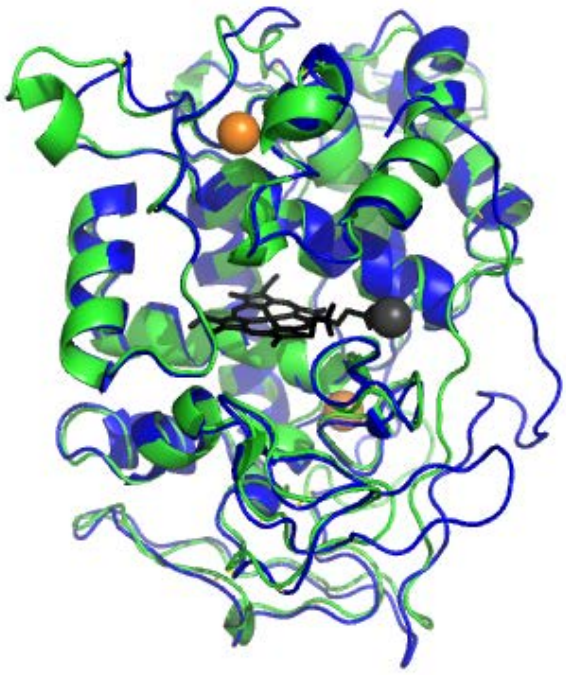

Figure 1-4 LiP and MnP aligned structure

PDB data was from protein data bank and aligned by PyMol.

LiP (PDB ID, 1LLP), MnP (1MNP) were shown in green and blue, respectively. Orange sphere was calcium and dark gray sphere was manganese.

References

[1] B. W. Matthews, H. Nicholson, and W. J. Becktel, “Enhanced protein thermostability from site-directed mutations that decrease the entropy of unfolding,” *Proc. Natl. Acad. Sci.*, vol. 84, no. 19, pp. 6663–6667, Oct. 1987.

[2] T. Alber, S. Dao-pin, K. Wilson, J. A. Wozniak, S. P. Cook, and B. W. Matthews, “Contributions of hydrogen bonds of Thr 157 to the thermodynamic stability of phage T4 lysozyme,” *Nature*, vol. 330, no. 6143, pp. 41–46, Nov. 1987.

[3] W. S. Sandberg and T. C. Terwilliger, “Influence of interior packing and hydrophobicity on the stability of a protein,” *Science*, vol. 245, no. 4913, pp. 54–57, Jul. 1989.

[4] L. J. Perry and R. Wetzel, “Disulfide bond engineered into T4 lysozyme: stabilization of the protein toward thermal inactivation,” *Science*, vol. 226, no. 4674, pp. 555–557, Nov. 1984.

[5] J. A. Wells and D. B. Powers, “In vivo formation and stability of engineered disulfide bonds in subtilisin.,” *J. Biol. Chem.*, vol. 261, no. 14, pp. 6564–6570, May 1986.

[6] R. T. Sauer, K. Hehir, R. S. Stearman, M. A. Weiss, A. Jeitler-Nilsson, E. G. Suchanek, and C. O. Pabo, “An engineered intersubunit disulfide enhances the stability and DNA binding of the N-terminal domain of .lambda. repressor,” *Biochemistry*, vol. 25, no. 20, pp. 5992–5998, Oct. 1986.

[7] M. Matsumura, W. J. Becktel, M. Levitt, and B. W. Matthews, “Stabilization of phage T4 lysozyme by engineered disulfide bonds,” *Proc. Natl. Acad. Sci.*, vol. 86, no. 17, pp. 6562–6566, Sep. 1989.

[8] R. Kuroki, Y. Taniyama, C. Seko, H. Nakamura, M. Kikuchi, and M. Ikehara, “Design and creation of a Ca2+ binding site in human lysozyme to enhance structural stability,” *Proc. Natl. Acad. Sci.*, vol. 86, no. 18, pp. 6903–6907, Sep. 1989.

[9] H. Sakuraba, K. Yoneda, I. Asai, H. Tsuge, N. Katunuma, and T. Ohshima, “Structure of l-aspartate oxidase from the hyperthermophilic archaeon Sulfolobus tokodaii,” *Biochim. Biophys. Acta - Proteins Proteomics*, vol. 1784, no. 3, pp. 563–571, Mar. 2008.

[10] K. S. P. Yip, T. J. Stillman, K. L. Britton, P. J. Artymiuk, P. J. Baker, S. E. Sedelnikova, P. C. Engel, A. Pasquo, R. Chiaraluce, V. Consalvi, R. Scandurra, and D. W. Rice, “The structure of Pyrococcus furiosus glutamate dehydrogenase reveals a key role for ion-pair networks in maintaining enzyme stability at extreme temperatures,” *Structure*, vol. 3, no. 11, pp. 1147–1158, Nov. 1995.

[11] M. Hennig, B. Darimont, R. Sterner, K. Kirschner, and J. N. Jansonius, “2.0 å structure of indole-3-glycerol phosphate synthase from the hyperthermophile Sulfolobus solfataricus: possible determinants of protein stability,” *Structure*, vol. 3, no. 12, pp. 1295–1306, Dec. 1995.

[12] T. Bulter, M. Alcalde, V. Sieber, P. Meinhold, C. Schlachtbauer, and F. H. Arnold, “Functional Expression of a Fungal Laccase in Saccharomyces cerevisiae by Directed Evolution,” *Appl. Environ. Microbiol.*, vol. 69, no. 2, pp. 987–995, Feb. 2003.

[13] K. Miyazaki and F. H. Arnold, “Exploring Nonnatural Evolutionary Pathways by Saturation Mutagenesis: Rapid Improvement of Protein Function,” *J. Mol. Evol.*, vol. 49, no. 6, pp. 716–720, 1999.

[14] L. Giver, A. Gershenson, P.-O. Freskgard, and F. H. Arnold, “Directed evolution of a thermostable esterase,” *Proc. Natl. Acad. Sci.*, vol. 95, no. 22, pp. 12809–12813, Oct. 1998.

[15] H. Zhao and F. H. Arnold, “Directed evolution converts subtilisin E into a functional equivalent of thermitase,” *Protein Eng.*, vol. 12, no. 1, pp. 47–53, Jan. 1999.

[16] U. Alcolombri, M. Elias, and D. S. Tawfik, “Directed Evolution of Sulfotransferases and Paraoxonases by Ancestral Libraries,” *J. Mol. Biol.*, vol. 411, no. 4, pp. 837–853, Aug. 2011.

[17] H. Flores and A. D. Ellington, “A modified consensus approach to mutagenesis inverts the cofactor specificity of Bacillus stearothermophilus lactate dehydrogenase,” *Protein Eng. Des. Sel.*, vol. 18, no. 8, pp. 369–377, Aug. 2005.

[18] S. Akanuma, Y. Nakajima, S. Yokobori, M. Kimura, N. Nemoto, T. Mase, K. Miyazono, M. Tanokura, and A. Yamagishi, “Experimental evidence for the thermophilicity of ancestral life,” *Proc. Natl. Acad. Sci.*, vol. 110, no. 27, pp. 11067–11072, Jul. 2013.

[19] H. Iwabata, K. Watanabe, T. Ohkuri, S. Yokobori, and A. Yamagishi, “Thermostability of ancestral mutants of Caldococcus noboribetus isocitrate dehydrogenase.,” *FEMS Microbiol. Lett.*, vol. 243, no. 2, pp. 393–398, Feb. 2005.

[20] K. Watanabe, T. Ohkuri, S. Yokobori, and A. Yamagishi, “Designing thermostable proteins: ancestral mutants of 3-isopropylmalate dehydrogenase designed by using a phylogenetic tree.,” *J. Mol. Biol.*, vol. 355, no. 4, pp. 664–674, Jan. 2006.

[21] K. Watanabe and A. Yamagishi, “The effects of multiple ancestral residues on the Thermus thermophilus 3-isopropylmalate dehydrogenase.,” *FEBS Lett.*, vol. 580, no. 16, pp. 3867–3871, Jul. 2006.

[22] H. Shimizu, S. Yokobori, T. Ohkuri, T. Yokogawa, K. Nishikawa, and A. Yamagishi, “Extremely thermophilic translation system in the common ancestor commonote: ancestral mutants of Glycyl-tRNA synthetase from the extreme thermophile Thermus thermophilus.,” *J. Mol. Biol.*, vol. 369, no. 4, pp. 1060–1069, Jun. 2007.

[23] K. Yamashiro, S. Yokobori, S. Koikeda, and A. Yamagishi, “Improvement of Bacillus circulans beta-amylase activity attained using the ancestral mutation method.,” *Protein Eng. Des. Sel.*, vol. 23, no. 7, pp. 519–528, Jul. 2010.

[24] S. Akanuma, S. Iwami, T. Yokoi, N. Nakamura, H. Watanabe, S. Yokobori, and A. Yamagishi, “Phylogeny-based design of a B-subunit of DNA gyrase and its ATPase domain using a small set of homologous amino acid sequences.,” *J. Mol. Biol.*, vol. 412, no. 2, pp. 212–225, Sep. 2011.

[25] T. K. Kirk and R. L. Farrell, “Enzymatic ‘Combustion’: The Microbial Degradation of Lignin,” *Annu. Rev. Microbiol.*, vol. 41, no. 1, pp. 465–501, Oct. 1987.

[26] M. TIEN and T. K. KIRK, “Lignin-Degrading Enzyme from the Hymenomycete Phanerochaete chrysosporium Burds,” *Sci.* , vol. 221 , no. 4611 , pp. 661–663, Aug. 1983.

[27] Y. Miki, M. Morales, F. J. Ruiz-Dueñas, M. J. Martínez, H. Wariishi, and A. T. Martínez, “Escherichia coli expression and in vitro activation of a unique ligninolytic peroxidase that has a catalytic tyrosine residue,” *Protein Expr. Purif.*, vol. 68, no. 2, pp. 208–214, Dec. 2009.

[28] G. Ghodake, S. Kalme, J. Jadhav, and S. Govindwar, “Purification and Partial Characterization of Lignin Peroxidase from Acinetobacter calcoaceticus NCIM 2890 and Its Application in Decolorization of Textile Dyes,” *Appl. Biochem. Biotechnol.*, vol. 152, no. 1, pp. 6–14, 2009.

[29] P. J. Harvey, H. E. Schoemaker, and J. M. Palmer, “Veratryl alcohol as a mediator and the role of radical cations in lignin biodegradation by Phanerochaete chrysosporium,” *FEBS Lett.*, vol. 195, no. 1–2, pp. 242–246, Jan. 1986.

[30] T. Johjima, N. Itoh, M. Kabuto, F. Tokimura, T. Nakagawa, H. Wariishi, and H. Tanaka, “Direct interaction of lignin and lignin peroxidase from Phanerochaete chrysosporium,” *Proc. Natl. Acad. Sci.* , vol. 96 , no. 5 , pp. 1989–1994, Mar. 1999.

[31] M. Chen, G. Zeng, Z. Tan, M. Jiang, H. Li, L. Liu, Y. Zhu, Z. Yu, Z. Wei, Y. Liu, and G. Xie, “Understanding Lignin-Degrading Reactions of Ligninolytic Enzymes: Binding Affinity and Interactional Profile,” *PLoS One*, vol. 6, no. 9, p. e25647, Sep. 2011.

[32] W. A. Doyle and A. T. Smith, “Expression of lignin peroxidase H8 in Escherichia coli: folding and activation of the recombinant enzyme with Ca2+ and haem,” *Biochem. J.*, vol. 19, pp. 15–19, 1996.

[33] T. M. Johnson and J. K.-K. Li, “Heterologous expression and characterization of an active lignin peroxidase from Phanerochaete chrysosporium using recombinant baculovirus,” *Arch. Biochem. Biophys.*, vol. 291, no. 2, pp. 371–378, Dec. 1991.

[34] W. Blodig, A. T. Smith, K. Winterhalter, and K. Piontek, “Evidence from Spin-Trapping for a Transient Radical on Tryptophan Residue 171 of Lignin Peroxidase,” *Arch. Biochem. Biophys.*, vol. 370, no. 1, pp. 86–92, Oct. 1999.

[35] T. Choinowski, W. Blodig, K. H. Winterhalter, and K. Piontek, “The crystal structure of lignin peroxidase at 1.70 Å resolution reveals a hydroxy group on the Cβ of tryptophan 171: A novel radical site formed during the redox cycle,” *J. Mol. Biol.*, vol. 286, no. 3, pp. 809–827, Feb. 1999.

[36] I. C. Kuan, K. A. Johnson, and M. Tien, “Kinetic analysis of manganese peroxidase. The reaction with manganese complexes.,” *J. Biol. Chem.*, vol. 268, no. 27, pp. 20064–20070, Sep. 1993.

[37] R. E. Whitwam, I. G. Gazarian, and M. Tien, “Expression of Fungal Mn Peroxidase in E. Coli and Refolding to Yield Active Enzyme,” *Biochem. Biophys. Res. Commun.*, vol. 216, no. 3, pp. 1013–1017, Nov. 1995.

[38] R. Whitwam and M. Tien, “Heterologous Expression and Reconstitution of Fungal Mn Peroxidase,” *Arch. Biochem. Biophys.*, vol. 333, no. 2, pp. 439–446, Sep. 1996.

[39] H. L. Youngs, M. D. Sollewijn Gelpke, D. Li, M. Sundaramoorthy, and M. H. Gold, “The Role of Glu39 in Mn II Binding and Oxidation by Manganese Peroxidase from Phanerochaete chrysosporium,” *Biochemistry*, vol. 40, no. 7, pp. 2243–2250, Jan. 2001.

[40] M. D. Sollewijn Gelpke, P. Moënne-Loccoz, and M. H. Gold, “Arginine 177 is involved in Mn(II) binding by manganese peroxidase.,” *Biochemistry*, vol. 38, no. 35, pp. 11482–9, Aug. 1999.

[41] M. Sundaramoorthy, K. Kishi, M. H. Gold, and T. L. Poulos, “Preliminary Crystallographic Analysis of Manganese Peroxidase from Phanerochaete chrysosporium,” *J. Mol. Biol.*, vol. 238, no. 5, pp. 845–848, May 1994.

[42] G. Nie, N. S. Reading, and S. D. Aust, “Relative Stability of Recombinant Versus Native Peroxidases fromPhanerochaete chrysosporium,” *Arch. Biochem. Biophys.*, vol. 365, no. 2, pp. 328–334, May 1999.

[43] S. Camarero, S. Sarkar, F. J. Ruiz-Dueñas, M. J. Martínez, and A. T. Martínez, “Description of a versatile peroxidase involved in the natural degradation of lignin that has both manganese peroxidase and lignin peroxidase substrate interaction sites.,” *J. Biol. Chem.*, vol. 274, no. 15, pp. 10324–10330, Apr. 1999.

[44] M. Pérez-Boada, F. J. Ruiz-Dueñas, R. Pogni, R. Basosi, T. Choinowski, M. J. Martínez, K. Piontek, and A. T. Martínez, “Versatile Peroxidase Oxidation of High Redox Potential Aromatic Compounds: Site-directed Mutagenesis, Spectroscopic and Crystallographic Investigation of Three Long-range Electron Transfer Pathways,” *J. Mol. Biol.*, vol. 354, no. 2, pp. 385–402, Nov. 2005.

[45] G. R. J. Sutherland and S. D. Aust, “The Effects of Calcium on the Thermal Stability and Activity of Manganese Peroxidase,” *Arch. Biochem. Biophys.*, vol. 332, no. 1, pp. 128–134, Aug. 1996.

[46] N. S. Reading and S. D. Aust, “Engineering a Disulfide Bond in Recombinant Manganese Peroxidase Results in Increased Thermostability,” *Biotechnol. Prog.*, vol. 16, no. 3, pp. 326–333, 2000.

[47] C. Miyazaki and H. Takahashi, “Engineering of the H2O2-binding pocket region of a recombinant manganese peroxidase to be resistant to H2O2.,” *FEBS Lett.*, vol. 509, no. 1, pp. 111–114, Nov. 2001.

[48] C. Miyazaki-Imamura, K. Oohira, R. Kitagawa, H. Nakano, T. Yamane, and H. Takahashi, “Improvement of H2O2 stability of manganese peroxidase by combinatorial mutagenesis and high-throughput screening using in vitro expression with protein disulfide isomerase,” *Protein Eng. Des. Sel.*, vol. 16, no. 6, pp. 423–428, Jun. 2003.

[49] S. L. Timofeevski, G. Nie, N. S. Reading, and S. D. Aust, “Substrate Specificity of Lignin Peroxidase and a S168W Variant of Manganese Peroxidase,” *Arch. Biochem. Biophys.*, vol. 373, no. 1, pp. 147–153, Jan. 2000.

[50] T. Mester and M. Tien, “Engineering of a manganese-binding site in lignin peroxidase isozyme H8 from Phanerochaete chrysosporium.,” *Biochem. Biophys. Res. Commun.*, vol. 284, no. 3, pp. 723–728, Jun. 2001.

[51] L. Gu, C. Lajoie, and C. Kelly, “Expression of a Phanerochaete chrysosporium manganese peroxidase gene in the yeast Pichia pastoris.,” *Biotechnol. Prog.*, vol. 19, no. 5, pp. 1403–9, 2003.

[52] E. Garcia-Ruiz, D. Gonzalez-Perez, F. J. Ruiz-Dueñas, A. T. Martínez, and M. Alcalde, “Directed evolution of a temperature-, peroxide- and alkaline pH-tolerant versatile peroxidase.,” *Biochem. J.*, vol. 441, no. 1, pp. 487–98, Jan. 2012.

Chapter 2. Ancestral mutants of lignin peroxidase

1. Summary

Stabilizing enzymes from mesophiles of industrial interest is one of the greatest challenges of protein engineering. The ancestral mutation method, which introduces inferred ancestral residues into a target enzyme, has previously been developed and used to improve the thermostability of thermophilic enzymes. In this report, we studied the ancestral mutation method to improve the chemical and thermal stabilities of *Phanerochaete chrysosporium* lignin peroxidase, a mesophilic fungal enzyme. A fungal ancestral lignin peroxidase sequence was inferred using a phylogenetic tree comprising Basidiomycota and Ascomycota fungal peroxidase sequences. Eleven mutant enzymes containing ancestral residues were designed, heterologous expressed in *Escherichia coli* and purified. Several of these ancestral mutants showed higher thermal stabilities and increased specific activities and/or k_{cat}/K_M than those of wild-type lignin peroxidase.

2. Purpose

In this study, we applied ancestral mutation to stabilized the recombinant LiP from Basidiomycota, *Phanerochaete chrysosporium* strain UMHA 3641. A composite phylogenetic tree without any thermophilic organisms was constructed and used to infer the ancestral amino acids. The ancestral mutation form of LiP were then characterized and compared with wild-type recombinant LiP.

3. Material

Veratryl alcohol (VA; 2, 6-dimethoxybenzyl alcohol), oxidized glutathione and hemin chloride were purchased from Sigma-Aldrich (St Louis, MO, USA). Other chemicals were obtained from Wako Chemicals (Tokyo, Japan) and were all of analytical grade.

4. Method

4.1. Phylogenetic analysis

The amino acid sequences of ligninolytic peroxidase, including LiP (30 sequences), MnP (45 sequences) and VP (7 sequences) from Basidiomycota and LiP (3 sequences) from Ascomycota, were retrieved by a BLASTP search using wild-type lignin peroxidase of *P. chrysosporium* strain UAMH 3641 as the query sequence. LiP sequence from *P. chrysosporium* was provided By Professor Sonoki (Azabu University). The sequences were aligned using the program CLUSTAL X 2.0 [1] with its default parameters and then manually adjusted. A composite LiP/MnP/VP phylogenetic tree was constructed using the Neighbor-Joining method with the program found in the CLUSTAL X 2.0 package [1]. Well-aligned regions (198 amino acid residues) were selected using the program GBLOCKS 0.91 [2]. Forty-nine sequences of LiP (16 sequences), MnP (27 sequences) and VP (4 sequences) from Basidiomycota, and LiP (2 sequences) from Ascomycota representing main branches of the tree were selected for further analysis (Table 2-7). Composite LiP/MnP/VP phylogenetic trees were then inferred by maximum likelihood (ML) method using the program Treefinder (October 2008) [3] and the program PhyML 2.4.4. [4]. The four-category model of discrete Gamma distribution model, which allows different substitution rates among sites, was employed. The WAG substitution model [5] was used as the substitution matrix for amino acids. Because the statistical support of some branch points were not significant, a “semi-exhaustive” search of a ML tree was then performed. We firstly assumed fixed branching orders for several groups in which the statistical support were considered high. We then listed all possible tree topologies with the program Molphy [6] using the same set of conditions. The top 1000 tree topologies of each analyses estimated by Molphy (JTT model) were used for the ML analysis with TREE-PUZZLE 5.2 program (WAG+G model) [7].

Because the results obtained with Treefinder and PhyML were slightly different, tree topologies with the top 50 likelihood in the Treefinder and PhyML analyses were used for further investigation. The likelihood of 100 tree topologies was assessed using CODEML program of the PAML3.14 package [8]. The best ML tree was selected and then ancestral amino acids were inferred using the same conditions.

4.2. Gene construction

The LiP cDNA from *Phanerochaete chrysosporium* strain UAMH 3641 cloned into pPDB-GB (pPDB-LiP) was generously provided by Prof. S. Sonoki (Department of Environmental Science, Azabu University, Japan). The LiP gene (lacking the N-terminal signal sequence) was amplified by the polymerase chain reaction (PCR). The PCR was performed using pPDB-LiP plasmid as template and the following pair of oligonucleotide primers: pLiPf (5'-GGAGATATACATATGGCCACCTGTTCCAACGGCAA-3') and pLiPr (5'-GTGCGGCCGCAAGCTTAAGCACCCGGAGGCGGAGGG-3'). *Ex Taq* DNA polymerase (Takara Bio, Ōtsu, Japan) was used for the PCR. Gene amplification involved an initial denaturation step of 94 ˚C for 3 min, followed by 25 cycles of denaturation, annealing and extension (94 ˚C for 30 sec, 55 ˚C for 1 min, and 72 ˚C for 2 min), then 72 ˚C for 7 min. The amplified wild-type LiP gene was digested with *Nde*I and *Hin*dIII and ligated into pET21a (+). The resulting plasmid was named pET-LiP.

The inferred ancestral amino acid residues were introduced into the expression plasmid pET-LiP by using a QuikChange Lightning Site-Directed Mutagenesis Kit (Stratagene, La Jolla, CA). The primer sequences are listed in Table 2-6. Clones harboring mutations were selected in *E. coli* XL10-GOLD. The sequence of each mutant was determined with an Applied Biosystems ABI PRISM 3130x sequencer (Applied Biosystems, Foster City, CA) and the clones were used for gene expression in *E. coli* BL21 (DE3).

4.3. Expression and purification

Wild-type LiP protein and its ancestral mutants were produced in *E. coli* BL21 (DE3). Cells harboring the respective plasmid were cultured in Terrific Broth medium (12 g polypepton, 24 g yeast extract, 4 mL glycerol, 2.31 g KH_2PO_4, 12.5 g K_2HPO_4 in 1 L) supplemented with ampicilin (0.1 mg/mL) at 37 ˚C. When the optical density ($OD_{600\ nm}$) of the culture reached 0.6-0.8 heterologous expression was induced by addition of isopropyl-β-D-thiogalactopyranoside (IPTG) to a final concentration of 0.5 mM, and the culture was then incubated for a further 4 hr at 37 ˚C. Cells were harvested and disrupted by sonication in ice cold resuspension buffer containing 10 mM Tris-HCl (pH 8.0), 1 mM ethylenediaminetetraacetic acid (EDTA), 5 mM dithiothreitol (DTT), 50 μM phenylmethylsulfonyl fluoride and 1 % (v/v) Triton X-100. The recombinant LiPs were

accumulated as inclusion bodies. Insoluble fractions were harvested and washed three times with buffer A (10 mM Tris-HCl (pH 8.0), 1 mM EDTA, 2 mM DTT and 1 % (v/v) Triton X-100). The pellets were resuspended in buffer A containing 8 M urea and incubated at room temperature for 1 hr. The denaturated-reduced protein was diluted to 2 M urea in refolding solution: 10 mM $CaCl_2$, 0.7 mM oxidized glutathione, 30 μM hemin chloride (1 mM stock solution in 0.1 N NaOH) in 50 mM Tris-HCl (pH 8.0). The refolding mixture was incubated at room temperature for 12-14 hr with continuous stirring in the dark.

The mixture was dialyzed against 10 mM sodium acetate buffer (pH 6.0), 5 mM $CaCl_2$ at 4 ˚C for 12-14 hr with five changes of buffer. The sample was then recovered and centrifuged at 60,000*g* for 20 min and the supernatant concentrated using an amicon YM-10 unit (Merck, Darmstadt, Germany).

To purify each sample, supernatant was applied onto a DEAE Sepharose Fast Flow anion-exchange column (GE Healthcare Bioscience, Piscataway, NJ) and after washing the column with the same buffer, bound proteins were eluted with 0.6 M NaCl in 10 mM sodium acetate buffer (pH 6.0) supplemented with 1 mM $CaCl_2$. The appropriate fractions were pooled, diluted with 10 mM sodium acetate buffer (pH 6.0) supplemented with 1 mM $CaCl_2$, applied onto a HiTrapQ column (GE Healthcare Bioscience) and eluted with a 0.01-0.6 M NaCl gradient in 10 mM sodium acetate buffer (pH 6.0) supplemented with 1 mM $CaCl_2$. Fractions with the highest activity were pooled and used for the following experiments.

4.4. Enzyme assay

Enzyme concentrations were determined by the alkaline-pyridine hemochrome method using an extinction coefficient of 34.4 mM^{-1} cm^{-1} at 557 nm for heme *b* [9]. Enzymatic activities were determined by monitoring the oxidation of veratryl alcohol (VA) to veratryl aldehyde. The absorbance change at 310 nm was recorded with a DU7400 spectrometer (Beckman, Fullerton, CA). The assay buffer was 50 mM tartrate (pH 2.5), 2 mM VA and 0.5 mM H_2O_2. Reaction was initiated by adding 0.5 mM H_2O_2. An extinction coefficient of 9300 M^{-1} cm^{-1} at 310 nm was used for the veratryl aldehyde [10]. One enzyme unit was defined as 1 μmol veratryl aldehyde formed per minute.

The pH dependence of specific activities was measured in 50 mM tartrate buffer (pH 2.0-4.5) and in 50 mM acetate buffer (pH 4.0-5.5) at 25 ˚C. The temperature dependence of LiP activities was measured at 25, 30, 40, 50 and 55 ˚C.

The values of the Michaelis constant (K_M) for the substrate VA and the catalytic constant (k_{cat}), were determined from steady-state kinetic analysis in the assay buffer with VA concentrations between 50 μM and 5000 μM. To determine the K_M value for H_2O_2, the concentration was varied between 10 and 500 μM, while the VA concentration was fixed at 2 mM. The kinetic constants were obtained by nonlinear least-square fitting of the steady-state

velocity data to the Michaelis-Menten equation using the Enzyme Kinetics module of SigmaPlot (Systat Software, San Jose, CA).

Thermal inactivation of LiP was studied by incubating LiP in 50 mM tartrate (pH 2.5) at 37 ˚C. Further experiments were carried out according to the previously described method where LiP was incubated in 20 mM Tris-SO_4 (pH 7.9) at 51 ˚C [11].
Inactivation of LiP in the presence of H_2O_2 was studied by incubating LiP in 50 mM tartrate buffer (pH 2.5) supplemented with 0.2 mM H_2O_2 at 25 ˚C.

4.5. Thermal melting profile

Structural stability was estimated by measuring circular dichroism at 222 nm using a J-720 spectropolarimeter (JASCO, Tokyo, Japan). The enzyme concentration was 0.4 mg/mL in 20 mM potassium phosphate buffer, pH 7.0, and the temperature was increased at 1 ^{o}C per minute.

5. Result

5.1. Inference of ancestral amino acids of fungal peroxidase

Eighty-five amino acid sequences related to wild-type LiP sequences were obtained from the NCBI database and aligned (Supplementary figure 2-1). Well-aligned regions were selected by GBLOCKS. A neighbor-joining (NJ) tree was then constructed using these 85 sequences. On the basis of the NJ tree topology, 49 representative sequences, 16 LiP (including wild-type LiP), 27 MnP and 4 VP from Basidiomycota and 2 Ascomycota LiP, were selected for further phylogenetic analyses. ML trees were constructed using Treefinder and PhyML. The tree topologies were assessed by CODEML. Figure 2-1 shows the best likelihood composite phylogenetic tree of the selected fungal ligninolytic peroxidase, constructed from 198 well-aligned sites of the 49 fungal peroxidase sequences. The sources and accession numbers of the proteins are listed in (Table 2-7). In Figure 2-1, marked branches indicate the selected ancestral positions: node63 is the branching point of Basidiomycota and Ascomycota, node60 and node62 are the two ancestors of LiP and MnP.

Ancestral residues of these nodes were inferred by the ML using the tree as the effort tree. Figure 2-2 shows the sequences of inferred ancestral residues. We then compared the sequences of wild-type LiP with the ancestral sequences (Figure 2-2). Eleven selected regions where the wild-type LiP residues differed from residues of the ancestral sequences were identified. When selecting the mutation sites, the tertiary structure and spatial location of these residues were not taken into consideration. Mutants m1, m2, m3, m4, m5, m6, m7, m8, m9, m10 and m11 correspond to Ala36Glu, Val45Thr, Lys92Glu/Leu93Ala, Ala110Gln, Ala116Gly/Leu117Val, His149Asp, Gly198Ser, Gln209Met, Ile235Leu, His239Phe/Thr240Leu/Ile241Leu, Phe254Met mutation(s), respectively. All mutation sites are shown in the tertiary structure (Figure 2-3). Each ancestral combination of residues was introduced into LiP by site-directed mutagenesis. All of the mutant enzymes were overexpressed in *E. coli* and then purified for characterization.

5.2. Enzyme stability

The activities of most of the ancestral mutant enzymes were similar to the wild-type enzyme. However three mutant enzymes (m1, m2 and m4) showed significantly lower activity than the wild-type enzyme at 37 °C (Figure 2-4). After incubation at 37 °C for 30 min, the wild-type enzyme retained 17 % of its initial activity, whereas the ancestral mutants, m5, m8, m10 and m11, retained 28.0, 33.5, 86.2 and 18.4 % of their initial activity, respectively (Table 2-1).

The activity of the enzymes was also measured after incubation in the presence of hydrogen peroxide. Specifically, enzymes were incubated with 0.2 mM H_2O_2 at 25 ^{o}C (Figure 2-5) and their activity was measured at set times. After 5 min incubation with 0.2 mM H_2O_2,

wild-type retained 6.5 % of its initial activity, whereas four ancestral mutants, m2, m5, m10 and m11, retained 18.4, 29.6, 10.5 and 9.3 % of their initial activity, respectively (Table 2-2). Of all the LiP mutants, the ancestral mutant m4 retained the greatest proportion of enzymatic activity in the presence of H_2O_2, although its initial activity was very low (Table 2-2).

5.3. Steady-kinetics analysis

The specific activities of six ancestral mutant enzymes (m6, m7, m8, m9, m10 and m11) were larger than that of the wild-type LiP (Table 2-3). In particular, the ancestral mutant m10 showed significantly enhanced specific activity *i.e.*, 2.3-fold greater than that of wild-type LiP.

The kinetic parameters of the LiPs were estimated using steady-state kinetics obtained at 25 ˚C (Table 2-3). The k_{cat} for VA of eight ancestral mutants (m3, m5, m6, m7, m8, m9, m10 and m11) were larger than that of wild-type LiP. Ancestral mutant m10 showed remarkably improved k_{cat} (3.4-fold higher than that of the wild-type enzyme). Eight of eleven ancestral mutants (m3, m5, m6, m7, m8, m9, m10 and m11) showed a k_{cat}/K_M ratio (specificity constant) for VA higher than that of the wild-type enzyme. The increased k_{cat}/K_M of ancestral mutants was caused by an improvement of k_{cat}. However, nine of eleven ancestral mutants (m1, m2, m3, m4, m5, m6, m8, m9 and m11) showed improved K_M values for H_2O_2. The k_{cat} for H_2O_2 of two mutants (m7 and m10) was higher than that of the wild-type enzyme. Eight of the ancestral mutants (m1, m5, m6, m7, m8, m9, m10 and m11) showed high k_{cat}/K_M for H_2O_2. The ancestral mutant, m10 showed improved k_{cat} for VA and H_2O_2.

5.4. pH dependence

The pH dependence of the wild-type enzyme and selected ancestral mutants, m5 and m10, showed similar tendencies: the specific activities increased as the pH decreased from pH 5.5 (Figure 2-7).

5.5. Temperature dependence

Figure 2-6 shows the temperature dependence of the enzyme activity. Wild-type LiP showed the highest activity at 30 °C. Four ancestral mutants (m6, m7, m10 and m11) exhibited greater activities than that of the wild-type enzyme. Activity of the wild-type enzyme decreased at temperatures above 30 °C. Three ancestral mutants (m8, m10 and m11) exhibited higher activity at temperatures greater than 30 °C. In particular, ancestral mutant m10 showed the highest activity at 40 °C *i.e.*, activity approximately 1.7-fold that at 25 °C (Figure 2-6).

5.6. Thermal melting profile

The thermal melting profiles of the wild-type and ancestral mutant m10 enzymes were also measured (Figure 2-8). T_m values of the wild-type enzyme and m10 were 50.1 ± 0.2 ^oC and 51.9 ± 0.7 ^oC, respectively.

6. Discussion

6.1. Phylogenetic analysis

In our analysis of the phylogenetic tree, two LiPs from Ascomycota *Pyrenophora tritici-repentis* were used as the outgroup for Basidiomycota peroxidases. LiPs formed a cluster in Basidiomycota enzymes, except for BAE46585 from *Trametes cervina*.

MnPs were clustered as two groups. The first group consists of MnPs from *P. chrysosporium* and the second group consists of MnPs from *Trametes versicolor*. Previously, Floudas *et al.,* proposed an evolutionary process for the lignin degrading peroxidases of fungi [12]. The tree topology obtained from our analysis is similar to that reported by Floudas *et al.* According to the geologic time reported by Floudas *et al.,* our node 63 and node 62 correspond to the Silurian period in the Paleozoic era (*ca.* 403 million years ago) and the Permian period in the Triassic era (*ca.* 270 million years ago), respectively.

6.2. Characteristics of the ancestral mutation sites

All improved mutants were located on a α helix region of the protein (Table 2-4). However, a few mutations were located on loop or β sheet regions of the protein, making the correlation between thermal stability and mutation site unclear. Moreover, there was no obvious relationship between protein stability and location of the mutation site in terms of distance from the active site and calcium ions. All mutation sites were separated from the heme prosthetic group, tryptophan171 and two calcium ions. In other words, the residues locating near these factors were not selected as mutation site.

FoldX was the computer algorithm to predict the effect of mutation from tertiary structure information[13]. In Table 2-4, the total energy value of most stable mutant, m10, was the most smallest. However the correlation between total energy and stability didn’t observe.

6.3. The reasons of increasing stability

Chou and Fasman reported the secondary structural prediction of proteins from their amino acid sequence[14]. According to their report, glutamate, methionine, alanine and leucine are amino acids strong α-helix former. Phenylalanine and isoleucine are α-helix former. Proline and glycine are strong α-helix breaker. The most stable ancestral mutant was m10 and its mutation was H239F/T240L/I241L and they located on the α-helix (Table 2-4). The α-helix formation can be attributed to the increased stability induced by ancestral mutation.

Accessible surface area of Phenylalanine 239, leucine 240 and leucine 241 is 24 % 38 % and 0 % respectively. This indicates that F239 and L240 located on the surface, I241

located in the interior. The crystal structure analysis of ancestral LiP wasn't done, so the 1B80 (Protein ID, [15]), the most homologous enzyme, was used to estimate the tertiary structure. The structure around I241L is shown in Figure 2-9. From the figure, the mutation I241L may have improved the packing in the hydrophobic core.

6.4. Comparing thermostability of glycosylated LiP

Figure 2-10 shows thermal inactivation time-course conditions used in a previous report *i.e.*, LiP was incubated in 20 mM Tris-SO_4 (pH 7.9) at 51 °C [11]. Under these conditions, wild-type LiP activity fell to less than 20 % of its original value after 10 min incubation, while ancestral mutants, m10 retained 65 % of their activity. Nie *et al.* reported that the thermal stability of recombinant LiP H8, which was expressed in *E. coli*, was lower than that of the corresponding native LiP H8 isolated from *P. chrysosporium*. Native glycosylated LiP H8 maintained *ca.* 50 % of its activity after incubation for 10 min at 51 °C, whereas recombinant LiP H8 was completely inactivated by this treatment. Wild-type LiP used in this study has 99.1 % sequence identity with LiP H8 isoform from *P. chrysosporium.* Recombinant LiP, m10, expressed in *E. coli* showed higher thermal stability than that of native LiP H8.

6.5. Comparison with the consensus approach

Watanabe *et al.*, classified ancestral mutants of IPMDH into two groups, dominant and minor ancestral mutants [16]. The dominant ancestral mutants have the ancestral residue, which is also a consensus residue, while the minor mutants have the ancestral residue that is not a consensus residue. In this study, there were seven dominant mutants (m1, m2, m4, m5, m6, m9 and m10) and four minor mutants (m3, m7, m8 and m11) (Table 2-5). Thermostability of two mutants (m8 and m11) in four minor mutants, were improved. Two mutants (m5 and m10) among seven dominant mutants showed higher thermal stability than the wild-type enzyme. We excluded a dominant mutant m4, which showed very low activity. Accordingly, it is not possible to judge whether the consensus residue is responsible for increased thermal stability. It is important to note that the ancestral residue was introduced into the wild-type consensus residue in three mutants (m7, m8 and m11). Two (m8 and m11) of the three mutants showed greater thermal stability over the wild-type enzyme. These results support the idea that the enhanced thermal stability is related to the ancestral residues, rather than the consensus residues.

6.6. Correlation between stability and conservation of the neighboring residues

Yamashiro *et al.*, argued that there is a correlation between thermostability and the extent to which the amino acid residues of an enzyme within 5 Å of the ancestral residue are conserved [17]. Successful mutation design can be efficiently performed using averaged

conserved value (ACV) as a design tool. Though only four mutants have an ACV higher than 0.80, two of them showed increased thermal stability in our experiments (Figure 2-12). The ACV values of the heme, distal and proximal calcium ions were high (*i.e.*, 0.61, 0.86 and 0.70, respectively), indicating that residues located near these factors are well conserved.

We have extended the method to select the mutation site from the primary amino acid sequence. We estimated the relationship between thermal stability and the conservation of the neighboring amino acids within seven residues in the primary sequence. If a wild-type residue and the ancestral residue were identical, the likelihood value was taken as the conservation value. However, if the wild-type and ancestral residue differed then the conservation value was 0. Finally, an averaged conservation value for neighboring residues on the primary amino acid sequence was calculated. This value is referred to as linear ACV. The linear ACV values were plotted against the remaining activity after incubation at 37 ^{o}C (Figure 2-11A) or in 0.2 mM H_2O_2 (Figure 2-11B). When the linear ACV value is greater than 0.9, mutants with improved thermal stability are obtained at high efficiency. Three of four mutants whose linear ACV was >0.9 showed improved thermal stability. A similar trend was observed when the window size was increased to eleven residues (Figure 2-13).

A comparable relationship between the linear ACV value and the effect of ancestral mutation was found for ancestral mutants of β-amylase (Figure 2-14) and IPMDH (Figure 2-15) reported previously. These results suggest that the mutants with higher ACV tend to show increased thermal stability. Thus, the linear ACV value can be used as an efficient method to select residues for mutation that will improve the thermal stability of the protein.

7. Conclusion

In this study, we introduced ancestral mutations into wild-type LiP from P. chrysosporium to improve its thermal stability. The recombinant ancestral mutant, m10 (H239F/T240L/I241L), showed improved thermal stability comparable to that of the glycosylated wild-type enzyme. Specific activity and k_{cat}/K_M of one of the ancestral mutants, m10, was improved by amino acid substitution. This is the first investigation to successfully improve enzyme stability by indentifying ancestral residues based on the dataset constructed from eukaryotic sequences. The linear ACV value can be used to select ancestral residues to efficiently enhance the thermal stability of enzymes.

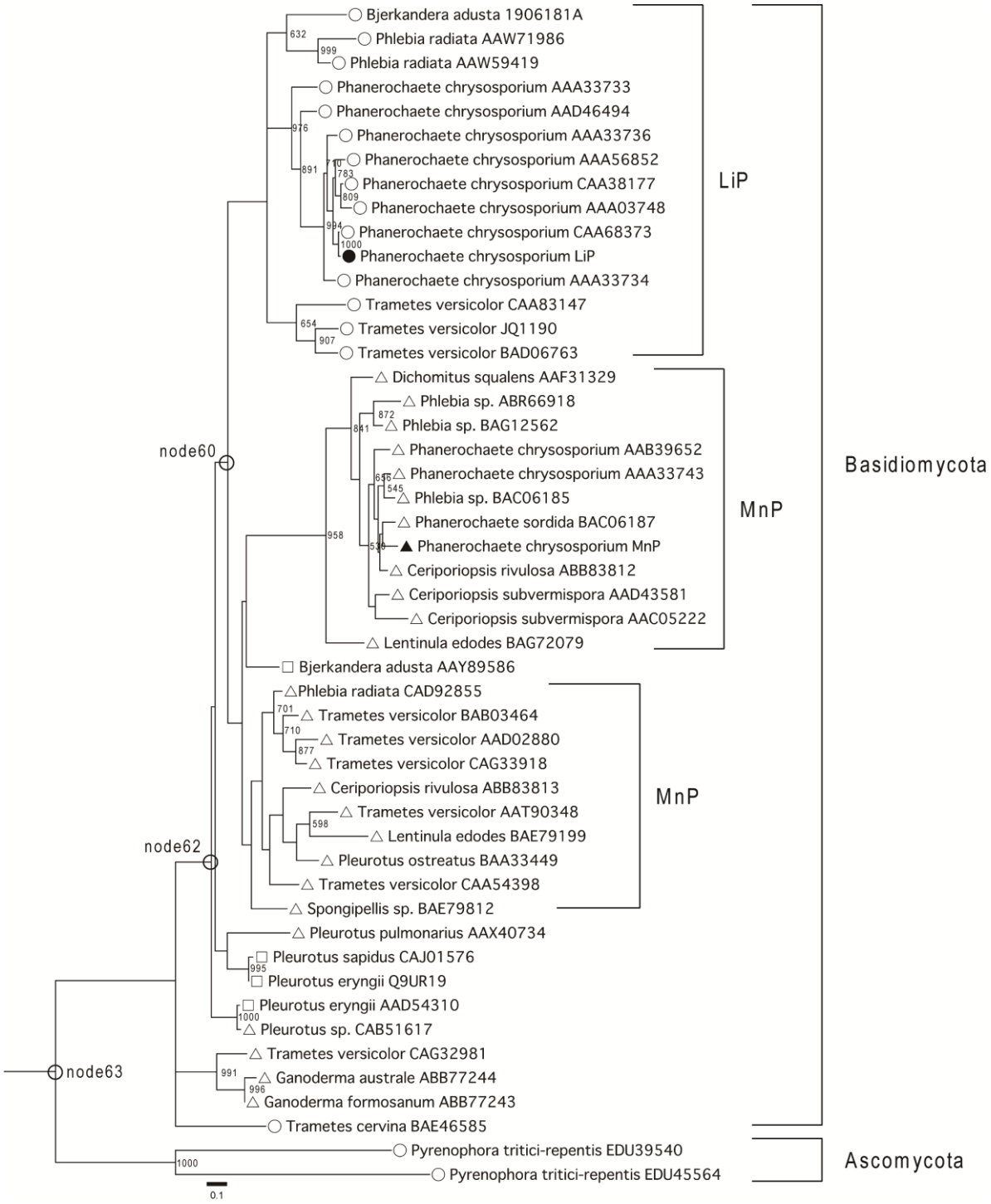

Figure 2-1. Phylogenetic tree

A composite phylogenetic tree of LiP, MnP and VP. The tree includes the selected species from Basidomycota and Ascomycota. Open circles, open triangles and open squares indicates LiPs, MnPs and VPs from Basidomycota, respectively. The filled circle and triangle represent LiP and MnP from *Phanerochaete chrysosporium* strain UMHA 3641, respectively. The phylogenetic tree was generated by the ML method as described in the Method section. The standard bar indicates 0.1 substitutions per site. The values indicate bootstrap confidence (1000 replicates).

Figure 2-2. Ancestral sequences

Multiple alignment of wild-type LiP with inferred ancestral amino acid sequences. Based on the phylogenetic tree in Figure2-1, ancestral amino acid residues at the node are identified by the ML method. The seven selected parts (34-53, 82-97, 102-124, 128-161, 164-210, 231-279 and 306-314 of wild-type LiP numbering) are shown. Mutation sites are indicates by boxes.

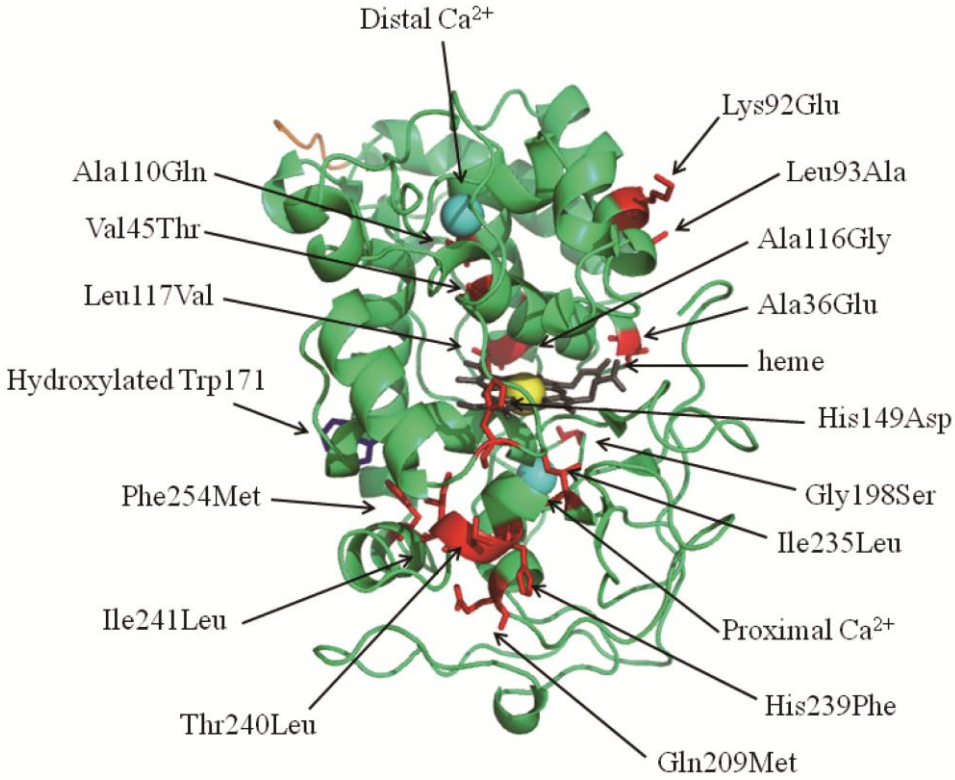

Figure 2-3. The three-dimensional structure of LiP and ancestral mutation points

The three-dimensional structure of recombinant P. chrysosporium LiP H8 (PDB accession number: 1B80 [18]). This figure was drawn using PyMOL (http://www.pymol.org/). Polypeptide chain, heme and heme iron atom are shown as solid light green ribbon, gray stick and yellow sphere, respectively. The distal and proximal Ca^{2+} ions are depicted as cyan spheres. The orange colored N-terminal region is shown with an extra five residues from the pro-sequence in this crystal structure. The β-hydroxylated Trp171, implicated to be involved in VA oxidations, is shown as a blue stick. The residues substituted with ancestral residues in this work are highlighted in red.

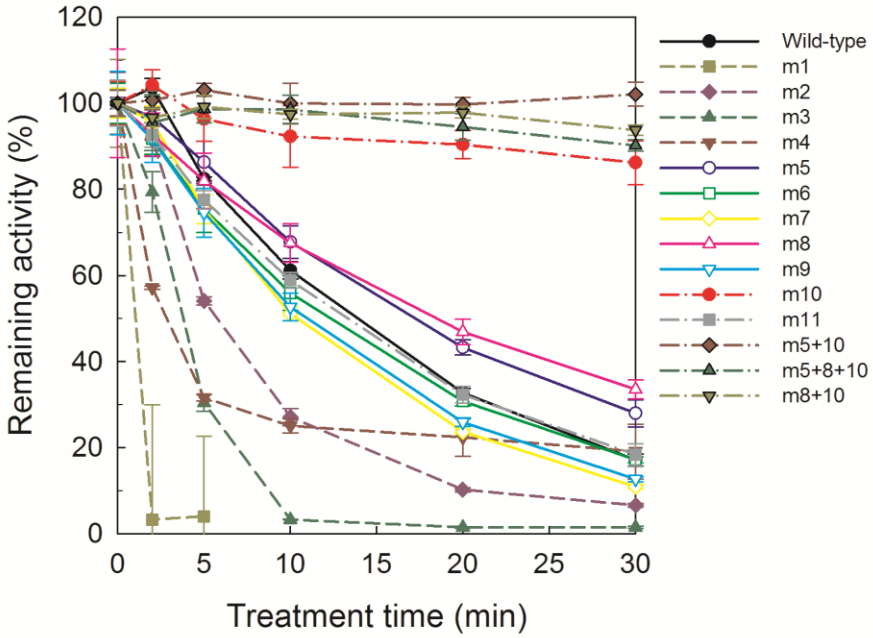

Figure 2-4. Time course of thermal inactivation of wild-type LiP and ancestral mutants

Incubation of the enzymes was carried out in 50 mM tartrate buffer (pH 2.5) containing 2 μM of each enzyme at 37 ^{o}C. The remaining enzyme activities were measured in 50 mM tartrate buffer (pH 2.5), 2 mM VA, 0.5 mM H_2O_2 and 0.2 μM enzyme. Reactions were initiated by the addition of H_2O_2.

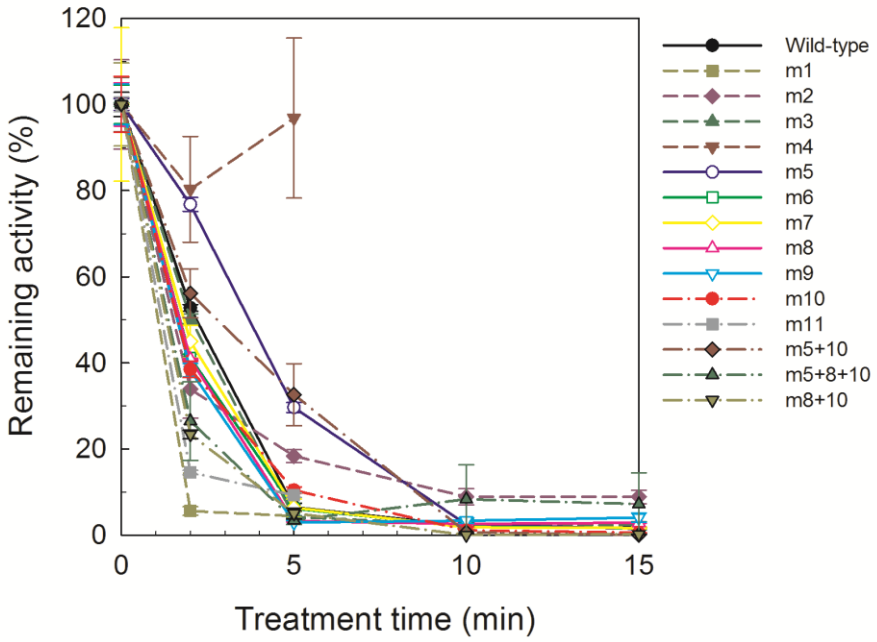

Figure 2-5. Residual activity of the wild-type enzyme and ancestral mutants after incubation in the presence of H_2O_2.

The incubation was carried out at 25 ^{o}C in 50 mM tartrate buffer (pH 2.5) containing 2 μM enzyme supplemented with 0.2 mM H_2O_2. The remaining enzyme activities were measured in 50 mM tartrate buffer (pH 2.5), 2 mM VA, 0.5 mM H_2O_2 and 0.2 μM enzyme. Reactions were initiated by addition of H_2O_2.

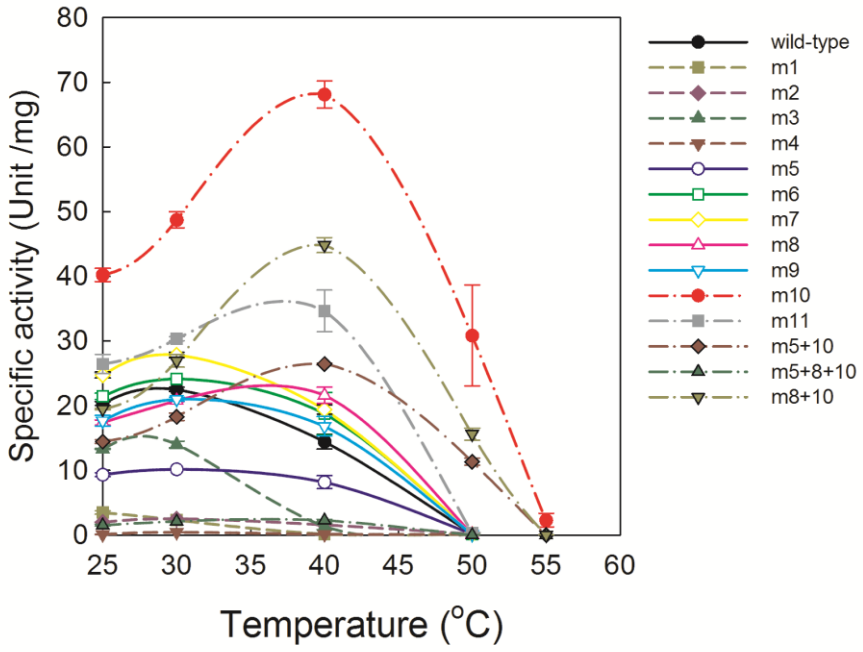

Figure 2-6. Temperature dependence of VA oxidation by wild-type LiP and ancestral mutants.

Reaction mixture contained 2 mM VA, 0.5 mM H_2O_2 and 0.2 μM of each enzyme in 50 mM tartrate buffer, pH 2.5. Reactions were initiated by the addition of H_2O_2.

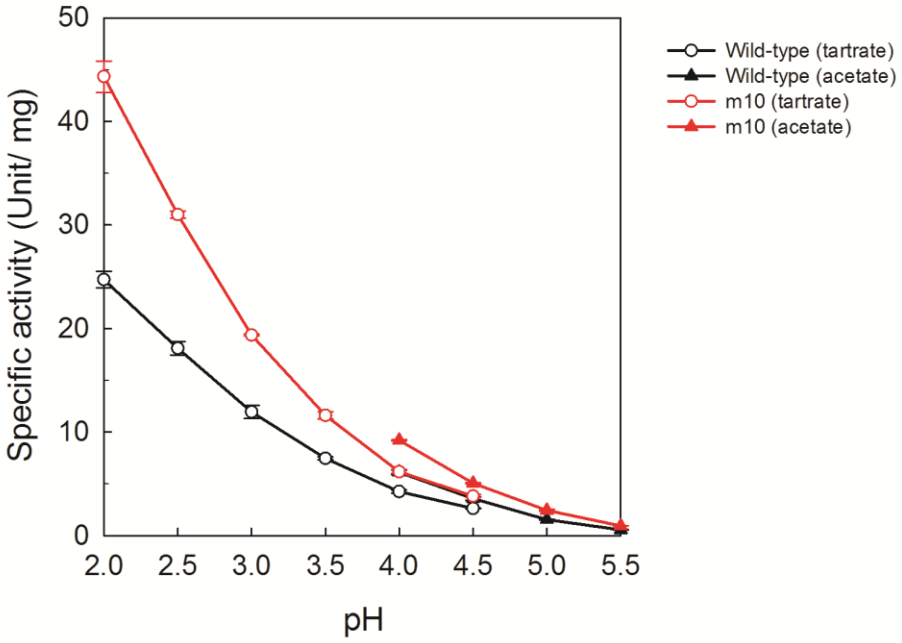

Figure 2-7. pH dependence of VA oxidation of wild-type and ancestral mutants of LiP.

Reaction mixture contains 2 mM VA and 0.5 mM H_2O_2 in 50 mM tartrate buffer, pH 2.0-4.5 (open circles) and 50 mM acetate buffer, pH 4.0-5.5 (closed triangles). Reactions were initiated by the addition of H_2O_2.

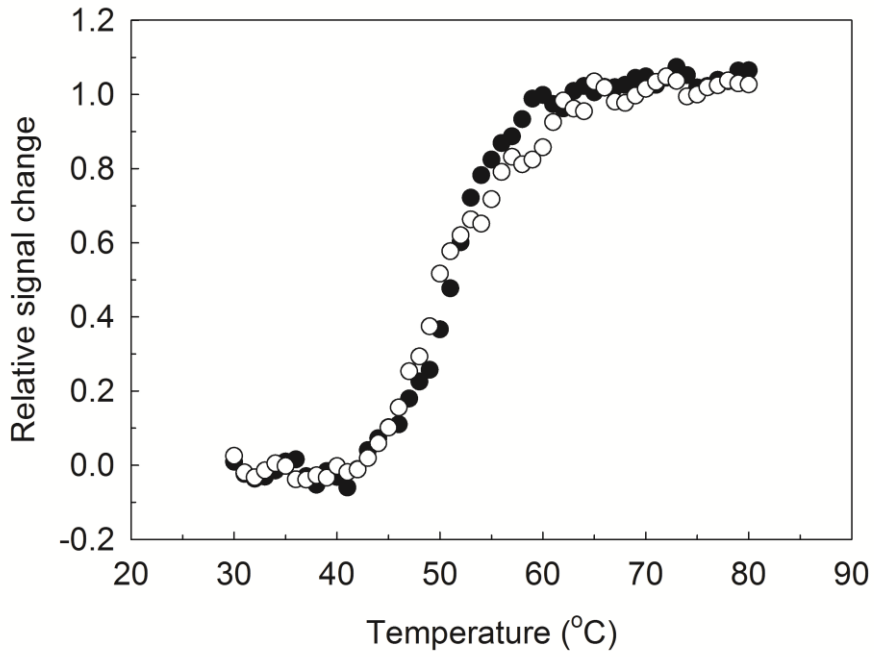

Figure 2-8. Thermal melting profile

Closed and open circle show m10 and wild-type LiP, respectively. Enzyme concentration was 0.4 mg/mL in 20 mM potassium phosphate buffer (pH 7.0). The temperature was increased 1 oC per minute. A J-720 spectropolarimeter (JASCO) was used to collect the data.

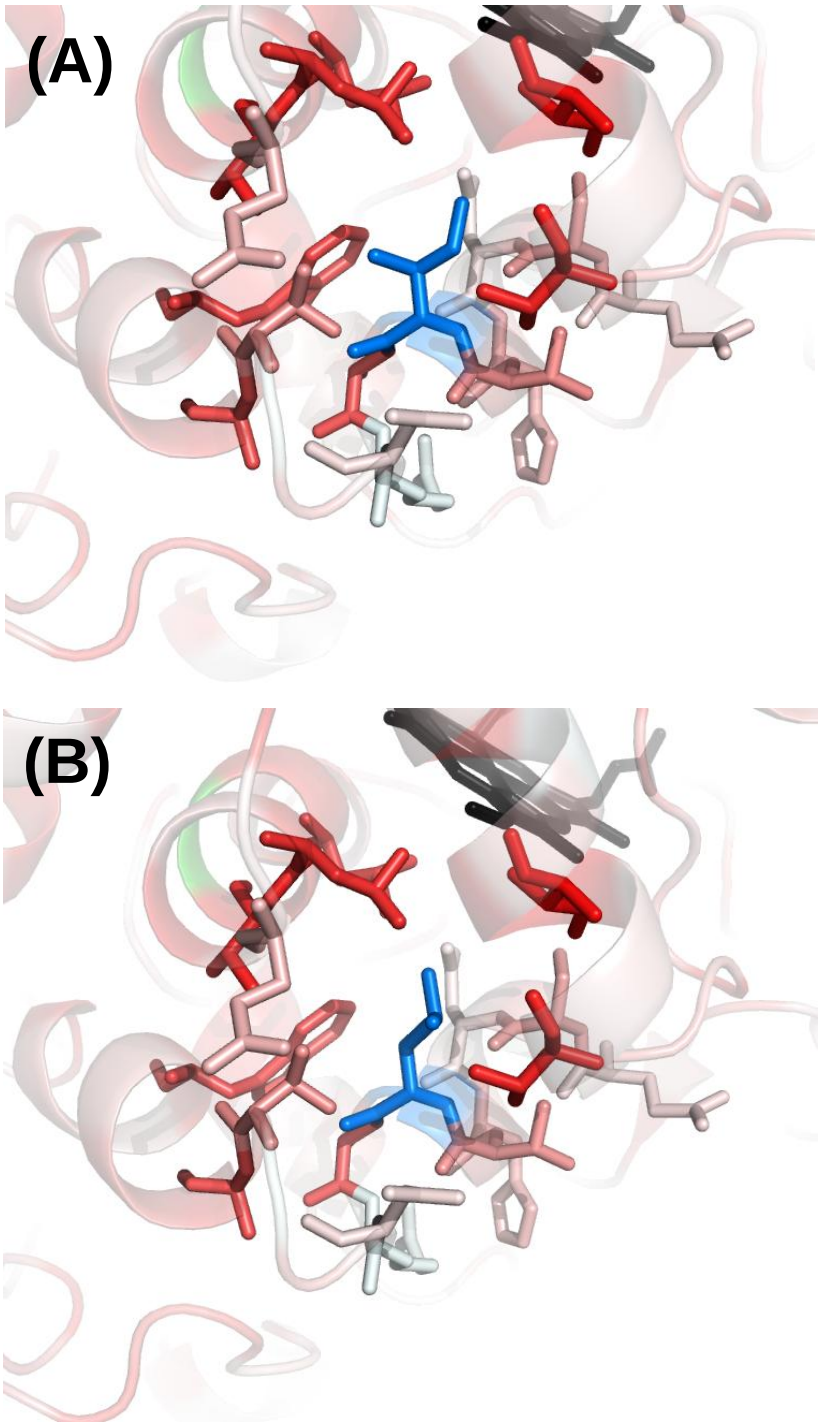

Figure 2-9. Mutation site of I241L

Dark red indicates higher hydrophobic residues, sickly red indicates hydrophobic amino acid residues. Blue stick indicates I241 or L241. Black stick is heme. (A) wild-type (I241) and (B) m10 (L241).

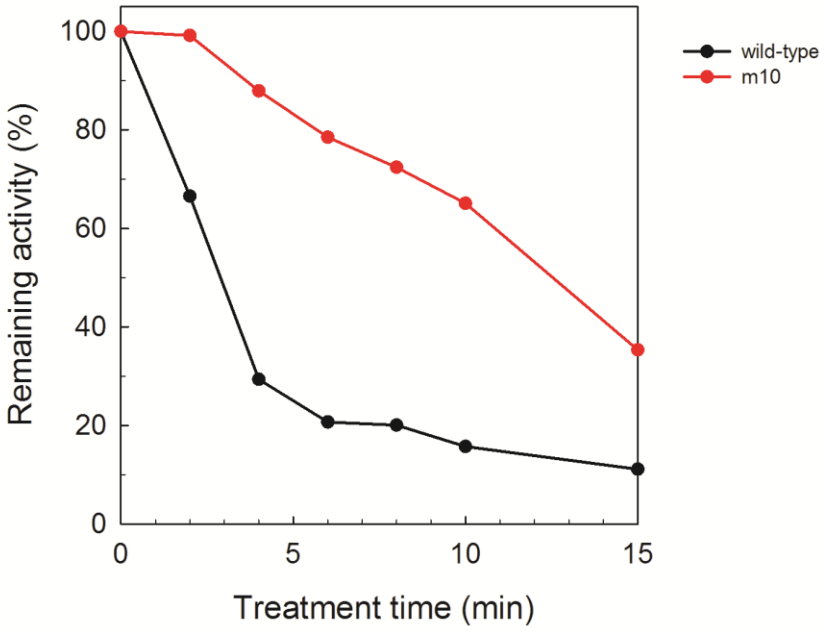

Figure 2-10. Time course of thermal inactivation of wild-type LiP and ancestral mutants, m10.

Enzymes were incubated at 51 ^{o}C in 20 mM Tris-SO4 buffer (pH 7.9). The remaining activities were measured in 50 mM acetate buffer (pH 4.5), 2 mM VA, 0.1 mM H_2O_2 and 0.2 μM enzyme. Reactions were initiated by the addition of H_2O_2.

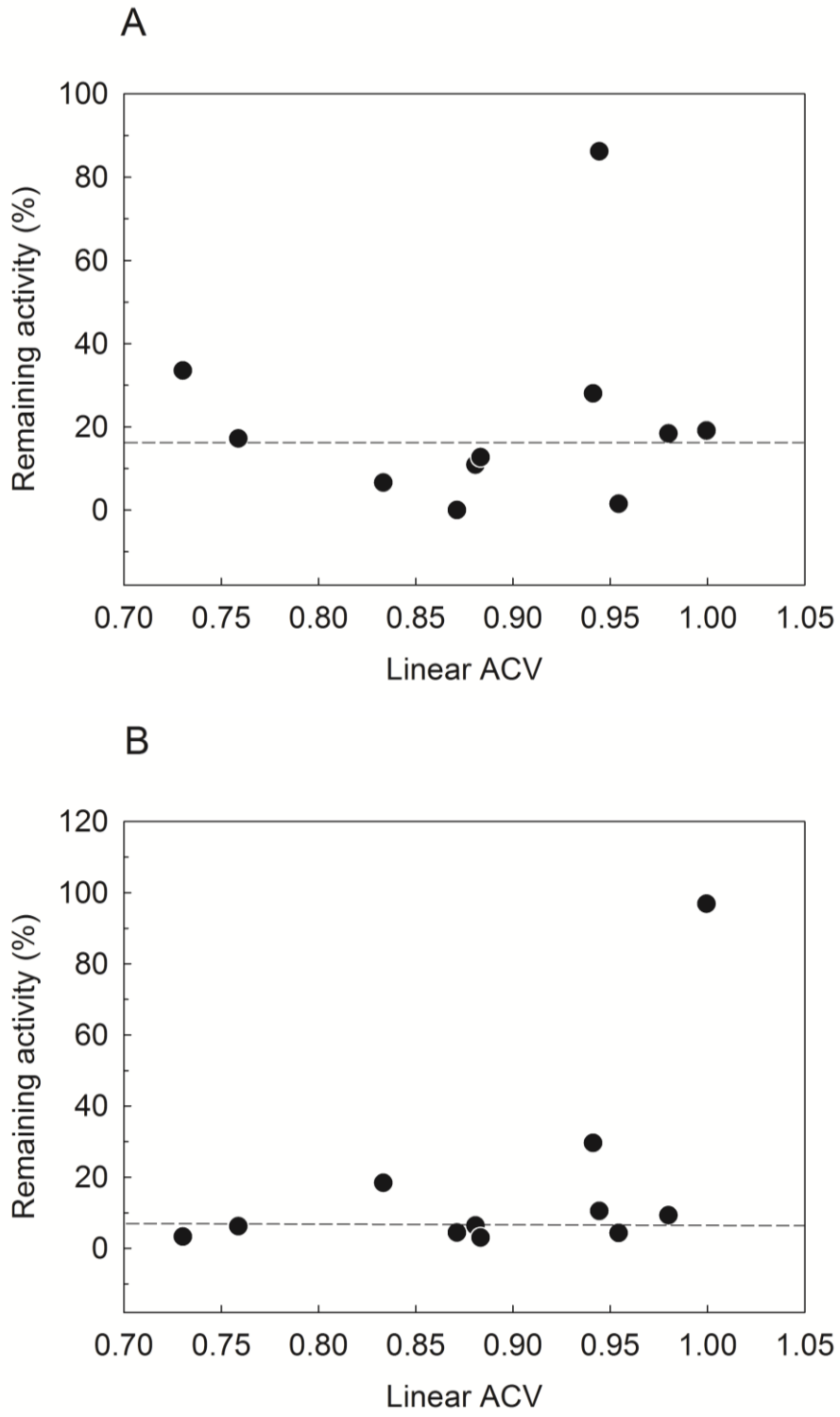

Figure 2-11. Correlation between thermostability and linear ACV.

The linear ACV values were plotted against remaining activity after treatment at 37 ^{o}C (Panel A). The linear ACV values were plotted against remaining activity after incubation with 0.2 mM H_2O_2 (Panel B). Dashed line indicates the remaining activity of the wild-type enzyme.

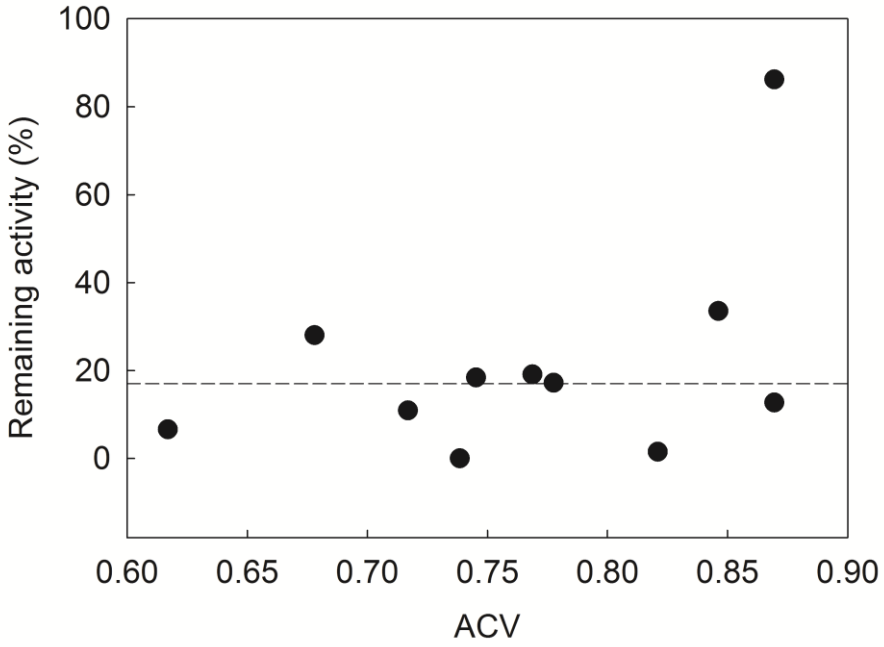

Figure 2-12. Correlation between thermostability and the ACV.

ACV values were plotted against remaining activity after incubation at 37 ^{o}C. Dashed line indicates remaining activity of the wild-type enzyme.

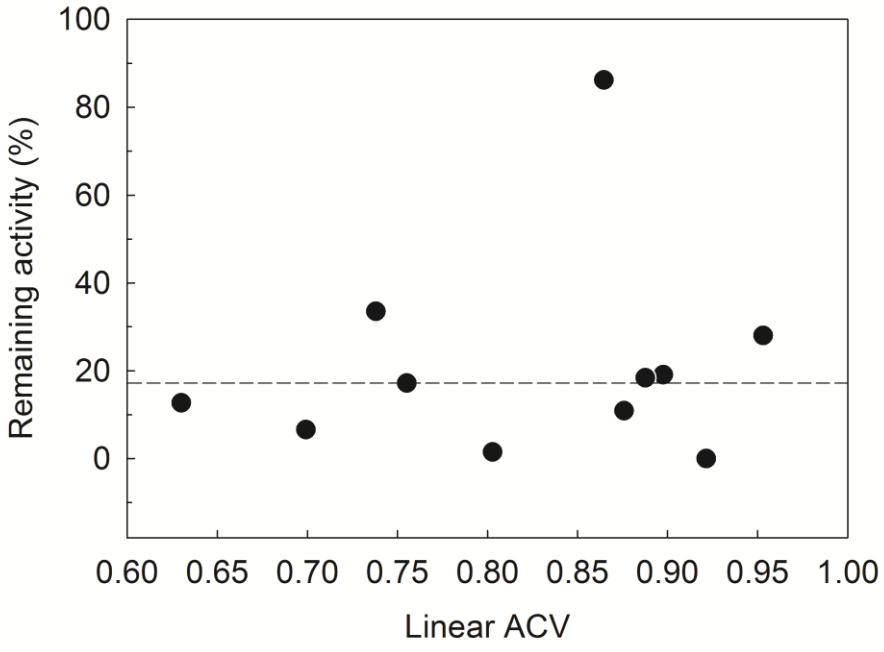

Figure 2-13. Correlation between thermostability and the linear ACV (window size 11).

Window size was 11. Linear ACV values were plotted against remaining activity after incubation at 37 ^{o}C. Dashed line indicates remaining activity of the wild-type enzyme.

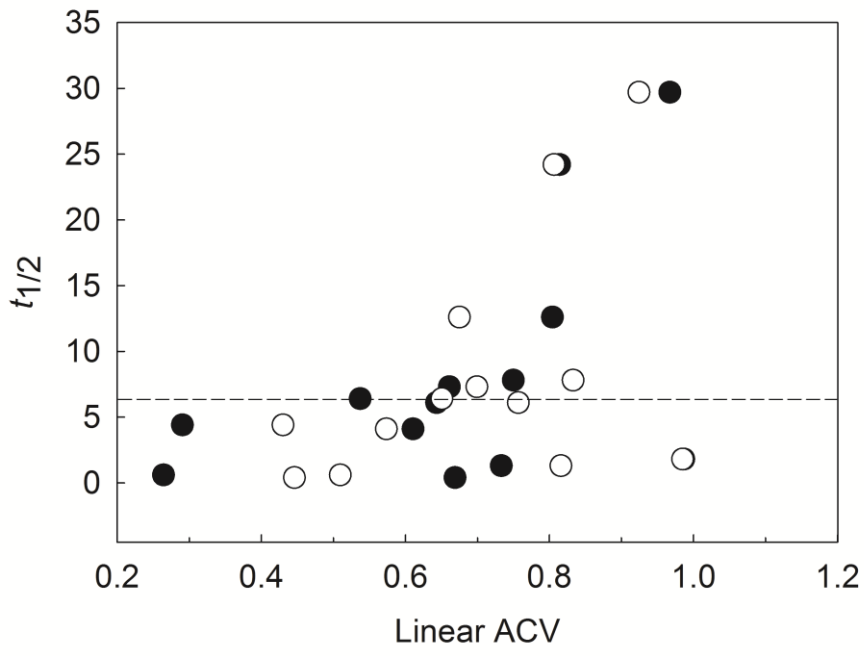

Figure 2-14. Correlation between thermostability and the linear ACV of β-amylase.

Closed circle indicates the linear ACV value of window size 5. Open circle indicate the linear ACV value of window size 7. $t_{1/2}$ values were plotted against linear ACV values. Dashed line indicates a $t_{1/2}$ of the wild-type enzyme.

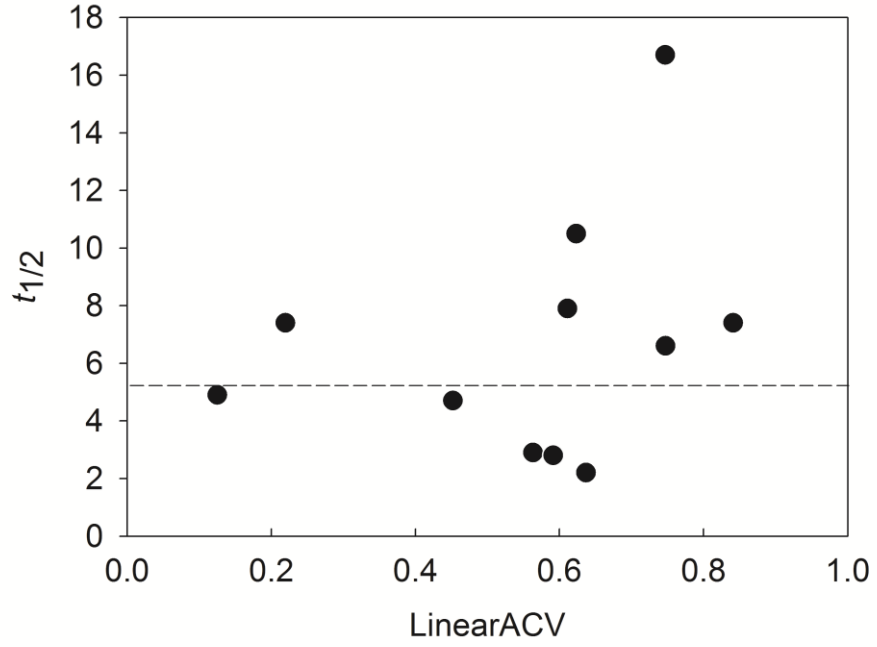

Figure 2-15. Correlation between thermostability and the linear ACV of IPMDH.

Closed circle indicates the linear ACV value of window size 9. $t_{1/2}$ values were plotted against linear ACV. Dashed line indicates a $t_{1/2}$ of the wild-type enzyme.

Table 2-1. Thermal inactivation at 37 °C treatment of wild-type LiP and ancestral mutants

	Specific activity (Unit/mg)			Remaining activity
	0 min	30 min		(%)
Wild-type	14.4 ± 0.0 (1.00)	2.5 ± 0.1 (1.00)		17.2 (1.00)
m1	5.6 ± 0.3 (0.39)	0.0 ± 0.0 (0.00)		0.0 (0.00)
m2	3.3 ± 0.1 (0.23)	0.2 ± 0.0 (0.08)		6.6 (0.38)
m3	12.6 ± 0.2 (0.88)	0.2 ± 0.0 (0.08)		1.5 (0.09)
m4	0.9 ± 0.0 (0.06)	0.2 ± 0.0 (0.08)		19.1 (1.11)
m5	14.6 ± 0.1 (1.01)	4.1 ± 0.3 (1.64)		28.0 (1.63)
m6	24.8 ± 0.7 (1.72)	4.3 ± 0.3 (1.72)		17.2 (1.00)
m7	25.6 ± 0.5 (1.78)	2.8 ± 0.1 (1.12)		10.9 (0.63)
m8	20.1 ± 1.5 (1.40)	6.7 ± 0.3 (2.68)		33.5 (1.95)
m9	19.4 ± 0.8 (1.35)	2.5 ± 0.1 (1.00)		12.7 (0.74)
m10	53.4 ± 1.6 (3.71)	46 ± 1.6 (18.4)		86.2 (5.01)
m11	22.1 ± 0.7 (1.53)	4.1 ± 0.3 (1.64)		18.4 (1.07)
m5+8	0.1 ± 0.0 (0.01)	0.0 ± 0.0 (0.00)		84.1 (4.89)
m5+10	14.0 ± 0.3 (0.97)	14.3 ± 0.1 (5.72)		102.1 (5.93)
m8+10	21.4 ± 0.2 (1.49)	20.1 ± 0.4 (1.40)		93.8 (5.45)
m5+8+10	4.4 ± 0.0 (0.31)	3.9 ± 0.0 (1.56)		90.2 (5.24)

The parenthesis value indicates the relative value.

Table 2-2. H_2O_2 resistance of wild-type LiP and ancestral mutants

	Specific activity (Unit/mg)			Remaining activity
	0 min	5 min		(%)
Wild-type	12.2 ± 0.2 (1.00)	0.8 ± 0.1 (1.00)		6.5 (1.00)
m1	3.9 ± 0.2 (0.32)	0.2 ± 0.0 (0.25)		4.4 (0.68)
m2	2.6 ± 0.2 (0.21)	0.5 ± 0.0 (0.63)		18.4 (2.83)
m3	10.0 ± 0.0 (0.82)	0.4 ± 0.0 (0.50)		4.3 (0.66)
m4	0.2 ± 0.0 (0.02)	0.2 ± 0.0 (0.25)		96.9 (14.9)
m5	11.3 ± 0.1 (0.93)	3.3 ± 0.1 (4.13)		29.6 (4.55)
m6	12.5 ± 0.3 (1.02)	0.8 ± 0.0 (1.00)		6.2 (0.95)
m7	15.3 ± 1.6 (1.25)	1.0 ± 0.2 (1.25)		6.4 (0.98)
m8	9.4 ± 0.3 (0.77)	0.3 ± 0.0 (0.38)		3.3 (0.51)
m9	8.8 ± 0.2 (0.72)	0.3 ± 0.0 (0.38)		3.0 (0.46)
m10	32.0 ± 1.2 (2.62)	3.4 ± 0.1 (4.25)		10.5 (1.62)
m11	3.3 ± 0.0 (0.27)	0.3 ± 0.0 (0.38)		9.3 (1.43)
m5+8	0.0 ± 0.0 (0.0)	0.0 ± 0.0 (0.00)		54.1 (8.32)
m5+10	14.3 ± 0.7 (1.17)	4.7 ± 1.2 (5.88)		32.6 (5.01)
m8+10	16.7 ± 0.8 (1.36)	0.8 ± 0.2 (1.00)		5.1 (0.78)
m5+8+10	5.5 ± 0.4 (0.45)	0.2 ± 0.0 (0.25)		3.5 (0.54)

The parenthesis value indicates the relative value.

Table 2-3. Steady-state kinetic parameters of wild-type and ancestral mutants

	Specific activity	VA			H_2O_2		
	(Unit/mg)	k_{cat} (/s)	K_M (μM)	k_{cat}/K_M (/s/μM)	k_{cat} (/s)	K_M (μM)	k_{cat}/K_M (/s/μM)
Wild-type	18.8 (1.00)	11.6 ± 0.1 (1.00)	93.4 ± 6.2 (1.00)	0.124 (1.00)	19.4 ± 0.0 (1.00)	59.5 ± 3.5 (1.00)	0.33 (1.00)
m1	8.7 (0.46)	9.6 ± 0.1 (0.83)	96.4 ± 5.3 (1.03)	0.099 (0.80)	3.9 ± 0.0 (0.20)	7.6 ± 0.4 (0.13)	0.51 (0.64)
m2	1.2 (0.06)	1.7 ± 0.4 (0.15)	504.3 ± 351.3 (4.10)	0.003 (0.04)	3.3 ± 0.0 (0.17)	18.5 ± 1.9 (0.31)	0.18 (0.55)
m3	12.1 (0.64)	17.4 ± 0.4 (1.50)	118.2 ± 12.1 (1.27)	0.147 (1.18)	13.4 ± 0.0 (0.69)	41.2 ± 3.9 (0.69)	0.32 (0.97)
m4	0.1 (<0.01)	0.2 ± 0.0 (0.02)	426.3 ± 67.2 (4.50)	<0.001 (<0.01)	0.1 ± 0.0 (0.01)	10.1 ± 4.9 (0.17)	0.005 (0.02)
m5	14.0 (0.74)	18.9 ± 0.2 (1.63)	122.8 ± 5.6 (1.31)	0.154 (1.24)	7.2 ± 0.0 (0.37)	47.2 ± 5.5 (0.79)	0.37 (1.12)
m6	26.7 (1.42)	18.7 ± 0.3 (1.61)	94.4 ± 7.4 (1.01)	0.198 (1.60)	19.2 ± 0.0 (0.99)	51.9 ± 3.5 (0.87)	0.36 (1.09)
m7	27.6 (1.47)	19.6 ± 0.2 (1.69)	120.5 ± 6.2 (1.29)	0.163 (1.31)	23.5 ± 0.6 (1.21)	65.3 ± 4.3 (1.10)	0.41 (1.24)
m8	21.0 (1.12)	13.8 ± 0.4 (1.19)	106.1 ± 15.6 (1.13)	0.13 (1.05)	16.5 ± 0.5 (0.85)	40.3 ± 4.2 (0.68)	0.43 (1.30)
m9	19.3 (1.03)	12.3 ± 0.1 (1.06)	64.7 ± 3.3 (0.69)	0.19 (1.53)	15.7 ± 0.4 (0.81)	36.3 ± 3.0 (0.61)	0.34 (1.03)
m10	43.3 (2.30)	39.7 ± 0.6 (3.42)	181.5 ± 11.6 (1.94)	0.219 (1.76)	34.2 ± 1.1 (1.76)	99.9 ± 8.6 (1.68)	0.41 (1.24)
m11	25.3 (1.35)	17.6 ± 0.3 (1.52)	121.7 ± 8.6 (1.30)	0.144 (1.16)	16.4 ± 0.0 (0.85)	40.2 ± 3.1 (0.68)	0.37 (1.12)
m5+8	0.0 (0.00)	Not Detected			0.1 ± 0.0 (0.01)	11.0 ± 4.1 (0.19)	0.01 (0.04)
m5+10	13.6 (0.72)	8.96 ± 0.3 (0.77)	139.7 ± 17.7 (1.50)	0.064 (1.94)	11.6 ± 0.4 (0.60)	74.38 ± 7.5 (1.25)	0.16 (0.47)
m8+10	24.1 (1.28)	13.4 ± 0.2 (1.16)	98.5 ± 8.1 (1.05)	0.136 (1.10)	15.2 ± 0.5 (0.79)	42.24 ± 5.3 (0.71)	0.36 (1.09)
m5+8+10	4.5 (0.24)	3.5 ± 0.1 (0.30)	109.7 ± 13.2 (1.17)	0.032 (0.26)	2.7 ± 0.1 (0.14)	22.7 ± 4.0 (0.38)	0.12 (0.36)

The parenthesis value indicates the relative value.

Table 2-4. Characteristics of ancestral mutation sites

Mutation site		Accessible surface area[a] (%)	Secondary structure[b]	Distance from active site ions (Å)[c]		Distance from Ca^{2+} ions (Å)[c]		⊿Total energy[d](kcal/mol)	Stability[e]
				From heme ion	From w171	From distal site	From proximal site		
m1	A36E	14	α	13.6	21.8	21.8	13.6	0.23	-
m2	V45T	1	α	10.2	15.1	8.8	18.4	0.18	-
m3	K92E	63	α	19.3	28.7	16.0	26.3	1.89	-
	L93A	40	α	19.3	28.1	17.7	24.4		
m4	A110Q	4	α	15.8	18.0	11.2	21.0	1.08	+
m5	A116G	0	α	15.0	18.1	19.1	14.1	2.81	+
	L117V	0	α	14.3	15.1	20.1	11.7		
m6	H149D	26	L	12.7	18.1	20.6	23.6	-0.51	±
m7	G198S	47	L	15.4	18.3	26.7	6.1	-0.05	-
m8	Q209M	2	α	17.4	15.6	32.1	14.3	-1.78	+
m9	I235L	9	β	9.7	16.8	24.1	15.6	-1.84	-
m10	H239F	24	α	12.9	14.8	27.0	16.2	-2.27	+
	T240L	38	α	14.4	15.0	26.9	19.3		
	I241L	0	α	13.2	11.4	25.1	17.9		
m11	F254M	4	α	17.8	9.0	29.3	12.2	0.63	+

[a]Accessible surface areas were calculated at the VADAR web server.

[b]Position of the mutated site in the modeled LiP structure: α, β and L represent helix, sheet and loop structure, respectively.

[c]Distances were estimated in the LiP-modeled structure.

[d]⊿Total energy was calculated by FoldX [13].

[e]The + or – indicates that the ancestral mutant has higher or lower stability than the wild-type after 37 ^{o}C heat treatment.

Table 2-5. The comparison of ancestral amino acid residues with consensus amino acid residues

Name	Wild-type residue	Ancestral residue	Consensus residue	Dominant or Minor	Stability[a]	Ancestral residues and its likelihood value						Consensus residue and its frequency			
						node60		node62		node63		1st	%	2nd	%
m1	A	E	E	D	-	E	(1.00)	E	(1.00)	E	(1.00)	E	(67.3)	A	(24.5)
m2	V	T	T	D	-	T	(1.00)	T	(1.00)	T	(1.00)	T	(69.4)	V	(18.4)
m3	K	E	N	M	-	E	(0.66)	E	(0.95)	E	(0.95)	N	(38.8)	E	(20.4)
	L	A	N			A	(0.86)	A	(0.99)	A	(0.86)	N	(22.4)	A	(20.4)
m4	A	Q	Q	D	+	Q	(1.00)	Q	(1.00)	Q	(1.00)	Q	(75.5)	A	(18.4)
m5	A	G	G	D	+	G	(1.00)	G	(1.00)	G	(1.00)	G	(57.1)	A	(42.9)
	L	V	V			V	(1.00)	V	(1.00)	V	(0.98)	V	(42.9)	L	(32.7)
m6	H	D	D	D	±	D	(1.00)	D	(1.00)	D	(1.00)	D	(71.4)	H	(28.6)
m7	G	S	G	M	-	E	(0.44)	S	(0.89)	S	(0.94)	G	(28.6)	F	(24.5)
m8	Q	M	Q	M	+	Q	(1.00)	M	(0.96)	M	(0.98)	Q	(53.1)	L	(32.7)
m9	I	L	L	D	-	L	(1.00)	L	(1.00)	L	(1.00)	L	(85.7)	I	(12.2)
m10	H	F	F	D	+	F	(0.71)	F	(0.95)	F	(0.99)	F	(49.0)	H	(28.6)
	T	L	A			L	(0.95)	L	(1.00)	L	(0.80)	A	(28.6)	L	(26.5)
	I	L	L			L	(0.99)	L	(1.00)	L	(1.00)	L	(71.4)	I	(20.4)
m11	F	M	F	M	+	F	(0.99)	M	(1.00)	M	(0.99)	F	(75.5)	M	(20.4)

[a]The + or – indicates that the ancestral mutant has higher or lower stability than the wild-type after 37 ^{o}C heat treatment.

Table 2-6. Names of the mutants and oligonucleotide sequence used for site-directed mutagenesis

Name	Mutation	Nucleotide sequence	
m1	Ala36Glu	Forward primer	5′-GGCGGCCAGTGCGGC***GAA***GAGGCGCACGAGTCG-3′
		Reverse primer	5′-CGACTCGTGCGCCTC***TTC***GCCGCACTGGCCGCC-3′
m2	Val45Thr	Forward primer	5′-GAGTCGATTCGTCTC***ACC***TTCCACGACTCCGTC-3′
		Reverse primer	5′-GACGGAGTCGTGGAA***GGT***GAGACGAATCGACTC-3′
m3	Lys92Glu/Leu93Ala	Forward primer	5′-CTCGACGAGATCGTC***GAAGCT***CAGAAGCCATTCGTT-3′
		Reverse primer	5′-AACGAATGGCTTCTG***AGCTTC***GACGATCTCGTCGAG-3′
m4	Ala110Gln	Forward primer	5′-CCTGGTGACTTCATC***CAG***TTCGCTGGTGCTGTC-3′
		Reverse primer	5′-GACAGCACCAGCGAA***CTG***GATGAAGTCACCAGG-3′
m5	Ala116Gly/Leu117Val	Forward primer	5′-TTCGCTGGTGCTGTC***GGTGTT***AGCAACTGCCCTGGT-3′
		Reverse primer	5′-ACCAGGGCAGTTGCT***AACACC***GACAGCACCAGCGAA-3′
m6	His149Asp	Forward primer	5′-GTCCCCGAGCCCTTC***GAC***ACTGTCGACCAAATC-3′
		Reverse primer	5′-GATTTGGTCGACAGT***GTC***GAAGGGCTCGGGGAC-3′
m7	Gly198Gln	Forward primer	5′-TTTGACTCTACCCCC***TCT***ATCTTCGACTCCCAG-3′
		Reverse primer	5′-CTGGGAGTCGAAGAT***AGA***GGGGGTAGAGTCAAA-3′
m8	Gln209Met	Forward primer	5′-TTCTTCGTCGAGACT***ATG***CTTCGTGGTACCGCC-3′
		Reverse primer	5′-GGCGGTACCACGAAG***CAT***AGTCTCGACGAAGAA-3′
m9	Ile235Leu	Forward primer	5′-CCTGGCGAAATTCGC***CTG***CAGTCCGACCACACT-3′
		Reverse primer	5′-AGTGTGGTCGGACTG***CAG***GCGAATTTCGCCAGG-3′
m10	His239Phe/Thr240Leu/Ile241Leu	Forward primer	5′-CGCATCCAGTCCGAC***TTCCTGCTG***GCCCGCGACTCACGC-3′
		Reverse primer	5′-GCGTGAGTCGCGGGC***CAGCAGGAA***GTCGGACTGGATGCG-3′
m11	Phe254Met	Forward primer	5′-TGTGAATGGCAGTCC***ATG***GTCAACAACCAGTGG-3′
		Reverse primer	5′-GGACTGGTTGTTGAC***CAT***GGACTGCCATTCACA-3′

Bold and italic letters indicate the mutated codons.

Table 2-7. List of gene-bank accession numbers and its species used for the phylogenetic tree construction

Accession No.	Enzyme type	Species
Basidiomycota		
AAA33736	LiP (*GLG6*)	*Phanerochaete chrysosporium*
AAA56852	LiP (LIG1)	*Phanerochaete chrysosporium* strain ME446
CAA38177	LiP (*lipA*)	*Phanerochaete chrysosporium* strain BKM1767
AAA03748	LiP	*Phanerochaete chrysosporium* strain BKM1767
CAA68373	LiP	*Phanerochaete chrysosporium* strain BKM1767
AAA33734	LiP	*Phanerochaete chrysosporium* strain BKM1767
AAD46494	LiP (*lipj*)	*Phanerochaete chrysosporium* strain BKM1767
AAA33733	LiP	*Phanerochaete chrysosporium* strain BKM1767
AAW59419	LiP (*lip1*)	*Phlebia radiata*
AAW71986	LiP (lip3)	*Phlebia radiata*
1906181A	LiP	*Bjerkandera adusta*
BAD06763	LiP	*Trametes versicolor* strain IFO1030
JQ1190	LiP (*VLG1*)	*Trametes versicolor*
CAA83147	LiP (*LPGV1*)	*Trametes versicolor* strain PRL 572
AAF31329	MnP (*mnp1*)	*Dichomitus squalens* strain PRL 572
ABR66918	MnP (*mnp2*)	*Phlebia sp*. B19 strain PRL 572
BAG12562	MnP (*mnp3*)	*Phlebia sp*. MG60
AAB39652	MnP (*mnp3*)	*Phanerochaete chrysosporium* MG60 strain OGC101
BAC06185	MnP (*mnp2*)	*Phlebia sp*. b19
AAA33743	MnP (*mnp1*)	*Phanerochaete chrysosporium*
BAC06187	MnP (*mnp3*)	*Phanerochaete sordida* strain ATCC90872
ABB83812	MnP (*mnpA*)	*Ceriporiopsis rivulosa* strain DSM 14618
AAC05222	MnP (*mnp1*)	*Ceriporiopsis subvermispora* strain FP 105752
AAD43581	MnP (*mnp2A*)	*Ceriporiopsis subvermispora* strain FP 105752
BAG72079	MnP (*mnp2*)	*Lentinula edodes*
AAY89586	VP	*Bjerkandera adusta strain* UAMH8258
BAE79812	MnP	*Spongipellis sp.* FERM P-18171
CAA54398	MnP (*PG V*)	*Trametes versicolor*
BAA33449	MnP (*mnp3*)	*Pleurotus ostreatus* strain IS-1
BAE79199	MnP (*mnp1*)	*Lentinula edodes*
AAT90348	MnP (*cmp1*)	*Trametes versicolor* strain KN9522
ABB83813	MnP (*mnpB*)	*Ceriporiopsis rivulosa* strain DSM 14618
CAG33918	MnP	*Trametes versicolor*

AAD02880	MnP (*mnp2*)	*Trametes versicolor* strain PRL 572
BAB03464	MnP (*CVMNP*)	*Trametes versicolor* strain IFO30340
CAD92855	MnP (*mnp3*)	*Phlebia radiate*
AAX40734	MnP (*MnP5*)	*Pheurotus pulmonarius*
CAJ01576	VP	*Pleurotus sapidus*
Q9UR19	VP (*vpl1*)	*Pleurotus eryngii*
AAD54310	VP (*vps1*)	*Pleurotus eryngii* strain ATCC90787
CAB51617	MnP (*mnp2*)	*Pleurotus sp.* Strain Florida
BAE46585	LiP	*Trametes cervina*
ABB77243	MnP (*mnp0109*)	*Ganoderma formosanum*
ABB77244	MnP	*Ganoderma austral*
CAG32981	MnP (*mrp*)	*Trametes versicolor*
Ascomycota		
EDU39540	LiP LG6	*Pyrenophora tritici-repentis* strain Pt-1C-BFP
EDU45564	LiP H2	*Pyrenophora tritici-repentis* strain Pt-1C-BFP

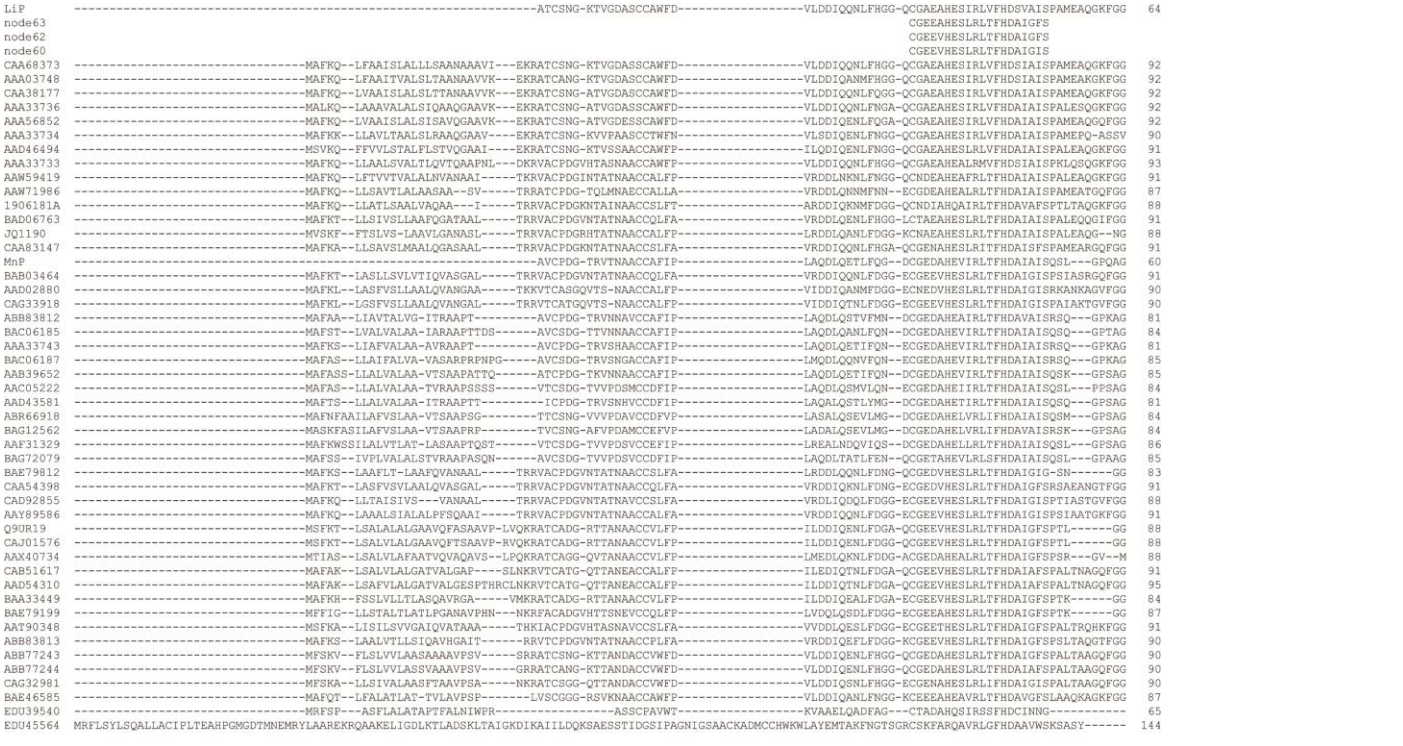

Supplementary figure 2-1. Multiple amino acid sequence alignment of 85 fungal peroxidases

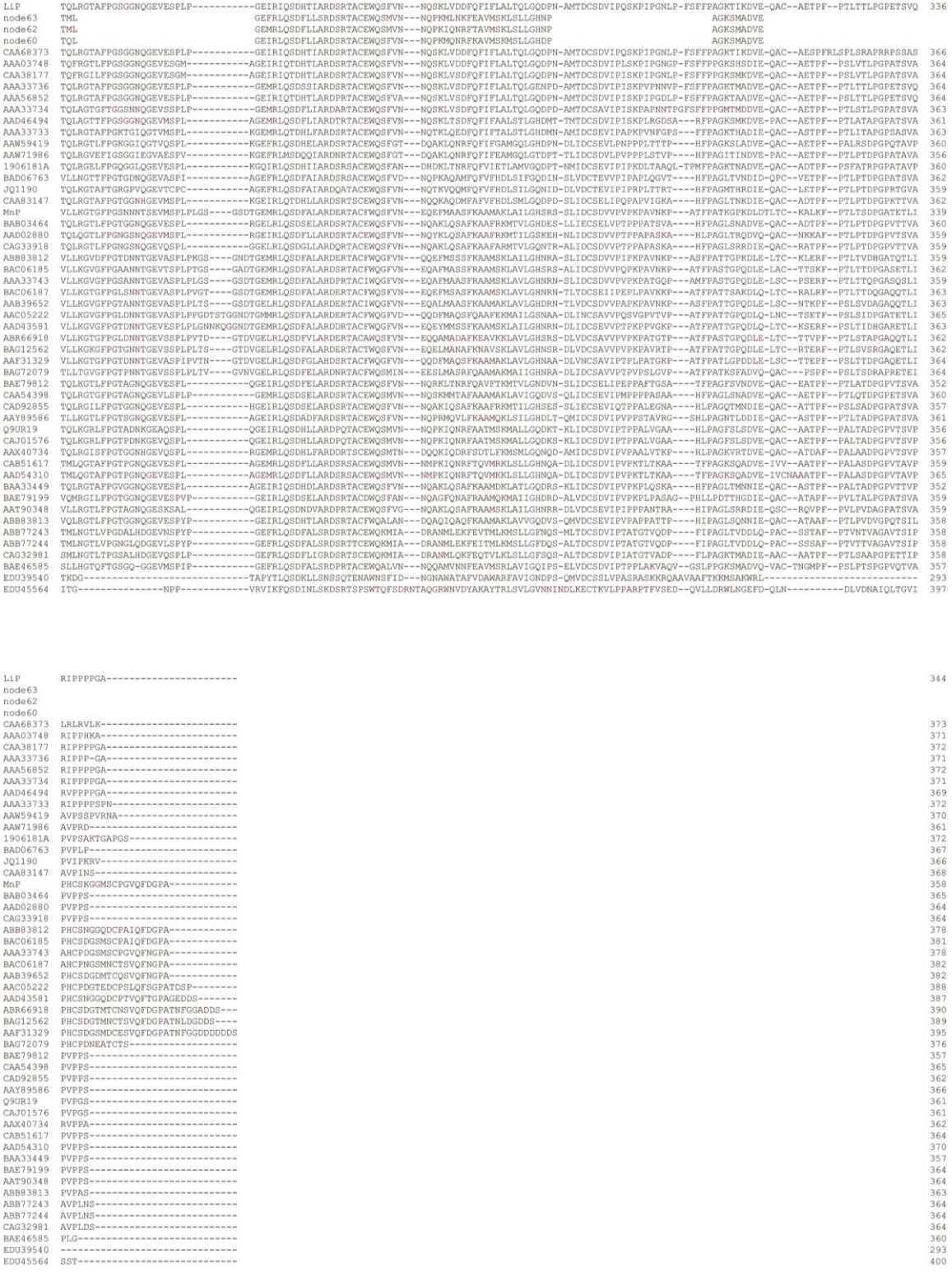

Supplementary figure 2-1. (continued)

References

[1] J. D. Thompson, T. J. Gibson, F. Plewniak, F. Jeanmougin, and D. G. Higgins, "The CLUSTAL_X Windows Interface: Flexible Strategies for Multiple Sequence Alignment Aided by Quality Analysis Tools," *Nucleic Acids Res.*, vol. 25, no. 24, pp. 4876–4882, Dec. 1997.

[2] J. Castresana, "Selection of conserved blocks from multiple alignments for their use in phylogenetic analysis.," *Mol. Biol. Evol.*, vol. 17, no. 4, pp. 540–552, Apr. 2000.

[3] G. Jobb, A. von Haeseler, and K. Strimmer, "TREEFINDER: a powerful graphical analysis environment for molecular phylogenetics.," *BMC Evol. Biol.*, vol. 4, no. 1, p. 18, Jun. 2004.

[4] S. Guindon and O. Gascuel, "A Simple, Fast, and Accurate Algorithm to Estimate Large Phylogenies by Maximum Likelihood," *Syst. Biol.*, vol. 52, no. 5, pp. 696–704, Oct. 2003.

[5] S. Whelan and N. Goldman, "A General Empirical Model of Protein Evolution Derived from Multiple Protein Families Using a Maximum-Likelihood Approach," *Mol. Biol. Evol.*, vol. 18, no. 5, pp. 691–699, May 2001.

[6] J. Adachi and M. Hasegawa, "MOLPHY Version 2.3:Programs for Molecular Phylogenetics Based on Maximum Likelihood Jun Adachi and Masami Hasegawa," *Comput. Sci. Monogr.*, vol. 28, pp. 1–150, 1996.

[7] H. A. Schmidt, K. Strimmer, M. Vingron, and A. von Haeseler, "TREE-PUZZLE: maximum likelihood phylogenetic analysis using quartets and parallel computing," *Bioinformatics*, vol. 18, no. 3, pp. 502–504, Mar. 2002.

[8] Z. Yang, "PAML: a program package for phylogenetic analysis by maximum likelihood," *Comput. Appl. Biosci. CABIOS*, vol. 13, no. 5, pp. 555–556, Oct. 1997.

[9] J. H. Fuhrhop and K. M. Smith, *Porphyrins and metalloporphyrins*. Amsterdam: Elsevier, 1975.

[10] M. Tien and T. K. Kirk, "Lignin-degrading enzyme from Phanerochaete chrysosporium: Purification, characterization, and catalytic properties of a unique

H(2)O(2)-requiring oxygenase.," *Proc. Natl. Acad. Sci. USA.*, vol. 81, no. 8, pp. 2280–2284, Apr. 1984.

[11] G. Nie, N. S. Reading, and S. D. Aust, "Relative Stability of Recombinant Versus Native Peroxidases fromPhanerochaete chrysosporium," *Arch. Biochem. Biophys.*, vol. 365, no. 2, pp. 328–334, May 1999.

[12] D. Floudas, M. Binder, R. Riley, K. Barry, R. A. Blanchette, B. Henrissat, A. T. Martínez, R. Otillar, J. W. Spatafora, J. S. Yadav, A. Aerts, I. Benoit, A. Boyd, A. Carlson, A. Copeland, P. M. Coutinho, R. P. de Vries, P. Ferreira, K. Findley, B. Foster, J. Gaskell, D. Glotzer, P. Górecki, J. Heitman, C. Hesse, C. Hori, K. Igarashi, J. A. Jurgens, N. Kallen, P. Kersten, A. Kohler, U. Kües, T. K. A. Kumar, A. Kuo, K. LaButti, L. F. Larrondo, E. Lindquist, A. Ling, V. Lombard, S. Lucas, T. Lundell, R. Martin, D. J. McLaughlin, I. Morgenstern, E. Morin, C. Murat, L. G. Nagy, M. Nolan, R. A. Ohm, A. Patyshakuliyeva, A. Rokas, F. J. Ruiz-Dueñas, G. Sabat, A. Salamov, M. Samejima, J. Schmutz, J. C. Slot, F. St. John, J. Stenlid, H. Sun, S. Sun, K. Syed, A. Tsang, A. Wiebenga, D. Young, A. Pisabarro, D. C. Eastwood, F. Martin, D. Cullen, I. V Grigoriev, and D. S. Hibbett, "The Paleozoic Origin of Enzymatic Lignin Decomposition Reconstructed from 31 Fungal Genomes," *Science*, vol. 336, no. 6089, pp. 1715–1719, Jun. 2012.

[13] J. Schymkowitz, J. Borg, F. Stricher, R. Nys, F. Rousseau, and L. Serrano, "The FoldX web server: an online force field," *Nucleic Acids Res.*, vol. 33, no. suppl 2, pp. W382–W388, Jul. 2005.

[14] P. Y. Chou and G. D. Fasman, "Secondary structural prediction of proteins from their amino acid sequence," *Trends Biochem. Sci.*, vol. 2, no. 6, pp. 128–131, Jun. 1977.

[15] W. Blodig, A. T. Smith, W. A. Doyle, and K. Piontek, "Crystal structures of pristine and oxidatively processed lignin peroxidase expressed in Escherichia coli and of the W171F variant that eliminates the redox active tryptophan 171. Implications for the reaction mechanism.," *J. Mol. Biol.*, vol. 305, no. 4, pp. 851–861, Jan. 2001.

[16] K. Watanabe, T. Ohkuri, S. Yokobori, and A. Yamagishi, "Designing thermostable proteins: ancestral mutants of 3-isopropylmalate dehydrogenase designed by using a phylogenetic tree.," *J. Mol. Biol.*, vol. 355, no. 4, pp. 664–674, Jan. 2006.

[17] K. Yamashiro, S. Yokobori, S. Koikeda, and A. Yamagishi, “Improvement of Bacillus circulans beta-amylase activity attained using the ancestral mutation method.,” *Protein Eng. Des. Sel.*, vol. 23, no. 7, pp. 519–528, Jul. 2010.

[18] W. Blodig, A. T. Smith, W. A. Doyle, and K. Piontek, “Crystal structures of pristine and oxidatively processed lignin peroxidase expressed in Escherichia coli and of the W171F variant that eliminates the redox active tryptophan 171. Implications for the reaction mechanism.,” *J. Mol. Biol.*, vol. 305, no. 4, pp. 851–861, Jan. 2001.

Chapter 3. Ancestral lignin degrading enzyme

1. Summary

In chapter 2, we constructed ancestral mutants of lignin peroxidase (LiP). Single, double and triple ancestral mutations were introduced into the amino acid sequence of LiP. In the next step in this chapter, an ancestral lignin degrading enzyme whose amino acid sequence was constructed entirely from ancestral amino acids was resurrected.

Eighty-three sequences homologous to lignin peroxidase (LiP) were collected and aligned using MAFFT. The multiple sequence alignment was adjusted manually and well-conserved region was selected by Gblocks. The WAG+G+F model was selected as the amino acid substitution model by Prottest. Phylogenetic tree was constructed using PhyML. The ancestral sequence was deduced using CODEML in PAML and the gap position was estimated using GASP. The ancestral sequence was named “ancestral ligninase” and the corresponding protein was expressed in *Escherichia coli* BL21 (DE3) and purified. It showed both manganese peroxidase (MnP) and LiP activities, although the former was lower than that of its counterpart from *Phanerochaete chrysosporium*. The remaining LiP and MnP activities of ancestral ligninase were higher than those of LiP and MnP from *P. chrysosporium* following a 15 min heat treatment. The T_m values, defined as the half denaturation temperature, of MnP, LiP and ancestral ligninase were 50 ^{o}C, 58 ^{o}C and 66 ^{o}C, respectively. The ancestral ligninase showed a higher T_m value than LiP and MnP.

These results indicated that a thermally stable enzyme can be designed by resurrecting the ancestral enzyme from a dataset consisting of a limited number of taxonomic species.

2. Purpose

In this study, we resurrected ancestral lignin degrading enzyme whose amino acid sequence was made of ancestral amino acids. The dataset used for phylogenetic analysis was limited only to Basidiomycota. The ancestral lignin degrading enzyme was characterized and then compared with modern lignin degrading enzymes, lignin peroxidase and manganese peroxidase from *Phanerochaete chrysosporium*. We estimated the stability of the ancestral enzyme.

3. Material

Veratryl alcohol (VA: 2, 6-dimethoxybenzyl alcohol), oxidized glutathione and hemin chloride were purchased from Sigma-Aldrich (St Louis, MO, USA). Other chemicals were obtained from Wako Chemicals (Tokyo, Japan) and all of analytical grade.

4. Method

4.1. Phylogenetic analysis

LiP-homologous 83 amino acid sequences were collected from the NCBI database by BLASTP. The amino acid sequences of LiP from *Phanerochaete chrysosporium* (PcLiP) and MnP from *P. chrysosporium* (PcMnP) was used as query sequences. Multiple sequence alignment was carried out using MAFFT 7.0[1] and were manually adjusted. 252 positions were selected using Gblocks 0.93[2] as well conserved region. WAG+G+F model[3] was selected by Prottest3.0[4]. Maximum likelihood tree was constructed with PhyML 3.0[5]. The ancestral sequence was estimated by CODEML in PAML[6]. Gap position was estimated by GASP[7]. Ancestral sequence obtained was named ancestral ligninase.

4.2. Construction of the ancestral ligninase gene

The ancestral ligninase gene was constructed by Eurofins Genomics (Tokyo, Japan) with *Escherichia coli* codon usage. In the gene, the *Nde*I was designed at the 5'end and the *Hin*dIII site was designed at its 3' end. The ancestral ligninase gene was digested with *Nde*I and *Hin*dIII and ligated into the same sites of pET21a (+) (Merck Millipore, Billerica, MA, USA). The sequence was confirmed using an Applied Biosystems ABI PRISM 3130x sequencer (Applied Biosystems, Foster City, CA, USA).

4.3. Expression and purification of the ancestral ligninase

E. coli BL21 (DE3) (Nippon Gene, Tokyo, Japan) was transformed with pET21a (+) harboring the ancestral ligninase gene. The *E. coli* was cultured in Terrific Broth medium (12 g polypeptone, 24 g yeast extract, 4 mL glycerol, 2.3 g KH_2PO_4, 12.5 g K_2HPO_4 in 1 L) supplemented with 50 μg/mL ampicillin at 37 ^oC. When the optical density ($OD_{600\ nm}$) of the culture reached 0.6-0.8, expression was induced by the addition of IPTG (isopropyl-β-$_D$-thiogalactopyranoside) to a final concentration of 0.5 mM and the culture was incubated for 4 hr at 37 ^oC. Cells were harvested and disrupted by sonication in ice cold resuspension buffer containing 20 mM Tris-HCl (pH8.0), 10 mM EDTA (ethylenediaminetetraacetic acid), 10 mM DTT (dithiothreitol), 1 % TritonX-100 and 1 mM PMSF (phenylmethylsulfonyl fluoride). The ancestral ligninase, PcMnP and PcLiP were expressed as inclusion bodies, which were washed three times with wash buffer containing 20 mM Tris-HCl (pH 8.0), 2 mM EDTA, 2 mM DTT and 1 % (v/v) TritonX-100. The pellet was resuspended in 8 M urea, 50 mM Tris-HCl (pH 8.0), 2 mM EDTA and 1 mM DTT and incubated at room temperature for 2 hr. The denatured, reduced proteins were diluted to 2 M urea in refolding solution, 50 mM Tris-HCl (pH 8.0), 1 mM $CaCl_2$, 0.7 mM oxidized glutathione and 5 μM hemin, and incubated at 4 ^oC overnight in the dark. The enzyme

mixtures were dialyzed exhaustively against 10 mM sodium acetate buffer (pH 6.0), 1 mM $CaCl_2$ at 4 ^oC for 12-14 hr, centrifuged at 60,000 *g* for 20 min and the supernatants concentrated using VIVA SPIN 6 (Sartorius Stedim Biotech, Gottingen, Germany).

To purify each sample, the supernatant was applied on a HiTrapQ HP column (GE Healthcare Bioscience, Piscataway, NJ, USA) and eluted with a 0.01-0.6 M NaCl gradient in 10 mM sodium acetate (pH 6.0) and 1 mM $CaCl_2$. Fractions with the highest activity were pooled and used for the next purification step. The pooled sample was applied on a Superdex75 gel filtration column (GE Healthcare Biosciences, Piscataway, NJ, USA), eluted in 10 mM sodium acetate (pH 6.0) and 1 mM $CaCl_2$, and the fractions with highest activity were pooled. The enzyme concentrations were determined using a BCA protein assay kit (Thermo Fisher Scientific, Waltham, MA, USA).

4.4. Thermal melting profile

The thermal stability of the ancestral ligninase was estimated by monitoring denaturation curves from circular dichroism measurements using a spectropolarimeter J720 (JASCO, Tokyo, Japan). The enzyme concentration was 0.3 mg/mL in 10 mM sodium acetate (pH 6.0) and 1 mM $CaCl_2$. The temperature was increased 1 ^oC per minute.

4.5. Activity assay

The enzymatic activity of LiP was measured by monitoring the oxidation of veratryl alcohol (VA) to veratryl aldehyde. An extinction coefficient ε_{310} = 9300 (M^{-1} cm^{-1}) was used for the activity assay[8]. The absorbance change at 310 nm was recorded with a DU7400 spectrometer (Beckman, Fullerton, CA, USA). The reaction mixture contained 50 mM tartrate buffer (pH2.5), 10 mM VA, 0.1 mM H_2O_2 and 1.5 μg/mL enzyme.

MnP activity was measured by monitoring Mn (III)-malonate complex formation using ε_{270} = 8500 (M^{-1} cm^{-1})[9]. The reaction mixture contained 50 mM malonate buffer (pH 4.5), 10 mM $MnSO_4$, 0.1 mM H_2O_2 and 1.5 μg/mL enzyme.

The steady-state kinetic parameters, i.e. the catalytic constant (k_{cat}) and the Michaelis constant (K_M), were estimated using the enzyme kinetics module of SigmaPlot (Systat Software, San Jose, CA, USA). The LiP activities of the ancestral ligninase and of PcLiP were measured at 47 ^oC and 37 ^oC, respectively, and the MnP activity of the ancestral ligninase and of PcMnP were measured at 62 ^oC and 42 ^oC, respectively.

5. Results

5.1. Phylogenetic analysis of the ancestral ligninase

83 sequences were used for the multiple sequence alignment shown in Figure 3-1. The list of protein IDs and species used for phylogenetic tree construction are shown in Table 1. The Phylogenetic tree (Figure 3-2) was constructed using the maximum likelihood method. Four peroxidases from *Arthromyces ramosus* (ARP) and *Coprinopsis cinerea* (CiP) were outgrouped in this phylogenetic tree. Some LiPs and VPs, such as LiP from *G. applanatum* BAA88392 and VP from *T. versicolor* AAB63460, were located at the deepest nodes. Most LiPs were clustered on branches and most MnPs were clustered in two groups in the tree. The DNA and corresponding amino acid sequence of the ligninase shown in Figure 3-2 were deduced and named the "ancestral ligninase". The amino acid sequence of the ancestral ligninase was estimated by CODEML in PAML program. The gap position of the amino acid sequence was estimated by GASP and 337 residues were selected as ancestral sequence was estimated by reverse translation. The restriction enzyme sites, *Nde*I and *Hin*dIII, were designed at 5' and 3' ends, respectively. The codon usage was adjusted to that of *E. coli*. The amino acid and DNA sequences of ancestral ligninase are shown in Figure 3-3.

5.2. Steady-state kinetics analysis

The kinetic parameters of the MnP and LiP activities were estimated for the ancestral ligninase, PcLiP and PcMnP (Table 2). The k_{cat} value of the ancestral ligninase was lower and the K_M value for VA was higher than those of PcLiP, resulting in a lower k_{cat}/K_M ratio than that of PcLiP. For H_2O_2, k_{cat}/K_M value of the ancestral ligninase was higher than that of PcLiP.

The k_{cat} for Mn (II) of the ancestral ligninase was lower than that of PcMnP. The K_M for Mn (II) of the ancestral ligninase was higher than that of PcMnP, resulting in a lower k_{cat}/K_M ratio for Mn (II) than for PcMnP. The same tendency was observed for H_2O_2.

5.3. Temperature dependence of the enzymatic activity

The temperature dependences of LiP and MnP activities were estimated and are shown in Figure 3-4. The LiP activities of PcLiP and of the ancestral ligninase were highest at 40 ^{o}C and 47 ^{o}C, respectively (Figure 3-4). The specific LiP activity at the optimum temperature for the ancestral ligninase was higher than that of PcLiP at its optimum temperature. The MnP activities of PcMnP and the ancestral ligninase were highest at 45 ^{o}C and 65 ^{o}C, respectively (Figure 3-5). The specific MnP activity of the ancestral ligninase at its optimum temperature was lower than that of PcMnP at its optimum temperature.

5.4. Thermal melting profile

Thermal stability was estimated by monitoring circular dichroism (CD) at 222 nm (Figure 3-6). The T_m values of the ancestral ligninase, PcMnP and PcLiP were 66 ^{o}C, 50 ^{o}C and 58 ^{o}C, respectively. The ancestral ligninase showed the highest T_m value, though this was lower than that of the versatile peroxidase from *Bjerkandera adusta*., 79 ^{o}C[10].

5.5. Remaining activity

The remaining activities of LiP (Figure 3-7) and MnP (Figure 3-8) after heat treatment were estimated. The T_h value was defined as the temperature where 50 % activity is lost after 15 min. The enzyme was incubated from 27 ^{o}C to 82 ^{o}C for 15 min, cooled on ice for 1 min and the activity was estimated. For LiP activity, the T_h values of the ancestral ligninase and of PcLiP were 60 ^{o}C and 49 ^{o}C, respectively. For MnP activity, the T_h values of the ancestral ligninase and of PcMnP were 59 ^{o}C and 43 ^{o}C, respectively. The T_h values of the ancestral ligninase estimated for these two reactions were higher than those of PcLiP and PcMnP.

6. Discussion

6.1. The effects of the dataset on thermal stability results

In previous studies, datasets consisting of archaeal, bacterial and eukaryal sequences were used to infer the sequences of ancestral enzymes. For example, the dataset consists of bacteria was used to infer ancestral sequence of DNA gyrase B subunit (GyrB) [11]. The ancestral GyrB had two T_m values, 65 ^oC and 80 ^oC[11]. The ancestral nucleoside diphosphate kinase (NDK) was resurrected from the dataset consisting of archaeal and bacterial sequences and its T_m values were about 100 ^oC[12]. Archaeal, bacterial and eukaryal sequences were used to infer the ancestors of elongation factor Tu (EF-Tu) [13]. In this study, a dataset consisting only of eukaryal sequences was used and the T_m value of the resurrected ancestral ligninase was 66 ^oC. This indicates that even a limited taxonomic dataset can be used to design a more stable enzyme.

6.2. The effects of the phylogenetic analysis method on the thermal stability

In previous studies of resurrecting ancestral enzymes, high thermal stabilities were interpreted to represent the high environ temperature of the host organism. In the current study, the ancestral sequence represents an era around 270 million years ago[14], when the earth temperature was not unusually high. The stability of an enzyme is often much higher than the growth temperature of the host organisms. For example, the T_m value of ribonuclease T1 from *Aspergillus oryzae* is 59.3 ^oC and the optimum growth temperature is 26 ^oC[15]. The ancestral ligninase was much more stable than the growth temperature of its host. Williams *et al*. reported that methods such as maximum parsimony and maximum likelihood that reconstruct a ‘best guess’ amino acid at each position overestimate the thermostability, while a Bayesian method that sometimes chooses less-probable residues from the posterior probability distribution does not [16]. This could be one reason for the high thermal stability of the ancestral ligninase.

6.3. The effects of the consensus method on thermal stability

The consensus method can also be used to improve thermal stability [17], [18]. This method was developed to engineer the immunoglobulin McPC603 V_κ domain and was based on the hypothesis that the immunoglobulin repertoire approximates a canonical ensemble of sequences, each derived from one of a set of germ-line sequences, which are selected in a process of random, independent mutations to be compatible with every aspect of antibody function[17]. The consensus amino acid sequence was estimated from the same dataset used in the present experiment, to compare the two methods. There were three positions whose consensus amino acid could not be uniquely determined. We constructed consensus sequences

from all eight combinations of the consensus residues. The amino acid sequence identity between the consensus and ancestral ligninase was 71.5 %. However, these eight consensus ligninases sequences showed no or low activity (data not shown), indicating that the ancestral method produced superior results in designing more stable and active LiP and MnP.

6.4. Thermal stability and the effect of glycosylation

The optimum temperature of ancestral ligninase was higher than those of PcLiP and PcMnP. Lignin degrading enzymes are secreted after glycosylation. LiP from *P. chrysosporium* (PDB ID: 1LLP) has three glycosylation sites; asparagine (N) 257, serine (S) 334 and threonine (T) 320[19]. N257, T320, S332 and S334 are also glycosylated in LiP from *Fusarium oxysporum* (PDB ID: 1QPA)[20]. In MnP from *P. chrysosporium*, N131 and S336 are both glycosylation sites (PDB ID: 1MNP and 1YYD)[21], [22]. We used peroxidase from *A. ramosus* (ARP) as an outgroup species and its glycosylation site is N143 (PDB ID: 1ARP)[23].

We aligned the amino acid sequences of these enzymes and the ancestral ligninase and searched for the glycosylation site in the ancestral ligninase (Figure 3-9). Most of the previously identified glycosylated residues were also found in the ancestral ligninase, indicating it was probably glycosylated in its nascent organism. Nie *et al*. reported that glycosylation contributed to the enzymatic stability of LiP and MnP [24]. Because the stabilities of glycosylated LiP and MnP were higher than those of the corresponding wild-type enzyme[24], the stability of the glycosylated ancestral ligninase may be higher than that of the non-glycosylated ancestral ligninase.

6.5. Comparison with other methods

Floudas *et al.* reported the phylogenetic tree of lignin degrading enzymes [14]. In their estimation, the ancestor was inferred to possess MnP activity but not LiP activity. In their tree, LiP has emerged once from MnP in the ancestor of *P. chrysosporium* and *Trametes versicolor.* To confirm the ancestral sequence, we added their sequence data into our dataset and deduced the ancestral sequence using our method. The constructed phylogenetic tree and amino acids in the active sites are shown in Figure 3-10. The CiP and ARP that formed an outgroup in Figure 3-2 formed an in-group following this analysis. The ancestor we inferred, shown in Figure 3-2 is indicated by a double asterisk. The amino acid residue at position 175 in the ancestral sequence estimated from this tree was alanine (A) 175 instead of aspartate (D) 175, suggesting that the ancestral enzyme possessed no LiP activity. These results suggest that the prediction of single residues and of activities depending on these single residues require special care in the selection of an appropriate dataset.

7. Conclusion

By constructing a dataset consisting only of Basidiomycota, and by selecting positions near the peroxidases from *A. ramosus* and *C. cinerea* as an ancestral node, an ancestral ligninase was engineered that showed two activities and that had high enzymatic stability than modern ligninase enzymes. The resurrecting of ancestral enzymes from limited datasets is a useful strategy to design thermally stable enzymes, however the prediction of enzymatic activities involving only a few residues requires special care.

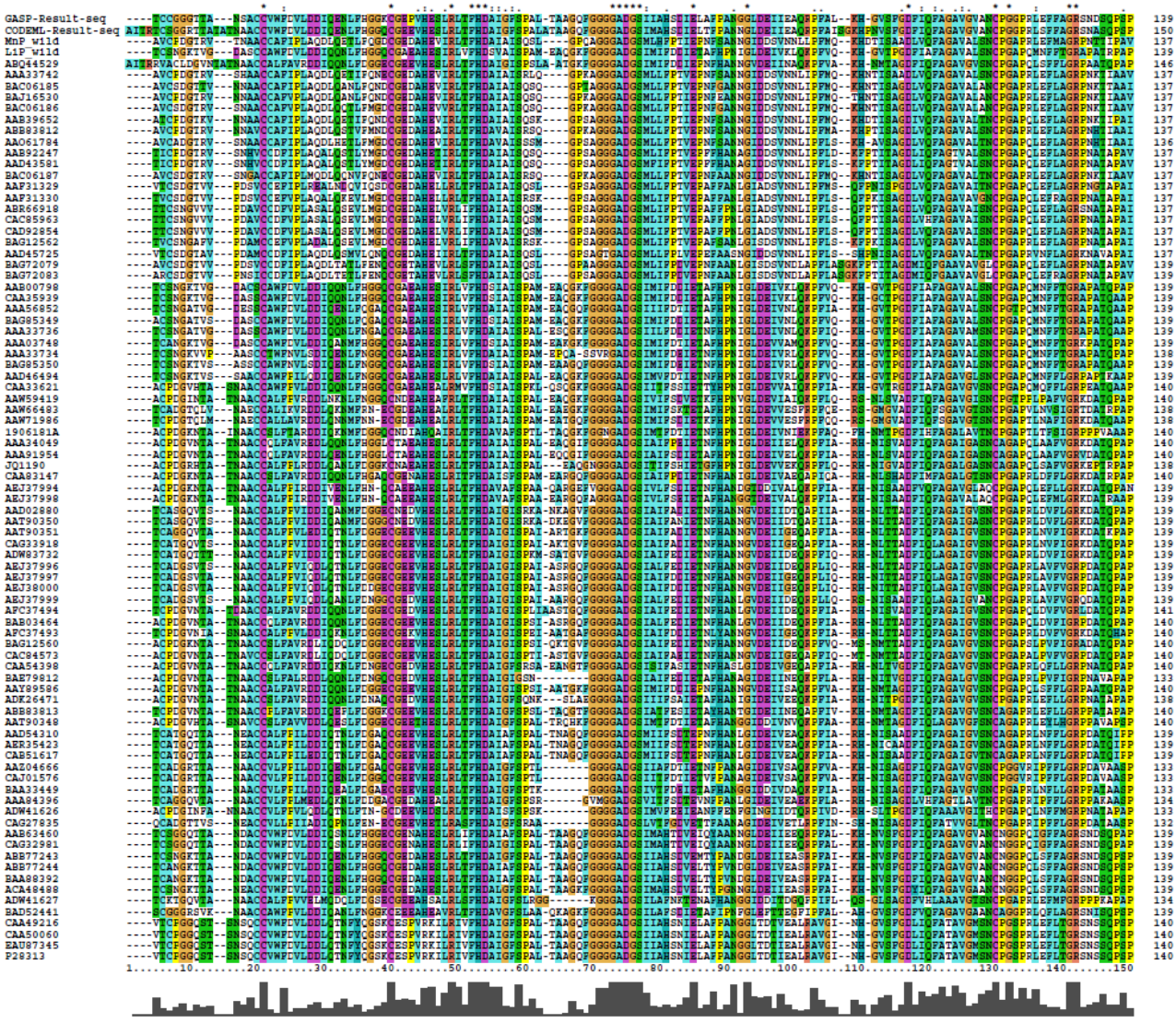

Figure 3-1.Multiple sequence alignment of lignin degrading enzymes

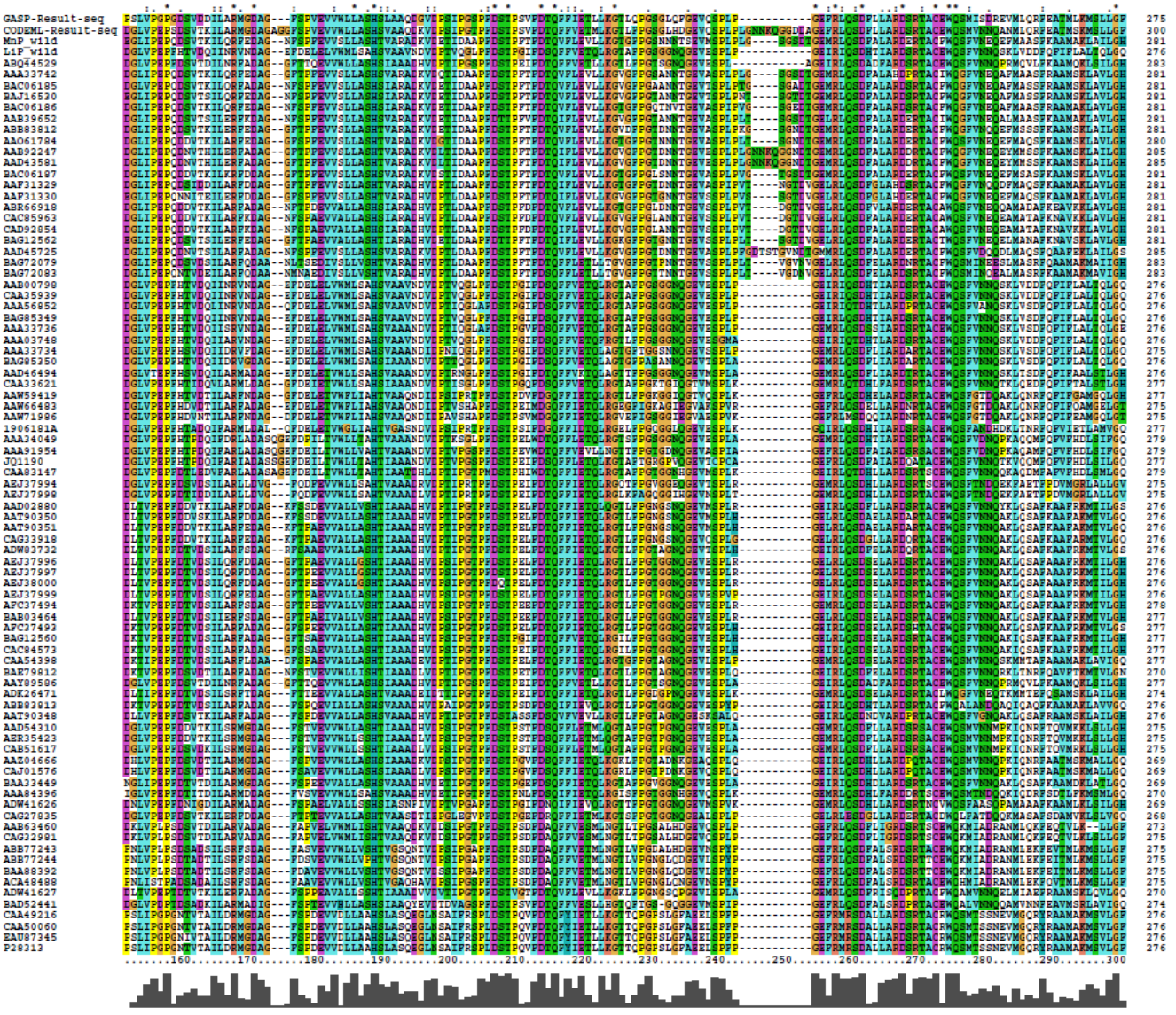

Figure 3-1. (Continued)

Figure3-1. (Continued)

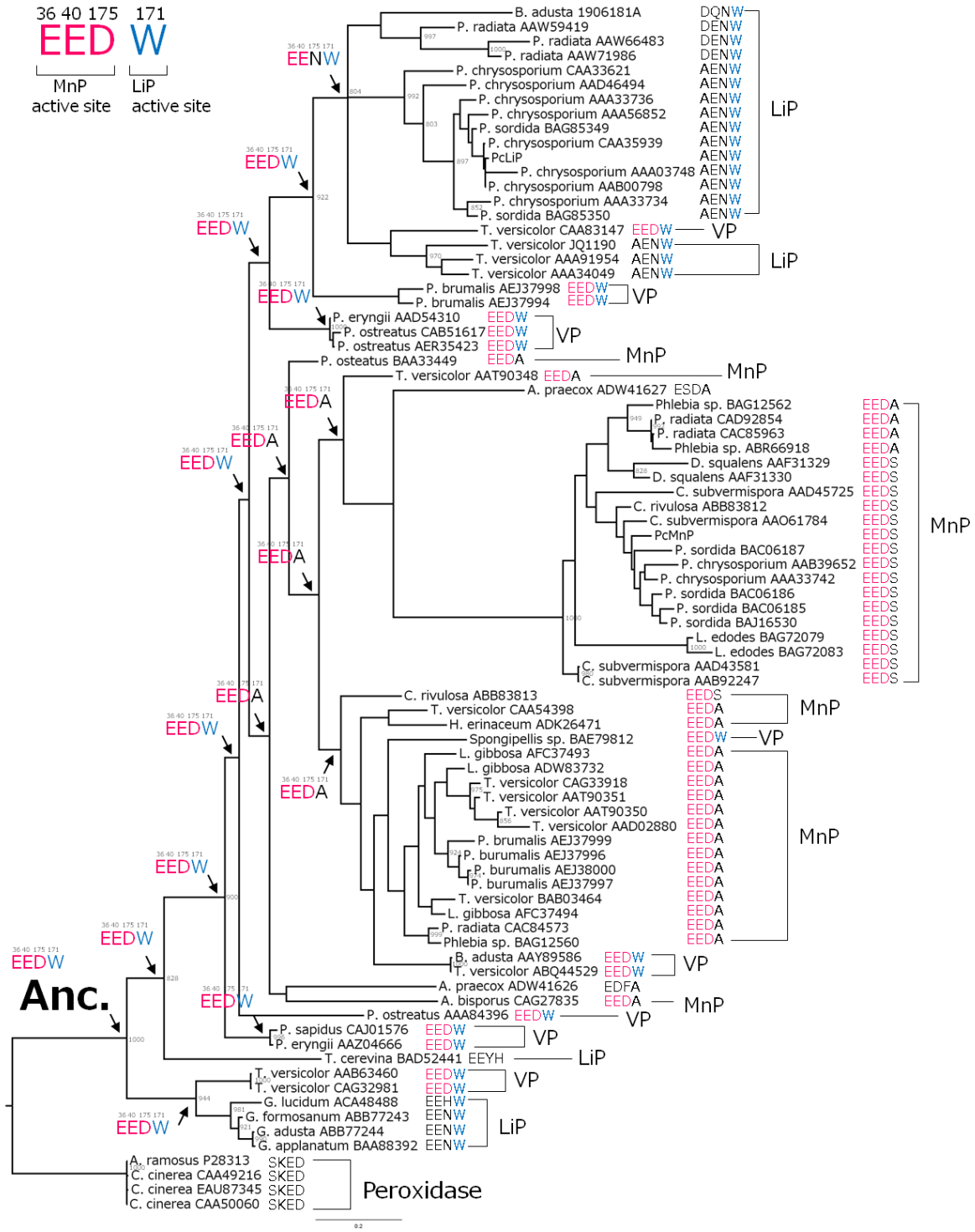

Figure 3-2.Phylogenetic tree of lignin degrading enzymes

The tree was inferred using the maximum likelihood method. The residues responsible for MnP activity (residues at positions 36, 40 and 175) and for LiP activity (position 171) are shown at their respective nodes and aligned at the right side. Red residues are the same as those in the MnP active site, and blue residues are the same as that in LiP active site residue. The standard bar represents 0.2 substitutions per sites.

>Ancestral ligninase DNA sequence

ATGACATGCTCTGGTGGCCGTACCACCGCCAATGCGGCCTGCTGTGTCTGGTTCGATGTGCT
GGACGATATTCAGGAGAACCTCTTTCATGGCGGTCAGTGCGGAGAGGAAGTTCATGAGAGCT
TGCGTCTGACTTTCCACGATGCCATTGGCTTCTCGCCAGCACTGACGGCAGCTGGGCAATTT
GGCGGAGGTGGTGCTGATGGGTCCATCATGGCGCATTCAGACATCGAACTGACCTTCCCGGC
TAACAATGGTCTTGATGAGATCATTGAAGCGCAACGCCCGTTTGCGATTAAGCACAACGTCA
GCTTTGGGGATTTCATCCAGTTTGCGGGTGCGGTAGGCGTTGCGAATTGTCCGGGTGGGCCA
CGGTTATCATTCTTTGCGGGCCGCAGCAACGCCAGTCAGCCCAGTCCAGATGGCCTGGTGCC
GGAACCCTCTGACTCCGTCACCAAAATCTTGGCCCGCATGGGAGATGCAGGCTTCTCTCCGG
TTGAAGTGGTCTGGTTACTCGCTAGTCACTCGGTTGCTGCCCAGGACAAAGTTGATCCGAGC
ATTCCTGGTACGCCGTTCGACTCAACTCCTAGCGTGTTCGATACCCAGTTCTTTGTGGAAAC
GATGCTGAAAGGTACGCTGTTTCCGGGTTCTGGCCTGCATGATGGCGAAGTGCAATCGCCCT
TACCAGGCGAATTTCGCCTGCAAAGCGACTTTCTGCTTGCGCGTGACTCACGTACCGCATGC
GAATGGCAGAGCATGGTGAATAACCAGGCCAACATGCTTCAACGCTTTGAAGCGACCATGTC
GAAGATGTCCCTGCTGGGCTTTGACCAGAGTGCGTTGACCGACTGTTCCGATGTCATCCCCA
CTGCCACTGGCACCGTTGCAGCTCCGTTTCTGCCGGCAGGGAAAACGATGGACGATATTGAG
GTAGCGTGTGCGTCGACACCGTTTCCTACACTGAGTGCAGCTCCAGGTCCGGTGACGAGCAT
TCCGCCTGTACCGCTCAATTAA

(1014 base)

>Ancestral ligninase amino acid sequence

MTCSGGRTTANAACCVWFDVLDDIQENLFHGGQCGEEVHESLRLTFHDAIGFSPALTAAGQF
GGGGADGSIMAHSDIELTFPANNGLDEIIEAQRPFAIKHNVSFGDFIQFAGAVGVANCPGGP
RLSFFAGRSNASQPSPDGLVPEPSDSVTKILARMGDAGFSPVEVVWLLASHSVAAQDKVDPS
IPGTPFDSTPSVFDTQFFVETMLKGTLFPGSGLHDGEVQSPLPGEFRLQSDFLLARDSRTAC
EWQSMVNNQANMLQRFEATMSKMSLLGFDQSALTDCSDVIPTATGTVAAPFLPAGKTMDDIE
VACASTPFPTLSAAPGPVTSIPPVPLN

(337 residues)

Figure 3-3. DNA and amino acid sequences of ancestral ligninase

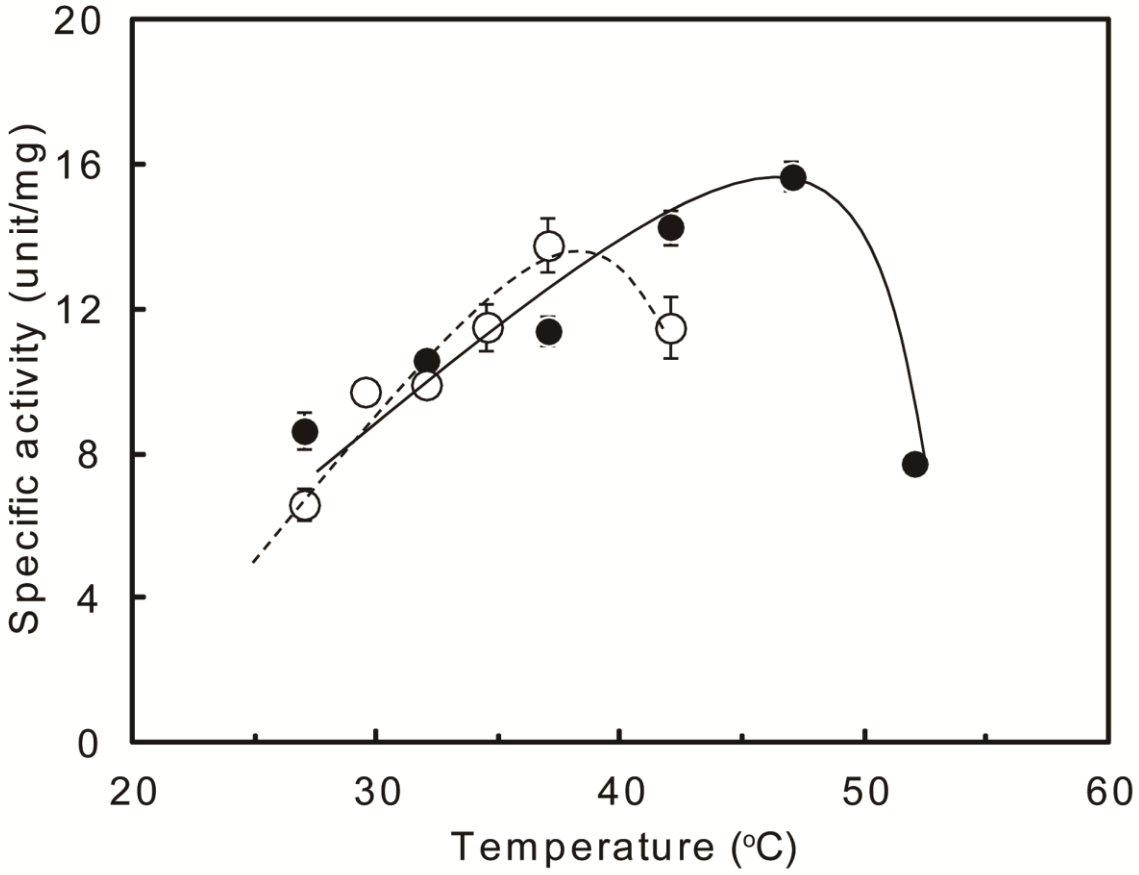

Figure 3-4.The temperature dependence of LiP activity

Closed and open circles indicate ancestral ligninase and PcLiP, respectively.

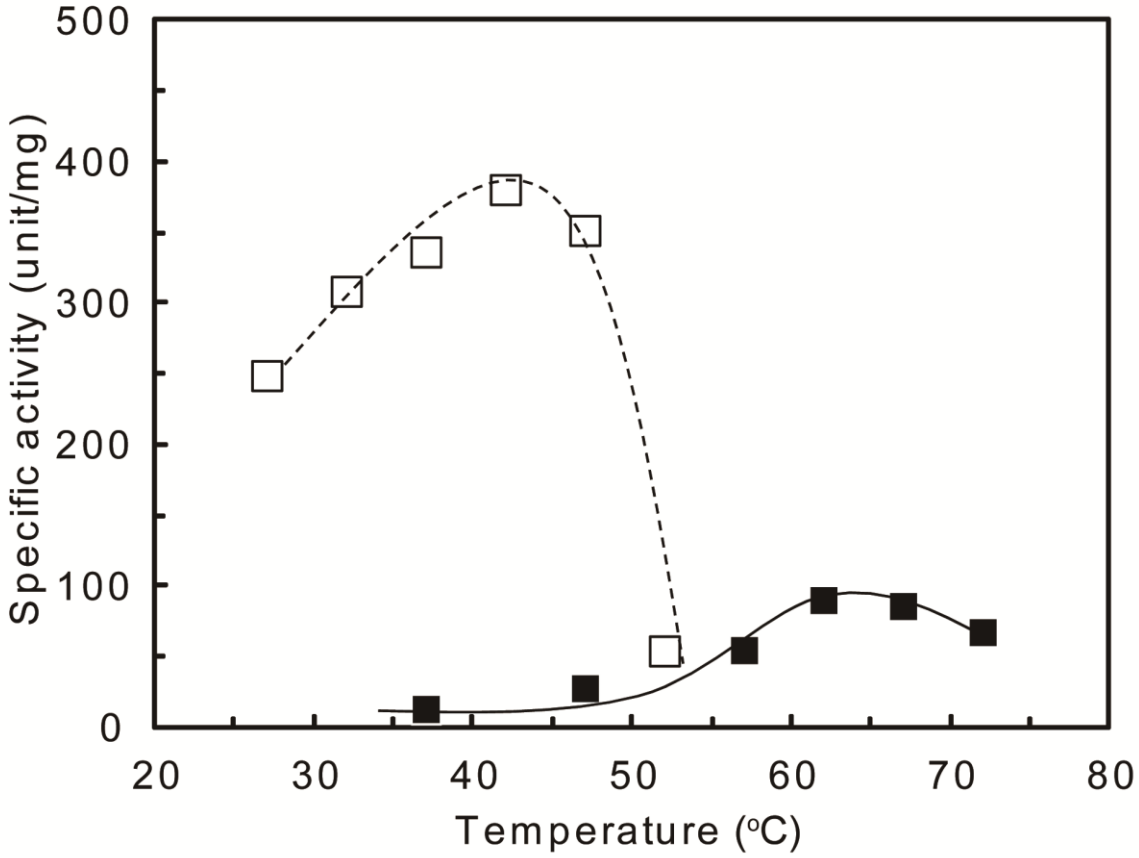

Figure 3-5.The temperature dependence of MnP activity

Closed and open squares indicate ancestral ligninase and PcMnP, respectively.

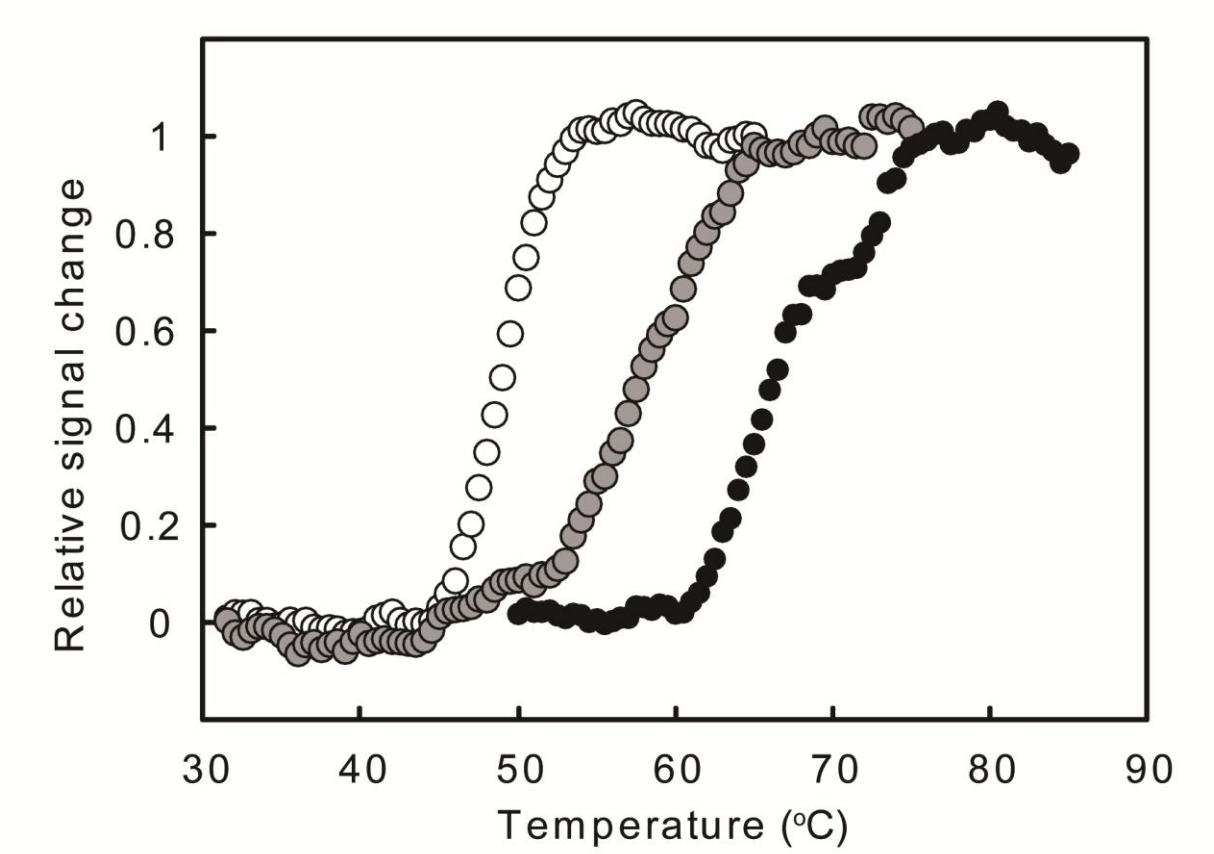

Figure 3-6.Thermal melting profile estimated by measuring CD at 222 nm

White, gray and black circles indicate ancestral ligninase, PcLiP and PcMnP, respectively. The protein concentration was 0.3 mg/mL in 10 mM acetate buffer (pH 6.0) containing 1 mM $CaCl_2$.

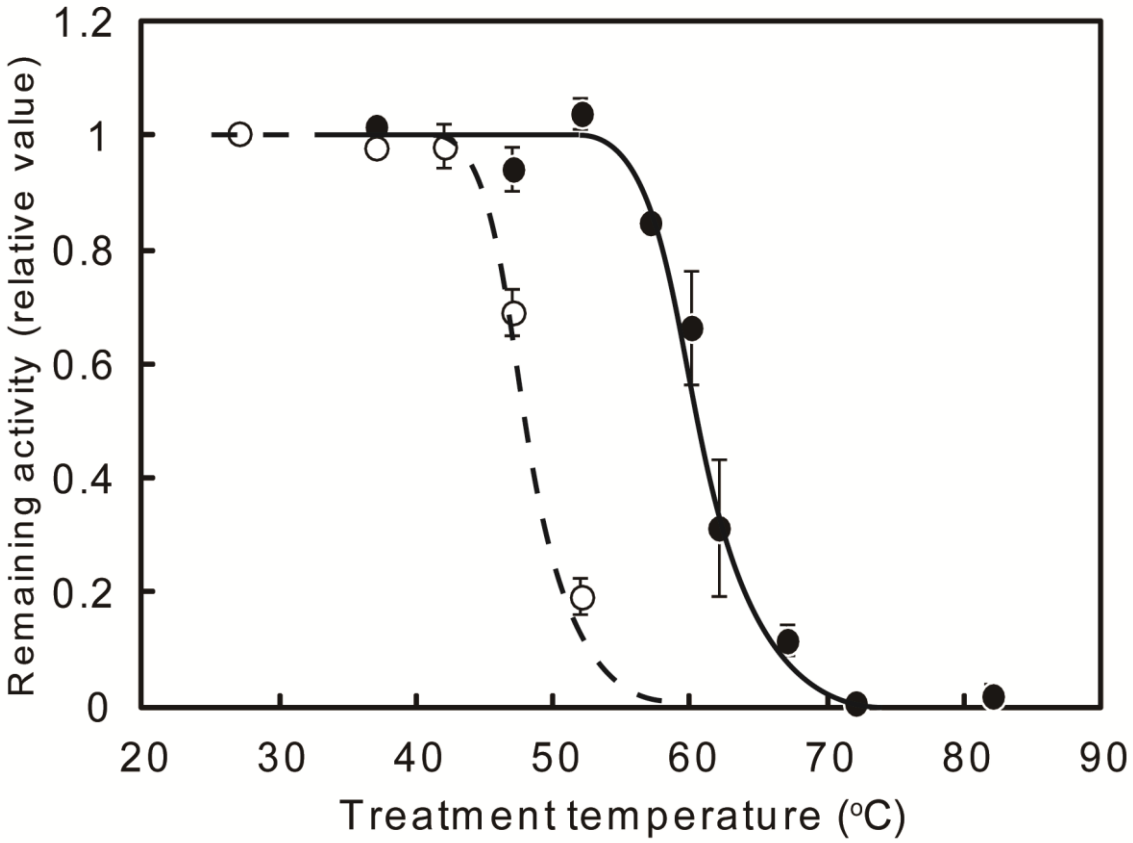

Figure 3-7.The remaining LiP activity after heat treatment for 15 min at the indicated temperatures.

Closed and open circles indicate the ancestral ligninase and PcLiP, respectively.

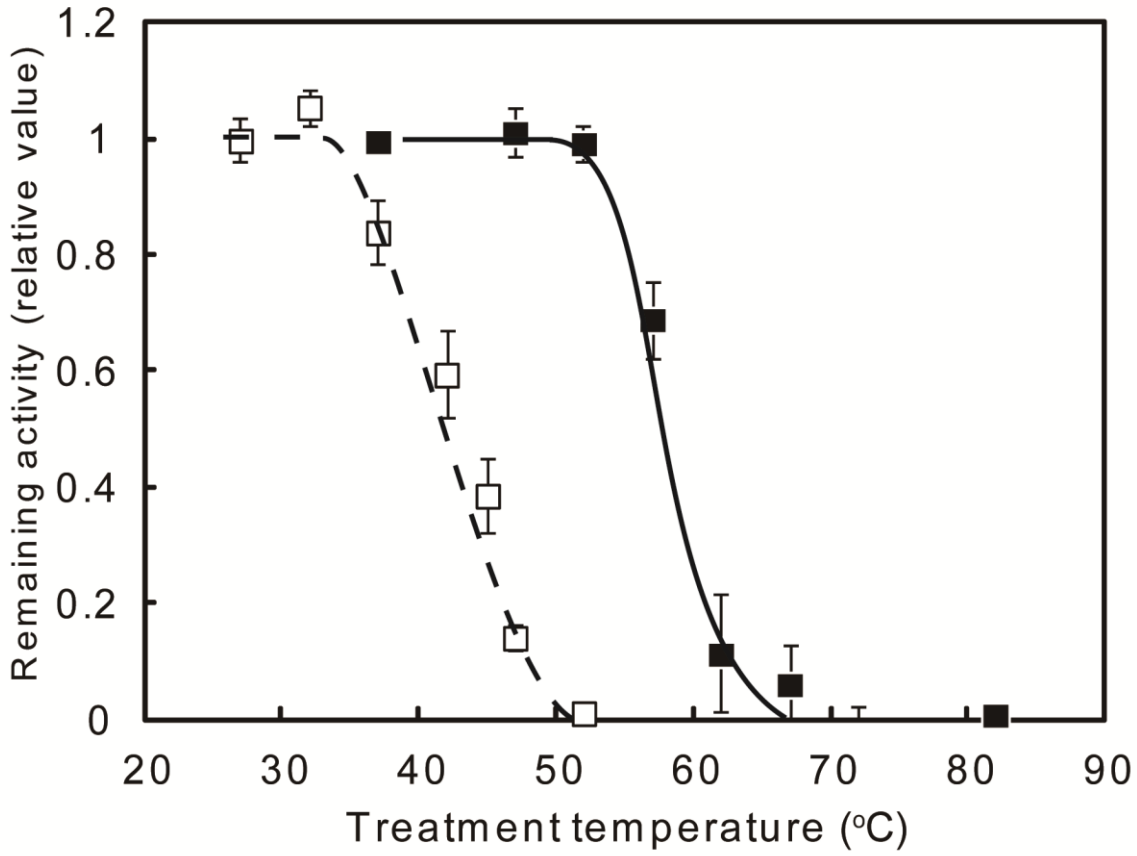

Figure 3-8.The remaining MnP activity after heat treatment for 15 min at the indicated temperatures.

Closed and open squares indicate the ancestral ligninase and PcMnP, respectively.

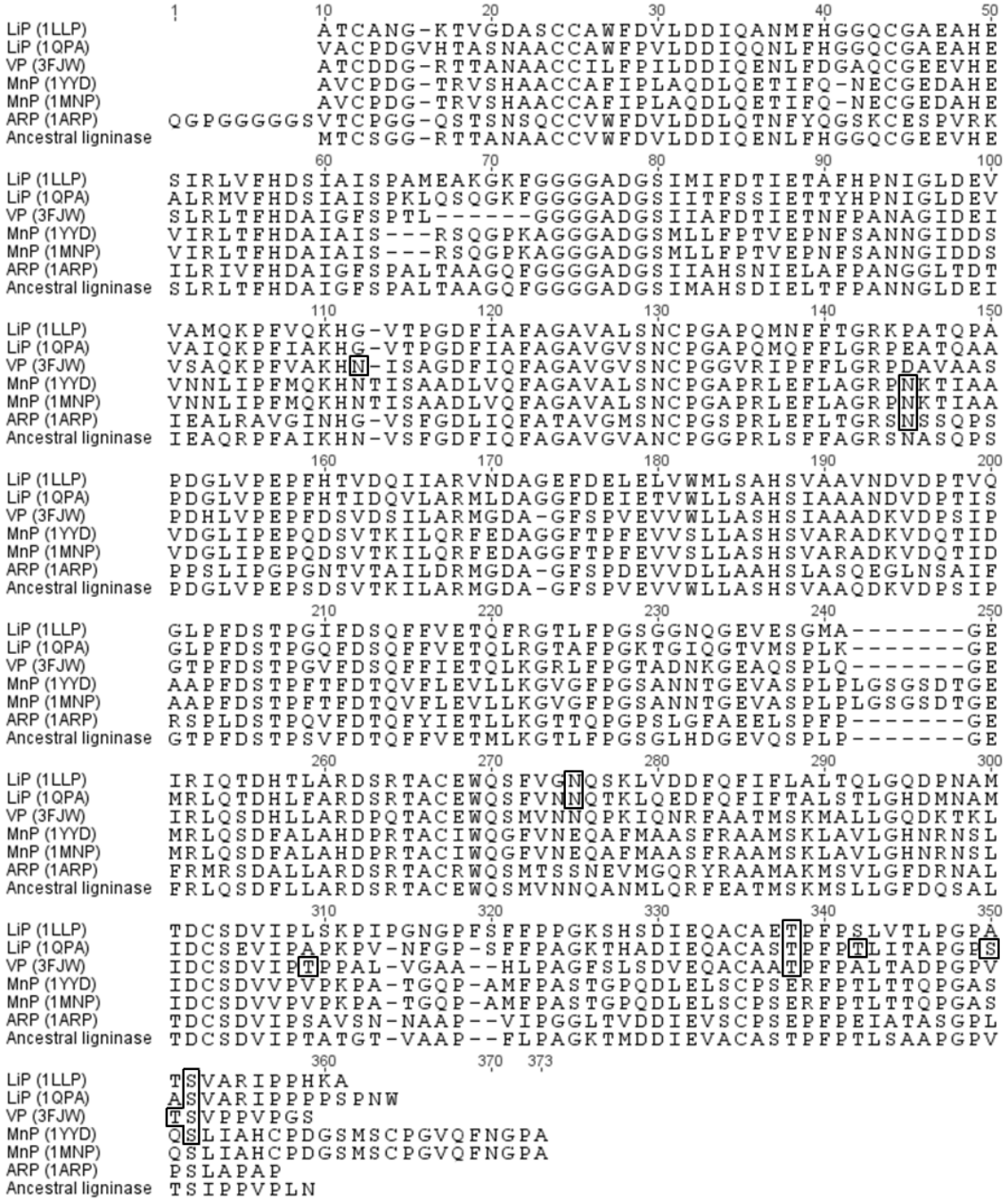

Figure 3-9.Glycosylation site

Alignment of amino acid sequences of two LiPs, one VP, two MnPs and the ancestral ligninase. The PDB IDs are in parentheses. The boxed residues indicate glycosylation sites.

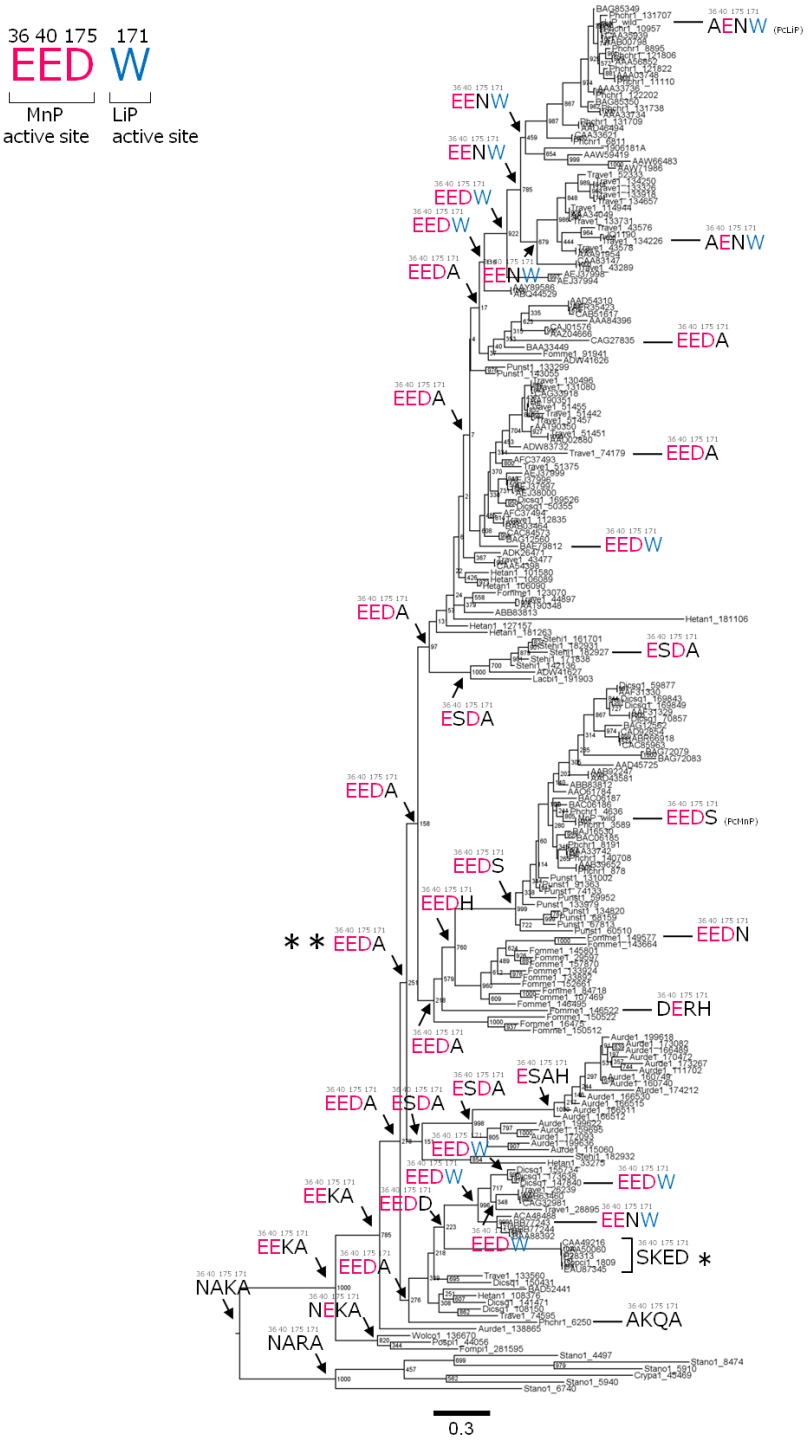

Figure 3-10. The maximum likelihood tree with sequences added

The single, double and triple asterisks indicate the outgroup and the ancestor position in Figure 3-2 and the ancestor of this tree, respectively. The amino acids comprising the active sites of selected nodes and sequences are shown. The residues responsible for MnP activity (residues at the position 36, 40 and 175) and LiP activity (position 171) are shown for respective nodes and aligned at right side. Red residues are the same as the MnP active site, and blue residues are the same as the LiP active site residue. The standard bar represents 0.3 substitutions per sites.

Table 1. List of protein IDs and its species used for phylogenetic tree construction

Protein ID	Enzyme name	Species
AAA33742	Manganese peroxidase I procedure	*Phanerochaete chrysosporium (OGC101)*
BAC06185	Manganese peroxidase isoform 1	*Phanerochaete sordida (YK-624, ATCC 90872)*
BAJ16530	Manganese peroxidase isoform 4	*Phanerochaete sordida (YK-624)*
BAC06186	Manganese peroxidase isoform 2	*Phanerochaete sordida (YK-624, ATCC 90872)*
AAB39652	Manganese peroxidase isozyme 3	*Phanerochaete chrysosporium (OGC101)*
ABB83812	Manganese peroxidase precursor	*Ceriporiopsis rivulosa (DSM 14618)*
AAO61784	peroxidase	*Ceriporiopsis subvermispora*
AAB92247	Manganese-dependent peroxidase	*Ceriporiopsis subvermispora (FP 105752)*
AAD43581	Manganese-dependent peroxidase precursor	*Ceriporiopsis subvermispora (FP 105757)*
BAC06187	Manganese peroxidase isoform 3	*Phanerochaete sordida (YK-624, ATCC 90872)*
AAF31329	Manganese peroxidase isoform 1	*Dichomitus squalens (CBS 432.34)*
AAF31330	Manganese peroxidase isoform 2	*Dichomitus squalens (CBS 432.34)*
ABR66918	Manganese peroxidase precursor	*Phlebia sp. (b19)*
CAC85963	Manganese peroxidase 2	*Phlebia radiata (79, ATCC 64658)*
CAD92854	Manganese peroxidase precursor	*Phlebia radiata (79, ATCC 64658)*
BAG12562	Manganese peroxidase 3	*Phlebia sp.MG60*
AAD45725	Manganese-dependent peroxidase precursor	*Ceriporiopsis subvermispora (FP105757)*
BAG72079	Manganese peroxidase	*Lentinula edodes (SR-1)*
BAG72083	Manganese peroxidase	*Lentinula edodes*
AAB00798	Lignin peroxidase isozyme H8	*Phanerochaete chrysosporium (BKM-F-1767)*
CAA35939	Lignin peroxidase precursor	*Phanerochaete chrysosporium (BKMF-1767, ATCC 24725)*
AAA56852	Ligninase	*Phanerochaete chrysosporium (ME446)*
BAG85349	Lignin peroxidase precursor	*Phanerochaete sordida (YK-624, ATCC 90872)*
AAA33736	Lignin peroxidase	*Phanerochaete chrysosporium (BKMF-1767, ATCC 24725)*
AAA03748	Lignin peroxidase	*Phanerochaete chrysosporium (BKM-F-1767, ATCC 24725)*

AAA33734	Ligninase precursor	*Phanerochaete chrysosporium (BKM-F1767, ATCC 24725)*
BAG85350	Lignin peroxidase precursor	*Phanerochaete sordida (YK-624, ATCC 90872)*
AAD46494	Lignin peroxidase	*Phanerochaete chrysosporium (BKM-F-1767)*
CAA33621	Lignin peroxidase	*Phanerochaete chrysosporium (BKMF 1767, ATCC 24725)*
AAW59419	Lignin peroxidase precursor	*Phlebia radiata (79, ATCC 64658)*
AAW66483	Lignin peroxidase precursor	*Phlebia radiata (79, ATCC 64658)*
AAW71986	Lignin peroxidase precursor	*Phlebia radiata (79, ATCC 64658)*
1906181A	Lignin peroxidase	*Bjerkandera adusta (IFO 5307)*
AAA34049	Lignin peroxidase	*Trametes versicolor (PRL572)*
AAA91954	Lignin peroxidase	*Trametes versicolor*
JQ1190	Lignin peroxidase VLG1 precursor	*Trametes versicolor (FP 72074, ATCC 12679)*
CAA83147	Lignin peroxidase isozyme LP7	*Trametes versicolor (PRL 572)*
AEJ37994	peroxidase MNP1	*Polyporus brumalis*
AEJ37998	Mn peroxidase MNP5	*Polyporus brumalis*
AAD02880	Manganese peroxidase	*Trametes versicolor (PRL 572)*
AAT90350	manganese peroxidase isozyme precursor	*Trametes versicolor (KN9522)*
AAT90351	Manganese peroxidase isozyme precursor	*Trametes versicolor (KN9522)*
CAG33918	Manganese-dependent peroxidase	*Trametes versicolor*
ADW83732	Manganese peroxidase	*Lenzites gibbosa (CB-1)*
AEJ37996	Mn peroxidase MNP3	*Polyporus brumalis*
AEJ37997	Mn peroxidase MNP4	*Polyporus brumalis*
AEJ38000	Mn peroxidase MNP4-1	*Polyporus brumalis*
AEJ37999	Mn peroxidase MNP6	*Polyporus brumalis*
AFC37494	Manganese peroxidase 3	*Lenzites gibbosa (CB-1)*
BAB03464	Manganese peroxidase	*Trametes versicolor (IFO30340)*
AFC37493	Manganese peroxidase 2	*Lenzites gibbosa (CB-1)*
BAG12560	Manganese peroxidase 1	*Phlebia sp. (MG60)*
CAC84573	Manganese peroxidase	*Phlebia radiata (79, ATCC 64658)*
CAA54398	peroxidase	*Trametes versicolor*
BAE79812	manganese peroxidase 1 precursor	*Spongipellis sp. (FERM P-18171)*

AAY89586	Versatile peroxidase	*Bjerkandera adusta (UAMH8258)*
ADK26471	Manganese peroxidase 1	*Hericium erinaceum*
ABB83813	Manganese peroxidase precursor	*Ceriporiopsis rivulosa (DSM 14618)*
AAT90348	Manganese peroxidase isozyme precursor	*Trametes versicolor (KN9522)*
AAD54310	Versatile peroxidase VPS1 precursor	*Pleurotus eryngii (CBS 613.91, ATCC 90787)*
AER35423	Manganese peroxidase	*Pleurotus ostreatus*
CAB51617	Manganese peroxidase 2	*Pleurotus ostreatus (Florida)*
AAZ04666	Versatile peroxidase precursor	*Pleurotus eryngii (CBS 458.79)*
CAJ01576	Putative versatile peroxidase	*Pleurotus sapidus*
BAA33449	Manganese peroxidase	*Pleurotus ostreatus (IS-1)*
AAA84396	Manganese peroxidase	*Pleurotus ostreatus (IFO 30160)*
ADW41626	Manganese peroxidase 2	*Agrocybe praecox (FBCC476)*
CAG27835	Manganese peroxidase enzyme	*Agaricus bisporus (D649, ATCC 62459)*
AAB63460	Manganese-repressed peroxidase	*Trametes versicolor (CU1)*
CAG32981	Manganese-repressed peroxidase	*Trametes versicolor*
ABB77243	Manganese peroxidase	*Ganoderma formosanum*
ABB77244	Manganese peroxidase	*Ganoderma australe*
BAA88392	Manganese peroxidase	*Ganoderma applanatum*
ACA48488	Manganese peroxidase	*Ganoderma lucidum (BCRC36123)*
ADW41627	Manganese peroxidase 1	*Agrocybe praecox (FBCC476)*
BAD52441	Lignin peroxidase	*Trametopsis cervina (WD550)*
CAA49216	peroxidase	*Coprinopsis cinerea (IFO 8371)*
CAA50060	peroxidase	*Coprinopsis cinerea (IFO 8371)*
EAU87345	peroxidase	*Coprinopsis cinerea (okayama7#130)*
P28313	Peroxidase:Flags:precursor	*Agaricales sp. (Arthromyces ramosus)*
ABQ44529	Versatile peroxidase	*Bjerkandera adusta*

Table 2. Steady-state kinetic parameters

	VA						H_2O_2					
	k_{cat} (/s)		K_M (mM)		k_{cat}/K_M (/s/mM)		k_{cat} (/s)		K_M (μM)		k_{cat}/K_M (/s/μM)	
Ancestral ligninase	7.3 ± 0.6	(1.00)	4.2 ± 1.2	(1.00)	1.7 ± 0.5	(1.00)	4.9 ± 0.2	(1.00)	6.4 ± 1.1	(1.00)	0.8 ± 0.1	(1.00)
PcLiP	8.4 ± 0.2	(1.16)	0.2 ± 0.0	(0.05)	41.9 ± 7.4	(24.7)	9.3 ± 0.5	(1.91)	36.0 ± 5.7	(5.62)	0.26 ± 0.1	(0.34)

	Mn (II)						H_2O_2					
	k_{cat} (/s)		K_M (mM)		k_{cat}/K_M (/s/mM)		k_{cat} (/s)		K_M (μM)		k_{cat}/K_M (/s/μM)	
Ancestral ligninase	35.1 ± 1.6	(1.00)	0.30 ± 0.1	(1.00)	129.9 ± 18.6	(1.00)	30.0 ± 0.7	(1.00)	3.2 ± 0.3	(1.00)	9.4 ± 2.3	(1.00)
PcMnP	303.0 ± 6.9	(8.64)	0.10 ± 0.1	(0.41)	2715.3 ± 232.1	(20.9)	310.6 ± 24.4	(10.4)	20.9 ± 6.4	(6.53)	14.9 ± 3.8	(1.59)

Relative values are shown in parentheses.

References

[1] K. Katoh and D. M. Standley, “MAFFT Multiple Sequence Alignment Software Version 7: Improvements in Performance and Usability,” *Mol. Biol. Evol.*, vol. 30, no. 4, pp. 772–780, Apr. 2013.

[2] J. Castresana, “Selection of conserved blocks from multiple alignments for their use in phylogenetic analysis.,” *Mol. Biol. Evol.*, vol. 17, no. 4, pp. 540–552, Apr. 2000.

[3] S. Whelan and N. Goldman, “A General Empirical Model of Protein Evolution Derived from Multiple Protein Families Using a Maximum-Likelihood Approach,” *Mol. Biol. Evol.*, vol. 18, no. 5, pp. 691–699, May 2001.

[4] D. Darriba, G. L. Taboada, R. Doallo, and D. Posada, “ProtTest 3: fast selection of best-fit models of protein evolution.,” *Bioinformatics*, vol. 27, no. 8, pp. 1164–1165, Apr. 2011.

[5] S. Guindon, J.-F. Dufayard, V. Lefort, M. Anisimova, W. Hordijk, and O. Gascuel, “New algorithms and methods to estimate maximum-likelihood phylogenies: assessing the performance of PhyML 3.0.,” *Syst. Biol.*, vol. 59, no. 3, pp. 307–321, May 2010.

[6] Z. Yang, “PAML: a program package for phylogenetic analysis by maximum likelihood,” *Comput. Appl. Biosci. CABIOS*, vol. 13, no. 5, pp. 555–556, Oct. 1997.

[7] R. J. Edwards and D. C. Shields, “GASP: Gapped Ancestral Sequence Prediction for proteins.,” *BMC Bioinformatics*, vol. 5, p. 123, Sep. 2004.

[8] M. Tien and T. K. Kirk, “Lignin-degrading enzyme from Phanerochaete chrysosporium: Purification, characterization, and catalytic properties of a unique H(2)O(2)-requiring oxygenase.,” *Proc. Natl. Acad. Sci. USA.*, vol. 81, no. 8, pp. 2280–2284, Apr. 1984.

[9] I. C. Kuan, K. A. Johnson, and M. Tien, “Kinetic analysis of manganese peroxidase. The reaction with manganese complexes.,” *J. Biol. Chem.*, vol. 268, no. 27, pp. 20064–20070, Sep. 1993.

[10] M. Mohorcic, M. Bencina, J. Friedrich, and R. Jerala, “Expression of soluble versatile peroxidase of Bjerkandera adusta in Escherichia coli.,” *Bioresour. Technol.*, vol. 100, no. 2, pp. 851–858, Jan. 2009.

[11] S. Akanuma, S. Iwami, T. Yokoi, N. Nakamura, H. Watanabe, S. Yokobori, and A. Yamagishi, “Phylogeny-based design of a B-subunit of DNA gyrase and its ATPase domain using a small set of homologous amino acid sequences.,” *J. Mol. Biol.*, vol. 412, no. 2, pp. 212–225, Sep. 2011.

[12] S. Akanuma, Y. Nakajima, S. Yokobori, M. Kimura, N. Nemoto, T. Mase, K. Miyazono, M. Tanokura, and A. Yamagishi, “Experimental evidence for the thermophilicity of ancestral life,” *Proc. Natl. Acad. Sci.*, vol. 110, no. 27, pp. 11067–11072, Jul. 2013.

[13] E. A. Gaucher, J. M. Thomson, M. F. Burgan, and S. A. Benner, “Inferring the palaeoenvironment of ancient bacteria on the basis of resurrected proteins,” *Nature*, vol. 425, no. 6955, pp. 285–288, Sep. 2003.

[14] D. Floudas, M. Binder, R. Riley, K. Barry, R. A. Blanchette, B. Henrissat, A. T. Martinez, R. Otillar, J. W. Spatafora, J. S. Yadav, A. Aerts, I. Benoit, A. Boyd, A. Carlson, A. Copeland, P. M. Coutinho, R. P. de Vries, P. Ferreira, K. Findley, B. Foster, J. Gaskell, D. Glotzer, P. Gorecki, J. Heitman, C. Hesse, C. Hori, K. Igarashi, J. A. Jurgens, N. Kallen, and P. Kersten, “The Paleozoic origin of enzymatic lignin decomposition reconstructed from 31 fungal genomes,” *Science*, vol. 336, pp. 1715–1719, 2012.

[15] C. N. Pace, G. R. Grimsley, J. A. Thomson, and B. J. Barnett, “Conformational stability and activity of ribonuclease T1 with zero, one, and two intact disulfide bonds.,” *J. Biol. Chem.*, vol. 263, no. 24, pp. 11820–11825, Aug. 1988.

[16] P. D. Williams, D. D. Pollock, B. P. Blackburne, and R. A. Goldstein, “Assessing the Accuracy of Ancestral Protein Reconstruction Methods,” *PLoS Comput Biol*, vol. 2, no. 6, p. e69, Jun. 2006.

[17] B. Steipe, B. Schiller, A. Plückthun, and S. Steinbacher, “Sequence Statistics Reliably Predict Stabilizing Mutations in a Protein Domain,” *J. Mol. Biol.*, vol. 240, no. 3, pp. 188–192, Jul. 1994.

[18] M. Lehmann, L. Pasamontes, S. F. Lassen, and M. Wyss, “The consensus concept for thermostability engineering of proteins.,” *Biochim. Biophys. Acta*, vol. 1543, no. 2, pp. 408–415, Dec. 2000.

[19] T. Choinowski, W. Blodig, K. H. Winterhalter, and K. Piontek, “The crystal structure of lignin peroxidase at 1.70 Å resolution reveals a hydroxy group on the Cβ of tryptophan 171: A novel radical site formed during the redox cycle,” *J. Mol. Biol.*, vol. 286, no. 3, pp. 809–827, Feb. 1999.

[20] A. Schmidt, C. Jelsch, P. Østergaard, W. Rypniewski, and V. S. Lamzin, “Trypsin Revisited: CRYSTALLOGRAPHY AT (SUB) ATOMIC RESOLUTION AND QUANTUM CHEMISTRY REVEALING DETAILS OF CATALYSIS,” *J. Biol. Chem.*, vol. 278, no. 44, pp. 43357–43362, Oct. 2003.

[21] M. Sundaramoorthy, K. Kishi, M. H. Gold, and T. L. Poulos, “Preliminary Crystallographic Analysis of Manganese Peroxidase from Phanerochaete chrysosporium,” *J. Mol. Biol.*, vol. 238, no. 5, pp. 845–848, May 1994.

[22] M. Sundaramoorthy, H. L. Youngs, M. H. Gold, and T. L. Poulos, “High-resolution crystal structure of manganese peroxidase: substrate and inhibitor complexes,” *Biochemistry*, vol. 44, pp. 6463–6470, 2005.

[23] N. Kunishima, K. Fukuyama, and H. Matsubara, “Crystal structure of the fungal peroxidase from Arthromyces ramosus at 1.9 A resolution. Structural comparisons with the lignin and cytochrome c peroxidases.,” *J. Mol. Biol.*, vol. 235, no. 1, pp. 331–344, Jan. 1994.

[24] G. Nie, N. S. Reading, and S. D. Aust, “Relative Stability of Recombinant Versus Native Peroxidases from Phanerochaete chrysosporium,” *Arch. Biochem. Biophys.*, vol. 365, no. 2, pp. 328–334, May 1999.

Acknowledgement

I gratefully acknowledge to Professor Akihiko Yamagishi, Tokyo University of Pharmacy and Life Sciences. Professor Yamagishi gave me a chance to commence this work and helpful advice. Grateful appreciation is lecture Shin-ichi Yokobori, Tokyo University of Pharmacy and Life Sciences, especially introducing phylogenetic analysis. Dr Manabu Ishida taught me experiment techniques. I am particularly indebted to associate professor Masatada Tamakoshi and assistant professor Satoshi Akanuma, Tokyo University of Pharmacy and Life Sciences, as well as to staff of the laboratory of extremophiles, Tokyo University of Pharmacy and Life Sciences.

Finally I grateful thank my family for their support during the course.